

**Investigations of Cation- $\pi$  Binding by Cyclophane Receptors in  
Aqueous Media**

**Thesis by  
Laura S. Mizoue**

**In Partial Fulfillment of the Requirements for the  
Degree of Doctor of Philosophy**

**California Institute of Technology  
Pasadena, California**

**1995**

**(Submitted October 12, 1994)**

## Acknowledgments

First of all, I would like to thank my advisor, Dennis Dougherty for his advice and guidance throughout my many years here at Caltech. I am very fortunate to have worked for someone whom I respect and admire, not only as a scientist, but as an educator and a person.

I am grateful to the members of the Dougherty group, both past and present, for sharing their scientific expertise and their words of wisdom. I would especially like to thank Rich Barrans, Pat Kearney, Alison McCurdy, Leslie Jimenez, Bob Kumpf, Sandro Mecozzi, Jon Forman, and Wenge Zhong for their advice on host-guest matters. I would also like to thank Silvia Cavagnero in the Chan group for her patient and unselfish assistance with various NMR experiments.

Many thanks go to those people who assisted me in the writing of this thesis. I am indebted to Jeff Clites, Pat Kearney, and Sarah Ngola for their critical reading of the manuscript, and to Jon Forman and Anthony West for their help in generating some of the figures.

There are also a number of people who deserve mention for having made day-to-day life here a little easier. I would like to thank Pat Kearney, Sandro Mecozzi, Wenge Zhong, and Jen Ma for making 249 Crellin a truly pleasant place to work, Cindy Kiser for fielding all of my molecular biology questions while I was writing props, and for letting me borrow/train/spoil her guide dogs, and Sonja Opstrup for listening to my travails, and then offering an optimist's viewpoint on the situation.

Finally, I would like to thank my entire family for their love and support, and for continually helping me to keep things in perspective.

## Abstract

The binding properties of two new cyclophane receptors in aqueous media were explored. Replacement of two benzene rings of the host P with furans or thiophenes was expected to enhance cation- $\pi$  interactions, but significant improvements in the binding of positively-charged guests were not observed. *Ab initio* calculations provided a rationalization for the experimental findings and a better understanding of the cation- $\pi$  interaction.

The binding in water of various guanidinium compounds to host P was also investigated. These molecules represented a new type of cationic guest for the receptor. Arginine was not measurably bound by P, but several alkylated guanidiniums were well bound, especially considering their high water solubility. Hexamethylguanidinium, a nonplanar molecule with  $D_3$  symmetry, was a particularly interesting guest which displayed enantioselective binding to P. In addition, some progress was achieved towards the synthesis of receptors that have either an amide or a carboxylate group attached to the rim of the cavity. The appended group is positioned such that it can form hydrogen bonds or electrostatic interactions with a bound guanidinium guest.

Finally, exploratory work was carried out towards the synthesis of a cyclophane host that possesses a disulfide near the binding cavity. This receptor was designed to mimic the acetylcholine binding site of the nicotinic acetylcholine receptor. Although various disulfide containing macrocycles were synthesized, they were not sufficiently water soluble to permit studies of their binding properties.

**Table of Contents**

Acknowledgments	ii
Abstract	iii
List of Figures	vi
List of Tables	viii
<b>Chapter 1: The Effects of Heterocyclic Rings on the Binding of Cationic Guests by a Cyclophane Receptor.</b>	<b>1</b>
Introduction and Background Information	2
Hosts F and T	9
Results and Discussion	10
Host Syntheses	10
CMC Studies	11
Binding Studies	12
Computational Studies	17
Conclusions	22
Experimental Section	24
References	28
<b>Chapter 2: The Aqueous Binding of Guanidinium Guests to a Cyclophane Receptor.</b>	<b>35</b>
Introduction	36
Results and Discussion	40
Binding Studies	40
Hexamethylguanidinium	42
Conclusions	46
Experimental Section	47
References	48

<b>Chapter 3: Progress Toward the Synthesis of Macrocycles with Appended Amide or Carboxylate Groups.</b>	<b>51</b>
Introduction	52
Results and Discussion	57
Progress Towards the Synthesis of the Amide Linker, 10a	59
Progress Towards the Synthesis of the Ester Linker, 10b	61
Progress Towards the Synthesis of the Amide Linker, 10c	64
Concluding Remarks	65
Experimental Section	67
References	75
<b>Chapter 4: Design of a Disulfide-Containing Macrocycle, a Model of the Nicotinic Acetylcholine Receptor Binding Site.</b>	<b>77</b>
Introduction	78
Results and Discussion	83
Disulfide Host Synthesis	84
Modification of the Disulfide Host	86
An N-Methyl Amide Macrocycle	90
Concluding Remarks	96
Experimental Section	99
References	08

**List of Figures**

- Figure 1.1.** Two Well-Studied Host Structures
- Figure 1.2**  $-\Delta G^\circ$  (kcal/mol) for Binding to Host P in Borate Buffer
- Figure 1.3.** CPK representations of the (S,S,S,S) enantiomer of host P in rhomboid (top) and toroid (bottom) binding conformations
- Figure 1.4** The Cation- $\pi$  Interaction
- Figure 1.5** Definition of Host Structures
- Figure 1.6** Synthesis of Hosts F and T
- Figure 1.7** Optimized 1:1 complexes of ammonium with benzene (Ia-Ic), thiophene (IIa-IIc), and furan (IIIa-IIIc)
- Figure 1.8** Calculated 6-31G\*\*//6-31G\*\* electrostatic potential surfaces for benzene (top), thiophene (middle), and furan (bottom)
- Figure 1.9** The angular dependence of the 6-31G\*\* binding energy of Na<sup>+</sup> to thiophene and furan
- Figure 2.1** Calculated relative aqueous (chloroform) solvation energies (kcal/mol) for cations and analogous neutral compounds
- Figure 2.2** A guanidinium ion stacked between aromatic rings
- Figure 2.3**  $-\Delta G^\circ$  (kcal/mol) in borate-d for guanidinium guests binding to host P
- Figure 2.4**  $-\Delta G^\circ$  (kcal/mol) for enantiomerically pure guests binding to host P in borate-d
- Figure 2.5** (a) NMR resonances of hexamethylguanidinium (8) when binding to host P. (b) Equilibrium relationships between the enantiomers of 8 ( $G_A$  and  $G_B$ ) and their complexes with P ( $HG_A$  and  $HG_B$ ). (c) CPK models of the two enantiomers of 8 based on calculated structures
- Figure 3.1** Host P shown with a CPK representation of a host-guest complex

- Figure 3.2** Host CP shown with a CPK representation of the host structure in one of several possible rhomboid conformations of the molecule
- Figure 3.3**  $-\Delta G^\circ$  (kcal/mol) in aqueous borate buffer for binding to Host CP/P
- Figure 3.4** Calculated AM1 electrostatic potential surfaces for the guanidinium guests 3 (left) and 6 (right)
- Figure 3.5** Definition of Host Structures
- Figure 3.6** Proposed synthesis of hosts 7a, 7b, and 7c
- Figure 3.7** Attempted synthesis of the Linker 10a
- Figure 3.8** Attempted Synthesis of the Ester Linker 10b
- Figure 3.9** A revised synthetic route towards the linker 10b
- Figure 3.10** Synthesis of the Linker 10c
- Figure 4.1** Schematic representation of a model of the nAChR
- Figure 4.2** A schematic model of the nAChR agonist binding site of *Torpedo marmorata*.
- Figure 4.3** Synthesis of a Disulfide-Containing Macrocycle
- Figure 4.4** N-Methylated Disulfide Host Synthesis
- Figure 4.5**  $^1\text{H}$  NMR spectra of macrocycle 19 in organic solvents
- Figure 4.6** Labelling Scheme for the Protons of Tetramethyl ester 19
- Figure 4.7**  $^1\text{H}$  NMR spectra of macrocycle 19 in mixed aqueous solvents
- Figure 4.8** Proposed Synthesis of a Disulfide Host

**List of Tables**

- Table 1.1**  $-\Delta G^\circ$  (kcal/mol) for binding to hosts F, T, P, and M in 10% v/v acetonitrile in borate-d
- Table 1.2** D values for the iminium guest **16** (top) and the tetraalkylammonium guest **5** (bottom) with hosts F, T, P, and M
- Table 1.3** Calculated relative binding energies for the 1:1  $\pi$ -complexes of benzene, thiophene, and furan with  $\text{NH}_4^+$  and  $\text{Na}^+$  cations

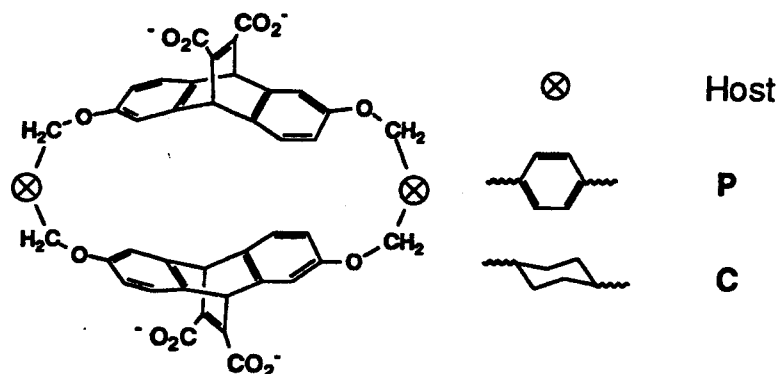


**Chapter 1: The Effects of Heterocyclic Rings on the Binding of Cationic Guests  
by a Cyclophane Receptor.**

## Introduction and Background Information

Supramolecular chemistry involves the study of molecules that are held together by noncovalent forces. Over the past decade, it has rapidly evolved into a broad, interdisciplinary field with developments and applications in chemistry, biology, and physics.<sup>1</sup> Many laboratories, including our own, have designed cyclophane-based macrocycles to investigate supramolecular complexation in water.<sup>2-14</sup> Much of the interest in these artificial receptors stems from their relevance to biological systems. Since they are considerably less complex and are easier to modify than their biological counterparts, these small, synthetic models have provided tremendous insight into the nature and magnitude of various fundamental interactions (hydrophobic effects, electrostatic interactions, solvent effects, and donor-acceptor interactions) that are responsible for molecular recognition.

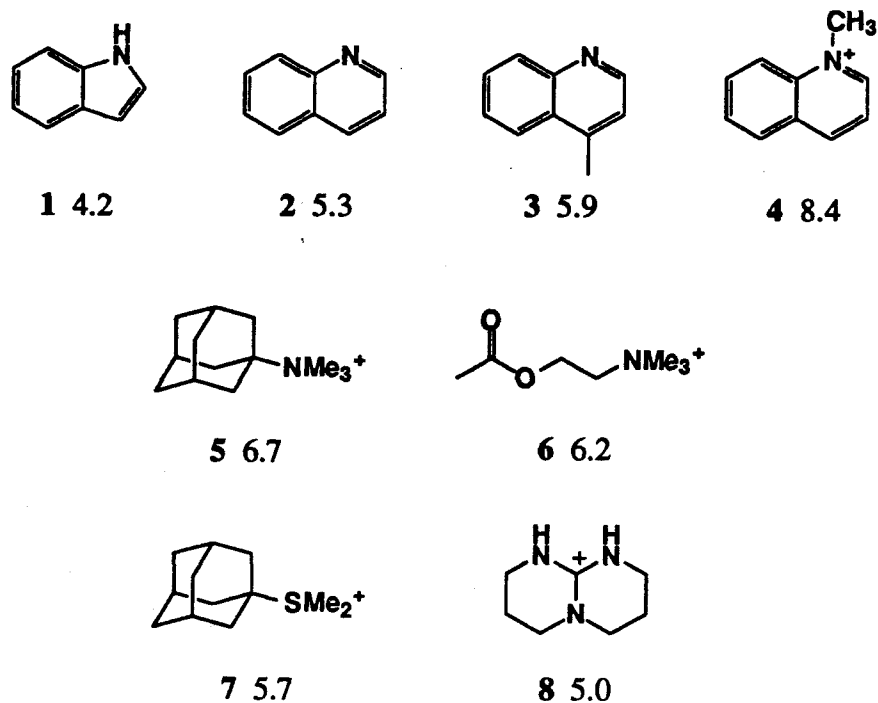
The Dougherty group's work in this area revolves around receptors that have the general structure shown in Figure 1.1. Our hosts are composed of two ethenoanthracene units that are connected via ether groups to a so-called "linker" (⊗). Various moieties have been introduced at the linker positions to produce different hosts that display different binding properties.<sup>13</sup> The ethenoanthracene unit serves two important functions. First, it provides a rigid, concave, hydrophobic surface that forms the basis of a well-defined binding cavity. Second, it places the water-solubilizing carboxylate groups in a position remote from the cavity. This presumably increases the hydrophobicity of the binding site and also prevents the carboxylates from directly interacting with bound guests. An additional feature of the ethenoanthracene is its  $C_2$  symmetry. It can be synthesized enantiomerically pure and then coupled to produce chiral host molecules.



**Figure 1.1.** Two Well-Studied Host Structures.

Our prototypical receptor is the host P, so designated because of its *p*-xylylene linkers (see Figure 1.1). Extensive studies of host P have shown that it binds with high affinities to a wide variety of guests that are quite water soluble.<sup>13</sup> Some representative guests and their free energies of binding ( $-\Delta G^\circ$  in kcal/mol) to host P in pH  $\sim$  9 borate buffer are illustrated in Figure 1.2.

A large component of the driving force for complexation in these systems is undoubtedly due to the hydrophobic effect. This is apparent from the high affinities seen with neutral electron-rich guests such as indole, **1**. Larger binding constants are observed with electron-deficient aromatic compounds such as quinoline, **2**. Since **1** and **2** are very similar in shape, the enhancement is probably reflective of strong donor-acceptor interactions with the electron-rich rings of the host, rather than improved size complementarity to the binding cavity.

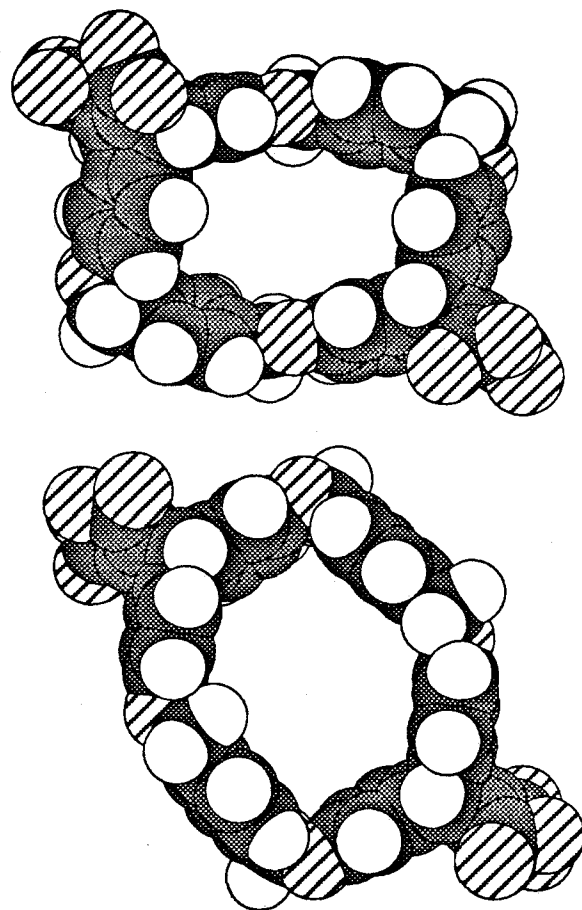


**Figure 1.2.**  $-\Delta G^\circ$  (kcal/mol) for Binding to Host P in Borate Buffer.

The data show that host P also binds extremely tightly to several different types of cationic guests. One such class of guests is typified by N-methylquinolinium, **4** and includes a number of N-alkylated quinolinium, isoquinolinium, pyridinium, and related molecules. We shall refer to these as iminium compounds with the understanding that the positive charge results from alkylation, not protonation, of a pyridine-type nitrogen. Other major classes of guests include the tetraalkylammonium (**5**, **6**), the sulfonium (**7**) and the guanidinium (**8**) compounds. (The guanidinium guests are discussed in more detail in Chapter 2.)

Although host P was designed to contain a rigid, preorganized binding site, CPK models and computer modelling suggest that it can adopt two distinct conformations to accommodate different guests. A  $C_2$ -symmetric

rhomboid conformation (see Figure 1.3, top) is best suited for binding flat, aromatic compounds. Naphthalene-sized guests such as **2** and **4** fit snugly within the cavity, thus maximizing both hydrophobic and  $\pi$ -stacking interactions. A more open,  $D_2$ -symmetric toroid conformation (see Figure 1.3, bottom) is better suited for binding the larger tetraalkylammonium compounds such as adamantyltrimethylammonium, **5**.

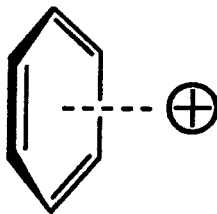


**Figure 1.3.** CPK representations of the  $S,S,S,S$  enantiomer of host P in rhomboid (top) and toroid (bottom) binding conformations. The rhomboid conformation is the X-ray structure of the tetraester with the methyl groups deleted for clarity; the toroid conformation was obtained by computer modelling. The oxygen atoms of the molecule are cross-hatched.

Originally, the existence of the two conformers was based primarily on specific NMR chemical shift patterns that the host protons displayed upon guest binding.<sup>13a</sup> More recently, circular dichroism (CD) data have provided additional support for the two-state model, as the changes in the CD spectra that occur when host P binds flat aromatic guests are significantly different from those seen when it binds the larger tetraalkylammonium guests.<sup>16</sup> Furthermore, an X-ray crystallographic structure of the tetramethyl ester of host P revealed a rhomboid conformation in excellent agreement with the predicted structure.<sup>17</sup> The X-ray analysis corroborated earlier results from <sup>1</sup>H NMR difference nOe experiments on the tetraester which suggested that the rhomboid conformation predominated in solution.<sup>13a</sup>

As alluded to earlier, host P shows an interesting preference for binding cationic over neutral guests. This is quite unusual, since the higher water solubility of the charged molecules should reduce their attraction to the hydrophobic binding site. These results suggest that cation- $\pi$  effects are operative in these systems.

The cation- $\pi$  interaction can be defined as the stabilizing force between a positive charge and the electron-rich face of a benzene ring (see Figure 1.4). It was first observed in the gas-phase binding of K<sup>+</sup> and other small ions to benzene.<sup>18</sup> Since then, the interaction has been seen in synthetic receptor systems from other laboratories,<sup>7,10,19</sup> and it has been proposed to play a significant role in determining protein structure and stability.<sup>20</sup> In addition, studies from our group have shown that cation- $\pi$  binding of transition states can lead to novel forms of catalysis.<sup>21</sup>



**Figure 1.4.** The Cation- $\pi$  Interaction.

The importance of cation- $\pi$  interactions in our host-guest complexes was further demonstrated when the benzene rings of host P were replaced with nonaromatic cyclohexyl groups to produce the host C (see Figure 1.1). Unlike host P, host C did not discriminate between positively-charged and neutral guests [guest ( $-\Delta G^\circ$ , kcal/mol): 4 (5.9), 3 (6.0)].<sup>13a</sup> Other compelling evidence was obtained from chloroform studies of the tetramethyl ester of host P.<sup>21</sup> In the absence of hydrophobic effects, significant binding of cationic guests was still observed [guest ( $-\Delta G^\circ$ , kcal/mol): 4 (3.5), 5 (2.1)], whereas neutral guests such as 2 were not measurably bound. These results also eliminated the possibility that electrostatic attractions with the carboxylates of host P were responsible for the enhanced binding of cations.

Perhaps the best quantitative measurement of the cation- $\pi$  effect can be obtained by comparing the host P binding affinities of guests 3 and 4 (see Figure 1.1). The two molecules are nearly identical in size, shape, and hydrophobic surface area, yet in water the cation is bound 2.5 kcal/mol more tightly than the neutral compound. This is probably a conservative estimate of the magnitude of the interaction, since the cost of desolvating the guest upon binding should be greater for the cation. In fact, calculated relative aqueous solvation energies revealed that 4 is better solvated than 3 by 46 kcal/mol.<sup>13b</sup>

Our investigations of cation- $\pi$  interactions in small, synthetic molecules led us to speculate about their possible roles in biological receptors, especially those that bind the ubiquitous neurotransmitter acetylcholine (ACh, 6). We had already demonstrated that host P binds ACh with a  $K_d = 25 \mu\text{M}$  at 298 °K in aqueous buffer (see Figure 1.1), a value comparable to those of biological binding sites.<sup>23</sup> A comprehensive search of the literature yielded two other interesting pieces of information. First, affinity-labeling, NMR, and mutagenesis experiments on the nicotinic acetylcholine receptor (nAChR) from the *Torpedo* electric organ had identified a number of conserved aromatic residues that lie near the binding site for ACh.<sup>26-28</sup> (The nAChR is the prototypical ligand-gated ion channel, and is discussed in greater detail in Chapter 4.) Second, the X-ray crystallographic structure of phosphocholine complexed to the antibody Fab McPC603 showed the trimethylammonium group of phosphocholine surrounded by three aromatic amino acids.<sup>25, 29</sup>

These observations led us to propose that the electron-rich rings of Trp, Tyr and Phe bind the quaternary ammonium ion of ACh through cation- $\pi$  interactions.<sup>30</sup> Our model was in sharp contrast to the widely-held assumption that the binding sites were anionic in nature. Conventional wisdom predicted that the carboxylate groups of Asp and Glu participated in favorable charge-charge interactions with the head group of ACh.

Our proposal gained considerable support with the subsequent determination of the X-ray structure of acetylcholinesterase (AChE) from *Torpedo*.<sup>31</sup> AChE terminates impulse transmission at cholinergic synapses by rapidly hydrolyzing ACh. The X-ray data revealed that the enzyme's active site lies at the bottom of a deep and narrow gorge. Remarkably, 14 highly conserved aromatic amino acids lie near the active site and along the gorge. The authors hypothesized that once the ACh is trapped at the opening of the



gorge, it rapidly diffuses down to the active site by interacting with the aromatic residues.

More recent studies point to the importance of cation- $\pi$  effects in other types of neurological receptors. For example, three-dimensional modelling of G-protein-coupled receptors suggests that conserved aromatic residues play a prominent role in binding cationic neurotransmitters.<sup>32</sup> In voltage-gated K<sup>+</sup> channels, mutagenesis studies<sup>33</sup> have revealed that the ion conduction pore is rich in aromatic residues; tetraethylammonium and other quaternary ammoniums inhibit the channel by binding to the pore region. Additionally, computational studies that we performed on a simple model of the K<sup>+</sup> channel led us to postulate that cation- $\pi$  interactions are responsible for the ion selectivity.<sup>34</sup>

Clearly, the studies of host P have helped establish the cation- $\pi$  interaction as a fundamental binding force in both artificial and natural receptors. They have also helped alter the common perception that benzene functions simply as a large, hydrophobic surface. The work that is detailed in this chapter extends our understanding of the cation- $\pi$  effect through both experimental and computational studies on a new generation of host molecules.

**Hosts F and T.** As part of an effort to gain further insight into the nature of the cation- $\pi$  interaction, we became interested in modifying the electronic properties of the host P. We decided to synthesize two new hosts, F and T, in which two benzene rings of host P have been replaced with furan and thiophene rings respectively (see Figure 1.5). Furan and thiophene are considered to be electron-rich ring systems,<sup>35</sup> so we anticipated that the new hosts would display enhanced cation- $\pi$  effects which would be manifested in stronger binding to cationic guests.

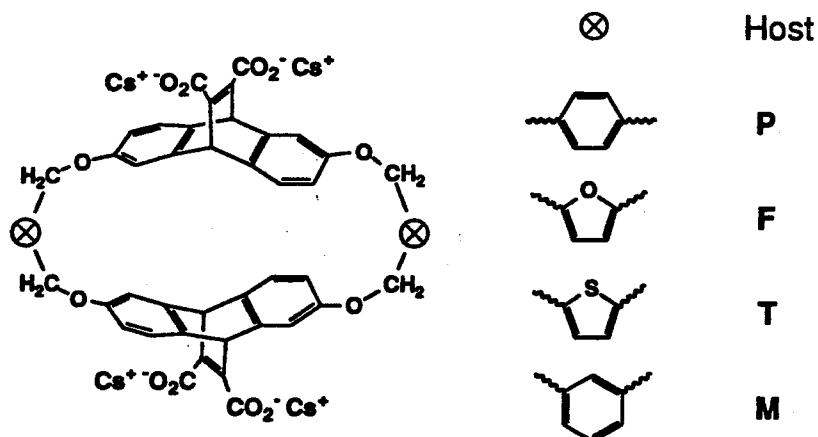


Figure 1.5. Definition of Host Structures.

## Results and Discussion.

**Host Syntheses.** The macrocycles were synthesized in a fairly straightforward manner, analogous to the procedure used to generate host P (see Figure 1.6).<sup>13a</sup> Enantiomerically pure ethenoanthracene **9** was coupled to the appropriate bis(chloromethyl) heterocycle (**10** or **11**) under high dilution conditions in anhydrous DMF using  $\text{Cs}_2\text{CO}_3$  as a base. The bis(chloromethyl) heterocycles were prepared as described in the literature.<sup>36</sup> Since both compounds **10** and **11** decomposed extremely rapidly, they were handled minimally and were stored under argon at  $-100\text{ }^\circ\text{C}$ . After isolating the desired macrocycle, a water-soluble host was obtained by hydrolyzing the methyl esters using excess  $\text{CsOH}$  in  $\text{DMSO}/\text{H}_2\text{O}$ . The reaction mixture was then passed through an  $\text{NH}_4^+$  ion exchange column, lyophilized, and dissolved in  $\text{pH} \sim 9$ , 10 mM deuterated cesium borate buffer (referred to as borate-d), producing a host solution for use in binding studies.

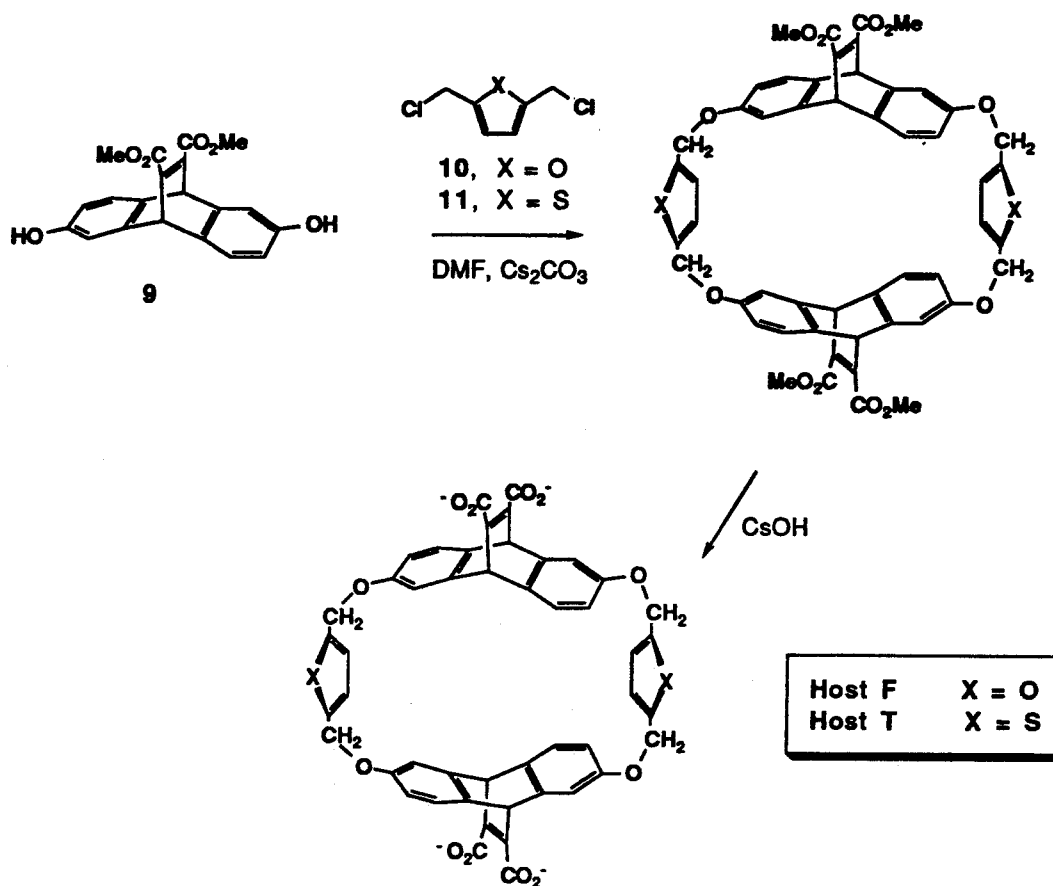


Figure 1.6. Synthesis of Hosts F and T.

**CMC Studies.** Before beginning binding studies on a particular host, it is very important to investigate its aggregation behavior in water. Since our macrocycles contain both hydrophobic and hydrophilic parts, they self-associate above a sufficiently high concentration known as the critical micellar concentration (CMC).<sup>2,37</sup> To ensure that only specific host-guest complexation is being measured, the experiments must be conducted below the CMC of the host. The CMC is determined by diluting a solution of the host and monitoring the chemical shifts of its resonances at several different

concentrations. Above the CMC, the chemical shifts are dependent upon the concentration, whereas below the CMC they are invariant.

A CMC study of host F in borate-d indicated that concentrations below 300  $\mu\text{M}$  were relatively free of aggregates. However, the data from several binding studies conducted in this medium gave extremely poor fits with our statistical analysis package. In our experience, this is usually indicative of some kind of aggregation phenomenon. Host T appeared to be even more prone to aggregate than host F. The  $^1\text{H}$  NMR spectrum of host T in borate-d showed severe broadening of the resonances. The peaks sharpened considerably upon addition of 10% v/v acetonitrile, and a CMC study of the host in this mixed buffer solution showed no signs of aggregation in concentrations as high as 1 mM. Consequently, binding studies of both hosts were performed in the mixed solvent system, where aggregation was completely suppressed.

**Binding Studies.** All binding constants for the hosts F and T were obtained using  $^1\text{H}$  NMR methods. Encapsulation by the host causes the protons of the guest to experience shielding and move considerably upfield. The host-guest complexes are in fast exchange, so the spectra display only time-averaged signals for the free and bound species.

In a typical binding experiment, a solution of the host was titrated with a solution of the guest, and the chemical shifts of the guest resonances were monitored. The host and guest concentrations were varied to ensure that the percentage-bound covered a broad range. The unknowns in the experiment were the association constant ( $K_a$ ) and the difference in chemical shift between the free and fully complexed guest protons (referred to as D values). A single  $K_a$  and the D value for each guest proton were determined

iteratively using the non-linear least-squares fitting programs EMUL/MULTIFIT, developed by Richard Barrans, Jr. in our group.<sup>38</sup> The programs fit the NMR data for all guest protons simultaneously; it has been demonstrated that this approach is superior to other methods commonly in use. Finally, to obtain an estimate of the error bars, a rigorous statistical analysis was performed on the data. Unless otherwise noted, the error bars were within  $\pm 0.2$  kcal/mol of the  $\Delta G^\circ$  values reported.

The binding data for several iminium and tetraalkylammonium guests are shown in Table 1.1; neutral guests such as **2** were not measurably bound in the mixed aqueous medium. We had expected that introduction of the heterocyclic ring systems would lead to dramatic increases in binding affinities, but this was not evident from the data. The  $\Delta G^\circ$  values for hosts T and P are nearly identical. The  $\Delta G^\circ$  values for host F appear to be slightly better than those of host P, however, most of the improvements fall within the allowable error.

The lack of significant differences between hosts T, F, and P led us to consider the possibility that the *meta*-linked host M (see Figure 1.5) might serve as a better hydrocarbon reference than host P in terms of both the size and flexibility of the linkers. Host M was synthesized, and its binding behavior was investigated. These data are also shown in Table 1.1.

A comparison of guest proton shielding patterns revealed that host M was indeed a more appropriate reference compound in most instances. The shielding patterns provide some information about the orientation of a guest within the binding pocket because protons that point out towards the solvent experience less shielding than those that penetrate further into the cavity. The D values for a typical iminium guest, **16**, and a typical tetraalkyl-

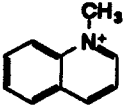
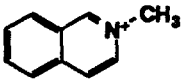
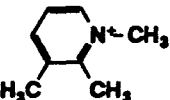
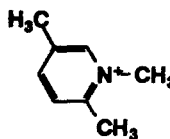
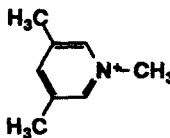
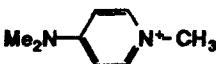
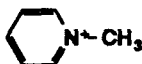
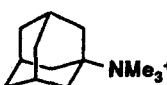

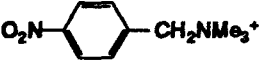
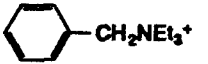
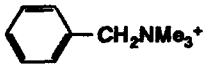
Guest		F	T	P	M
	4	5.2 <sup>a</sup>	5.1	5.8	5.2
	12	5.1	4.9	4.9	4.8
	13	4.5	4.3	4.3	4.4 <sup>a</sup>
	14	4.6	4.3	3.9	4.5
	15	4.6	4.2	4.3	4.3
	16	4.6	4.6	4.5	4.6
	17	3.7	<3.5	<3.5	<3.5
	5	3.7	4.0	4.1	<3.5
	18	3.7	<3.5	<3.5	<3.5
	19	4.1	<3.5	<3.5	<3.5
	20	3.5	<3.5	<3.5	<3.5
	21	3.9 <sup>b</sup>	<3.5	<3.5	<3.5

Table 1.1.  $-\Delta G^\circ$  (kcal/mol) for binding to hosts F, T, P, and M in 10% v/v acetonitrile in borate-d.

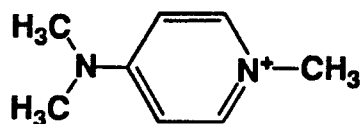
a  $\pm 0.3$  kcal/mol.

b  $\pm 0.4$  kcal/mol.

ammonium guest, 5, are illustrated in Table 1.2; the numbers have been scaled relative to the highest D-value in each experiment.

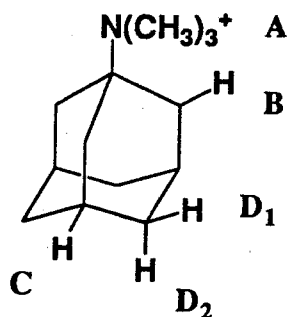
A comparison of the D values for guest 16 reveals that both host F and host T bind the flat aromatic molecule in a manner similar to host M. The 3, 5 protons of the guest are the most highly shielded, followed by the 2, 6 protons; for host P the relative ordering of the two types of protons is reversed. For guest 5, the upfield shift pattern of host F again resembles that of host M. The A and B protons are substantially shielded, and the shielding of D<sub>2</sub> is equivalent in magnitude to that of C and D<sub>1</sub>. This implies that the predominate association of the macrocycle is with the trimethylammonium group. The pattern for host T, on the other hand, more closely matches that of host P. The A and B protons are the most highly shielded, however the A protons are shielded to a lesser extent than for hosts F and M. The shieldings of the C and D<sub>1</sub> protons are comparable in magnitude, while that of D<sub>2</sub> is significantly less. This suggests that the guest is fully encapsulated within the binding cavity, with its D<sub>2</sub> protons pointed out towards solution. These observations show that the binding data of hosts F and T should be compared to host M, with the exception of the tetraalkyl-ammonium compounds whose binding to host T which should be compared to host P.

Returning to the  $\Delta G^\circ$  values in Table 1.1, it can be seen that the differences in binding affinities for the hosts P and M are small. Thus, even with inclusion of host M, no obvious trends emerge from the data. These results were certainly contrary to our original expectations. Puzzled by our experimental observations, we then turned to computational methods to help us understand the binding data.



16

Protons	F	T	P	M
N <sup>+</sup> -CH <sub>3</sub>	0.24	0.30	0.34	0.26
N(CH <sub>3</sub> ) <sub>2</sub>	0.40	0.47	0.76	0.42
3, 5	1.00	1.00	0.73	1.00
2, 6	0.81	0.77	1.00	0.75



5

A	1.00	0.72	0.61	1.00
B	0.92	1.00	1.00	0.86
C	0.38	0.40	0.43	0.56
D <sub>1</sub>	0.43	0.43	0.47	0.60
D <sub>2</sub>	0.35	0.29	0.29	0.55

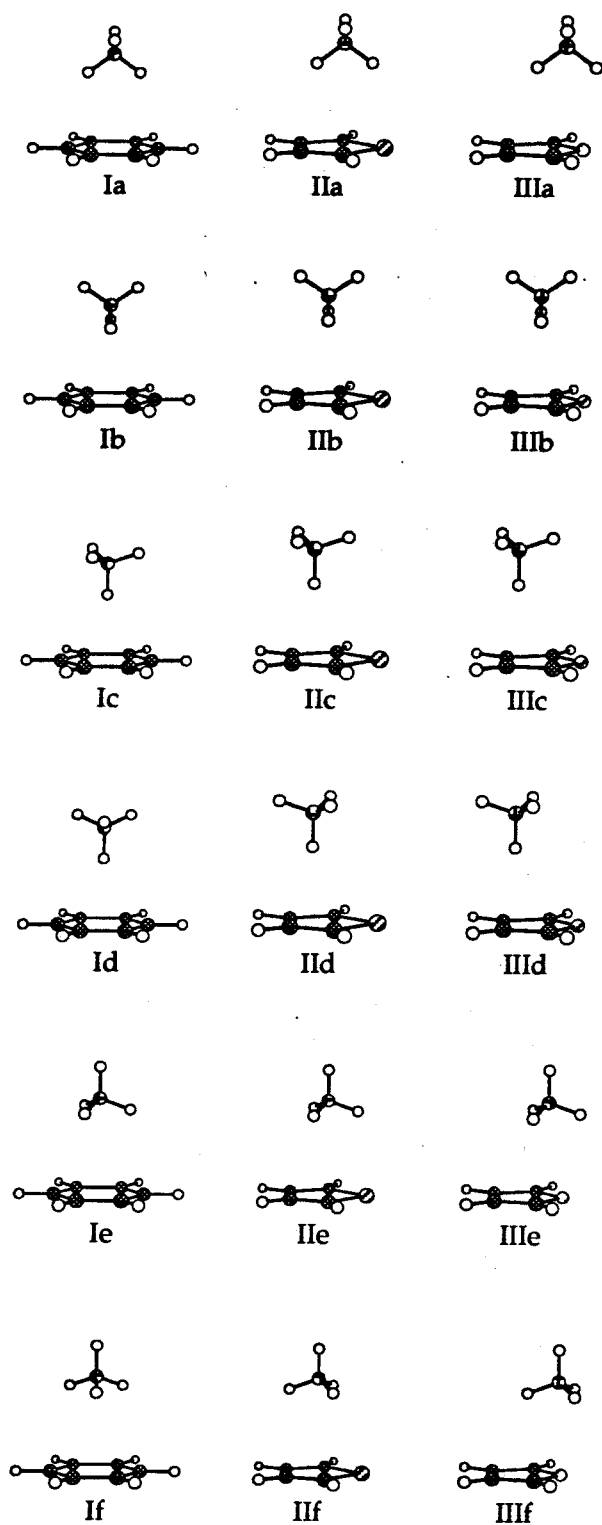
**Table 1.2.** D values for the iminium guest 16 (top) and the tetraalkylammonium guest 5 (bottom) with hosts F, T, P, and M. The numbers are scaled relative to the largest D value in each experiment.



**Computational Studies.** A number of *ab initio* computational studies of the cation- $\pi$  interaction were performed by Dr. Robert Kumpf in our group. To evaluate the differences between hosts P, F, and T, the gas-phase binding of  $\text{NH}_4^+$  to benzene, furan, and thiophene were investigated. The calculations involved geometry optimization at the HF-6-31G\*\* level followed by single-point energy evaluation at the MP2 level to account for electron correlation.<sup>39</sup> This level of theory provides results for benzene... $\text{NH}_4^+$  complexes that are in good agreement both with experiment and with previous calculations.<sup>18c,d</sup>

We emphasize that these are gas-phase calculations. In other work, we have shown that inclusion of aqueous solvation can have large effects when evaluating the interactions of different cations with the same aromatic species.<sup>33</sup> This is because cation desolvation energies are large and vary considerably with the cation structure. However, in the comparisons between benzene, furan, and thiophene the cation is kept constant, so to a good approximation the extent of ion desolvation should be similar. There will be some variation in the desolvation energies of the aromatic species, but we expect it to be small. Therefore, the gas-phase calculations should provide useful information for relative comparisons among the different hosts.

The calculated binding orientations of the complexes between  $\text{NH}_4^+$  and benzene, thiophene, and furan are illustrated in Figure 1.7. The binding energies are listed in Table 1.3. As is seen in Table 1.3,  $\text{NH}_4^+$  shows a clear preference for binding to benzene over furan and thiophene for all the binding geometries. In general, thiophene binds slightly better than furan.



**Figure 1.7.** Optimized 1:1 complexes of ammonium with benzene (Ia-I<sub>f</sub>), thiophene (IIa-II<sub>f</sub>), and furan (IIIa-III<sub>f</sub>).

<u>Complex</u>	<u><math>\Delta E</math></u>	<u><math>\Delta E_{MP2}</math></u>	<u><math>\Delta E_{lit}^{c,d}</math></u>
Ia	-15.1	-17.9	-16.3
IIa	-12.7	-15.2	
IIIa	-12.2	-15.3	
Ib	-15.1	-17.9	
IIb	-13.4	-16.6	
IIIb	-11.8	-14.7	
Ic	-13.9	-16.9	-15.2
IIc	-12.2	-15.7	
IIIc	-11.0	-14.0	
Id	-13.9	-16.9	
IIId	-12.1	-15.6	
IIIId	-10.9	-13.9	
Ie	-13.9	-16.2	-14.7
IIe	-12.5	-14.6	
IIIe	-11.8	-14.4	
If	-13.9	-16.2	
IIIf	-11.4	-13.9	
IIIIf	-10.6	-13.0	
C <sub>6</sub> H <sub>6</sub> ...Na <sup>+</sup>	-27.1		
C <sub>4</sub> H <sub>4</sub> S...Na <sup>+</sup>	-22.8		
C <sub>4</sub> H <sub>4</sub> O...Na <sup>+</sup>	-20.6		

**Table 1.3.** Calculated<sup>a</sup> relative binding energies<sup>b</sup> for the 1:1  $\pi$ -complexes of benzene, thiophene, and furan with NH<sub>4</sub><sup>+</sup> and Na<sup>+</sup> cations.

a 6-31G\*\*//6-31G\*\*

b in kcal/mol

c 3-21G//STO-3G

d Reference 18c

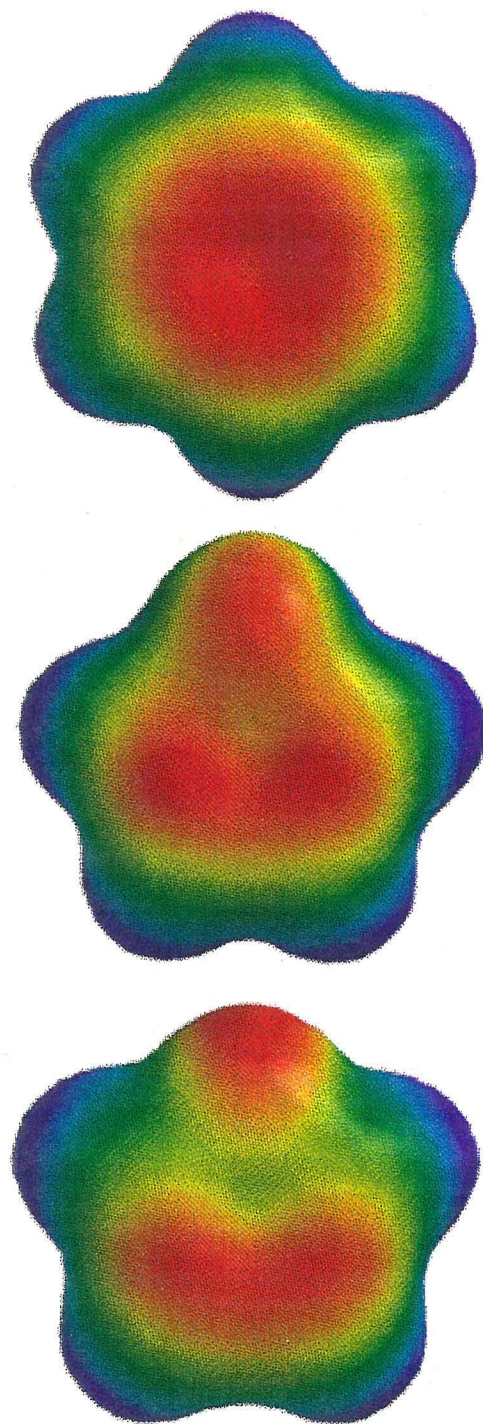
Similar trends are seen when Na<sup>+</sup> is substituted for NH<sub>4</sub><sup>+</sup> which also simplifies the calculations. These results are consistent with the lack of improvement we observed upon conversion of the host P (or M) to F or T.

Presumably, the cation- $\pi$  interaction results from a combination of fundamental forces such as charge-dipole, charge-quadrupole, charge-induced

dipole, and London dispersion terms. We believe, however, that the cation- $\pi$  effect is predominantly electrostatic in nature. We have shown that the gas-phase affinities for benzene follow the trend seen in conventional electrostatic binding<sup>34</sup> with  $\text{Li}^+ > \text{Na}^+ > \text{K}^+ > \text{Rb}^+$ , and in all of our binding studies we are able to rationalize the cation- $\pi$  interaction by treating benzene as a weak anion. Therefore, we also investigated the electrostatic potentials of the aromatic rings. They are shown pictorially in Figure 1.8 for benzene (top), thiophene (middle) and furan (bottom). In the color scheme, red represents the most negative value, and blue represents the most positive value.


As expected, benzene displays a large surface of partial negative charge directly over the center of the ring. With furan, the electronegative oxygen pulls electron density away from the center of the ring and introduces areas of electropositive character next to the heteroatom. The same effect is seen with thiophene, although to a lesser extent. This significantly diminishes the binding region over the face of the ring and suggests a reason for benzene binding more strongly to a simple cation.

The analysis reveals the flaw in the initial reasoning behind choosing furan and thiophene for our hosts. Furan and thiophene are considered to be electron-rich because of their high reactivity in electrophilic aromatic substitution reactions.<sup>35b</sup> Their reactivity results from stabilization of the developing positive charge of the transition state by the lone pairs of the heteroatom. The cation- $\pi$  interaction, however, is more nearly a ground-state effect. The  $\pi$  system distorts only slightly upon binding, so in this case, the ground-state electron distribution of the  $\pi$  system is more relevant.



**Figure 1.8.** Calculated 6-31G\*\*//6-31G\*\* electrostatic potential surfaces for benzene (top), thiophene (middle), and furan (bottom). Electrostatic potential surface values range from -20.0 (red) to +20.0 (blue) kcal/mol.

Lastly, for  $\text{Na}^+$  we probed the competition between cation- $\pi$  binding and interaction with the heteroatom lone pairs. The results are illustrated in Figure 1.9. The binding energies show that the interaction of the ion with furan is almost completely insensitive to orientation, whereas with thiophene the cation- $\pi$  interaction is clearly preferred.



<u>Angle <math>\theta</math></u>	<u><math>\Delta E</math></u>	<u><math>\Delta E</math></u>
0°	-20.7	-13.5
10°	-20.7	-13.6
20°	-20.5	-14.1
30°	-20.3	-14.7
40°	-20.0	-15.4
50°	-19.6	-16.2
60°	-19.2	-16.8
70°	-19.0	-17.4
80°	-19.0	-17.9
90°	-19.3	-18.7

**Figure 1.9.** The angular dependence of the 6-31G\*\* binding energy of  $\text{Na}^+$  to thiophene and furan. Energies are reported in kcal/mol.

## Conclusions

We have investigated the effects of replacing the benzene rings of host P with furan and thiophene. Contrary to our initial expectations, the new hosts F and T did not show any significant improvements in cation binding. Computational modelling supported and clarified our experimental findings. An examination of the electrostatic potential surfaces of the aromatic systems

was particularly enlightening, as it illustrated the importance of considering the ground-state electron distribution of the aromatic ring. This is in contrast to conventional notions of the electron-richness of the heterocyclic rings, which are based on their ability to stabilize a transition state.

Hosts F and T did not fulfill our original goal of enhancing the cation- $\pi$  effect in our macrocycles. The studies did, however, considerably expand our understanding of the cation- $\pi$  interaction. The work also neatly demonstrates how experiment and theory complement one other, and suggests how a combination of methods can be used to design systems with optimal binding properties.

## Experimental Section

**General Methods.** NMR spectra were recorded on either a General Electric QE-300, JEOL JNM GX-400, or Bruker AM-500 spectrometer. Routine spectra were referenced to the residual proton signals of the solvents and are reported in ppm downfield of 0.0 as  $\delta$  values. All coupling constants,  $J$ , are reported in Hz. Spectra from aqueous binding studies were referenced to an internal standard of 3,3-dimethylglutarate (DMG  $\delta$  1.09). Preparative centrifugal chromatography was performed on a Harrison Research Chromatotron model 792T using silica plates.

Host and guest stock solutions for the NMR binding experiments were prepared using a standard 10 mM deuterated cesium borate buffer at pH ~ 9 (referred to as borate-d). The buffer was prepared by dissolving high purity boric oxide (31.3 mg) in D<sub>2</sub>O (100 g). CsOD (467  $\mu$ L of a 1.0 M solution in D<sub>2</sub>O) was added, and the solution was mixed thoroughly.

The host solutions were quantified by NMR integrations against a primary standard solution of DMG in borate-d. Acetonitrile (10% v/v) was added to aliquots of these host solutions. Guest solutions for NMR binding studies were prepared by dissolution of the compounds in the appropriate volumes of 10% v/v acetonitrile in borate-d buffer. Guest solution concentrations were determined either by weight of solute or through NMR integrations against DMG. All binding studies were performed by subsequent addition of aliquots of guest solutions to an NMR tube containing a solution of host compound that was initially approximately 300  $\mu$ M. Binding data were fit to an appropriate association constant using the MULTIFIT or EMUL programs.<sup>38</sup> Error bars on the  $\Delta G^\circ$  values were obtained using the LUCIUS/PORTIA statistical analysis package.<sup>38</sup>



All gas-phase calculations were performed by Dr. Robert Kumpf using computational methods that have been described previously.<sup>13b</sup>

Guests 4, 5, and 12-21 were prepared by exhaustive alkylation of the appropriate amines, quinolines, isoquinolines, and pyridines with the appropriate iodoalkanes. For hosts F and T, the bis(chloromethyl) heterocycles, 10 and 11, were synthesized according to literature procedures.<sup>36</sup> In a slight modification of the purification protocol, 11 was isolated by quickly passing the crude product over a pad of silica gel and eluting with 10% ether in petroleum ether. Both heterocycles decomposed quite readily, and therefore were handled minimally and were stored under argon at -100 °C.

**Macrocyclizations.** As described previously,<sup>13a</sup> the tetramethyl ester of host P and host M were prepared by condensing ethenoanthracene 9 with *p*- or *m*-bis(bromomethyl)benzene in a suspension of cesium carbonate in anhydrous DMF. The tetramethyl esters of the new host compounds (F and T) were prepared similarly using the appropriate bis(chloromethyl)heterocycles, 10 and 11. In all macrocyclizations, enantiomerically pure ethenoanthracenes were coupled, although both *R,R* and *S,S* forms were used. The workup of the macrocyclic products differed slightly from that previously reported for host P. After the macrocyclizations were complete, the reactions were filtered, and the DMF was evaporated. The residues were then chromatographed over flash silica using 5% ethyl acetate in methylene chloride in order to separate the macrocyclic compounds from baseline impurities. The desired macrocycles were then isolated from higher order macrocycles using preparative centrifugal chromatography (silica plates, 5% ethyl acetate in CH<sub>2</sub>Cl<sub>2</sub>).

F, tetramethyl ester. Yield 5%; <sup>1</sup>H NMR (CDCl<sub>3</sub>) δ 7.08 (d, 4H, *J* = 9), 6.93 (d, 4H, *J* = 2), 6.47 (dd, 4H, *J* = 2, 8), 6.27 (s, 4H), 5.24 (s, 4H), 4.88 (AB, 8H, *J* = 14 Δ*v* =

18 Hz), 3.76 (s, 12H);  $^{13}\text{C}$  NMR ( $\text{CDCl}_3$ )  $\delta$  165.98, 156.21, 151.09, 147.06, 145.69, 136.28, 124.05, 112.28, 110.79, 110.47, 62.68, 52.36, 51.74; FAB-MS  $m/e$  889 ( $\text{M}^+$ ), 857 ( $\text{M}^+-\text{OMe}$ ), 537 ( $\text{M}^+-\text{ethenoanthracene}$ ); HRMS of  $\text{MNa}^+$  911.2308, calc. for  $\text{C}_{52}\text{H}_{40}\text{O}_{14}\text{Na}$  911.2316.

**T**, tetramethyl ester. Yield 8-18%;  $^1\text{H}$  NMR ( $\text{CDCl}_3$ )  $\delta$  7.14 (d, 4H,  $J = 8$ ), 6.92 (d, 4H,  $J = 2$ ), 6.86 (s, 4H), 6.47 (dd, 4H,  $J = 2, 8$ ), 5.25 (s, 4H), 5.11 (AB, 8H,  $J = 12$ ,  $\Delta\nu = 18$  Hz), 3.75 (s, 12H);  $^{13}\text{C}$  NMR ( $\text{CDCl}_3$ )  $\delta$  165.92, 155.61, 146.91, 145.77, 140.35, 136.22, 125.54, 124.05, 112.67, 109.71, 65.07, 52.36, 51.60; FAB-MS  $m/e$  921 ( $\text{M}^+$ ), 920 ( $\text{M}^+-1$ ), 919 ( $\text{M}^+-2$ ), 889 ( $\text{M}^+-\text{OMe}$ ), 569 ( $\text{M}^+-\text{ethenoanthracene}$ ); HRMS of  $\text{MNa}^+$  943.1862, calc. for  $\text{C}_{52}\text{H}_{40}\text{O}_{12}\text{S}_2\text{Na}$  943.1859.

**Ester Hydrolysis.** All tetraacid macrocycles were prepared by hydrolysis of the corresponding tetramethyl esters. In a typical procedure, the tetraester was dissolved in 1-2 mL of DMSO, and 10 equivalents of aqueous CsOH (1.0 M solution) was added which caused a white precipitate to form. The reaction mixture was stirred at room temperature for approximately three hours. Water (1-2 mL) was then added, and all solids dissolved. The solution was stirred overnight, and then frozen and lyophilized. The resulting residue was dissolved in a minimal amount of water and loaded onto a cation-exchange column (neutral pH, Dowex 50 X 4,  $\text{NH}_4^+$  form). The material was eluted with water that had been passed through a Milli-Q purification system. The fractions containing host were identified by their UV activity on TLC silica gel plates. The appropriate fractions were combined and lyophilized to obtain the desired free acids. Standard aqueous solutions of the hosts were prepared by adding the appropriate amount of aqueous CsOD (1.0 M in  $\text{D}_2\text{O}$ ), and diluting with borate-d to the desired volume.

**F**, tetraacid.  $^1\text{H}$  NMR (borate, referenced to internal DMG  $\delta$  1.09)  $\delta$  7.17 (d, 4H,  $J = 7$ ), 6.85 (d, 4H,  $J = 2$ ), 6.48 (dd, 4H,  $J = 2, 8$ ), 6.19 (br s, 4H), 5.21 (s, 4H).

**T**, tetraacid.  $^1\text{H}$  NMR (10%  $\text{CD}_3\text{CN}/90\%$  borate, referenced to internal DMG  $\delta$  1.09)  $\delta$  7.30 (d, 4H,  $J = 8$ ), 7.07 (d, 4H,  $J = 2$ ), 7.05 (s, 4H), 6.62 (dd, 4H,  $J = 2, 8$ ), 5.26 (s, 4H), 5.23 (AB, 4H,  $J = 13$ ,  $\Delta\nu = 22$  Hz).

**References**

1. Lehn, J.-M. *Science* **1993**, *260*, 1762-1762.
2. Diederich, F. *Cyclophanes*; The Royal Society of Chemistry: Cambridge, UK, 1991.
3. (a) Odashima, K.; Itai, A.; Iitaka, Y.; Koga, K. *J. Am. Chem. Soc.* **1980**, *102*, 2504-2505. (b) Soga, T.; Odashima, K.; Koga, K. *Tetrahedron Lett.* **1980**, *21*, 4351-4354. (c) Odashima, K.; Spoga, T.; Koga, K. *Tetrahedron Lett.* **1981**, *22*, 5311-5314.
4. (a) Tabushi, E.; Sasaki, H.; Kuřoda, Y. *J. Am. Chem. Soc.* **1976**, *98*, 5727-5728. (b) Tabushi, E.; Kimura, Y.; Yamamura, K. *J. Am. Chem. Soc.* **1981**, *103*, 6486-6492. (c) Tabushi, I.; Yamamura, K.; Nonoguchi, H.; Hirotsu, K.; Higuchi, T. *J. Am. Chem. Soc.* **1984**, *106*, 2621-2625.
5. (a) Ferguson, S. B.; Seward, E. M.; Diederich, F.; Sanford, E. M.; Chou, A.; Inocencio-Szweda, P.; Knobler, C. B. *J. Org. Chem.* **1988**, *53*, 5593-5595. (b) Smithrud, D. B.; Sanford, E. M.; Chao, I.; Ferguson, S. B.; Carcanague, D. R.; Evanseck, J. D.; Houk, K. N.; Diederich, F. *Pure & Appl. Chem.* **1990**, *62*, 2227-2236. (c) Smithrud, D. B.; Wyman, T. B.; Diederich, F. *J. Am. Chem. Soc.* **1991**, *113*, 5420-5426.
6. (a) Berscheid, R.; Lűer, I.; Seel, C.; Vűgtle, F. In *Supramolecular Chemistry*; V. Balzani and L. De Cola, Ed.; Kluwer Academic Publishers: The Netherlands, 1992; pp 71-86. (b) Seel, C.; Vűgtle, F. *Angew. Chem. Int. Ed. Engl.* **1991**, *30*, 442-444. (c) Ebmeyer, F.; Vűgtle, F. In *Bioorganic Chemistry Frontiers* Springer-Verlag: Berlin, 1990; Vol. 1; pp 145-158.

7. (a) Goodnow, T. T.; Reddington, M. V.; Stoddart, J. F.; Kaifer, A. E. *J. Am. Chem. Soc.* **1991**, *113*, 4335-4337. (b) Bernardo, A. R.; Stoddart, J. F.; Kaifer, A. E. *J. Am. Chem. Soc.* **1992**, *114*, 10624-10631.
8. (a) Lehn, J.-M. *Angew. Chem. Int. Ed. Engl.* **1988**, *27*, 89-112. (b) Dhaenens, M.; Lacombe, L.; Lehn, J.-M.; Vigneron, J.-P. *J. Chem. Soc., Chem. Commun.* **1984**, 1097-1099. (c) Dhaenens, M.; Lehn, J.-M.; Fernandez, M.-J. *New J. Chem.* **1991**, *15*, 873-877.
9. Whitlock, B. J.; Whitlock, H. W. *J. Am. Chem. Soc.* **1990**, *112*, 3910-3815.
10. (a) Schneider, H.-J.; Schiestel, T.; Zimmermann, P. *J. Am. Chem. Soc.* **1992**, *114*, 7698-7703. (b) Schneider, H.-J.; Güttes, D.; Scheider, U. *Angew. Chem. Int. Ed. Engl.* **1986**, *25*, 647-649. (c) Schneider, H.-J. *Angew. Chem. Int. Ed. Engl.* **1991**, *30*, 1417-1436. (d) Schneider, H.-J.; Blatter, T. *Angew. Chem. Int. Ed. Engl.* **1988**, *27*, 1163-1164. (e) Schneider, H.-J.; Blatter, T.; Simova, S.; Theis, I. *J. Chem. Soc., Chem. Commun.* **1989**, 580-581. (f) Schneider, H.-J.; Philippi, K.; Pöhlmann, J. *Angew. Chem. Int. Ed. Engl.* **1984**, *23*, 908-910. (g) Schneider, H.-J.; Theis, I. *Angew. Chem. Int. Ed. Engl.* **1989**, *28*, 753-754. (h) Schneider, H.-J.; Kramer, R.; Theis, I.; Zhou, M. *J. Chem. Soc., Chem. Commun.* **1990**, 276-278.
11. Webb, T. H.; Suh, H.; Wilcox, C. S. *J. Am. Chem. Soc.* **1991**, *113*, 8554-8555.
12. (a) Araki, K.; Shimizu, H.; Shinkai, S. *Chem. Lett.* **1993**, 205-208. Ikeda, A.; (b) Shinkai, S. *Tetrahedron Lett.* **1992**, *33*, 7385-7388. (c) Murakami, Y.; Kikuchi, J.; Ohno, T.; Hirayama, T. *Chem. Lett.* **1989**, 881-884. (d) Shinmyozu, T.; Sakai, T.; Uno, E.; Inazu, T. *J. Org. Chem.* **1985**, *50*, 1959-1963. (e) Hisaeda, Y.; Ihara, T.; Ohno, T.; Murakami, Y. *Tetrahedron Lett.* **1990**, *31*, 1027-1030. (f)

Murakami, Y.; Kikuchi, J.; Ohno, T.; Hirayama, T.; Hisaeda, Y.; Nishimura, H.; Snyder, J. P.; Steliou, K. *J. Am. Chem. Soc.* **1991**, *113*, 8229-8242.

13. (a) Petti, M. A.; Shepodd, T. J.; Barrans, R. E., Jr.; Dougherty, D. A. *J. Am. Chem. Soc.* **1988**, *110*, 6825-6840. (b) Kearney, P. C.; Mizoue, L. S.; Kumpf, R. A.; Forman, J. E.; McCurdy, A.; Dougherty, D. A. *J. Am. Chem. Soc.* **1993**, *115*, 9907-9919.
14. In aqueous media, hydrogen bonding generally has not been effectively utilized in synthetic receptors (except see: Rotello, V. M.; Viani, E. Z.; Deslongchamps, G.; Murray, B. A.; Rebek, J., Jr. *J. Am. Chem. Soc.* **1993**, *115*, 797-798). It has been well utilized in organic media.<sup>15</sup>
15. (a) Nowick, J. S.; Ballester, P.; Ebmeyer, F.; Rebek, J., Jr. *J. Am. Chem. Soc.* **1990**, *112*, 8902-8906. (b) Rebek, J., Jr. *Angew. Chem. Int. Ed. Engl.* **1990**, *29*, 245-255. (c) Rebek, J., Jr. *Science* **1987**, *235*, 1478-1484. Fan, E.; Van Arman, S. A.; (d) Kincaid, S.; Hamilton, A. D. *J. Am. Chem. Soc.* **1993**, *115*, 369-370. (e) Muehldorf, A. V.; Van Engen, D.; Warner, J. C.; Hamilton, A. D. *J. Am. Chem. Soc.* **1988**, *110*, 6561-6562. (f) Yoon, S. S.; Still, W. C. *J. Am. Chem. Soc.* **1993**, *115*, 823-824. (g) Wang, X.; Erickson, S. D.; Iimori, T.; Still, W. C. *J. Am. Chem. Soc.* **1992**, *114*, 4128-4137. (h) Hong, J.-I.; Namgoong, S. K.; Bernardi, A.; Still, W. C. *J. Am. Chem. Soc.* **1991**, *113*, 5111-5112.
16. Forman, J. E.; Barrans, R. E., Jr.; Dougherty, D. A., manuscript in preparation.
17. Forman, J. E.; Marsh, R. E.; Schaefer, W. P.; Dougherty, D. A. *Acta Cryst.* **1993**, *B49*, 892-896.
18. (a) Sunner, J.; Nishizawa, K.; Kebarle, P. *J. Phys. Chem.* **1981**, *85*, 1814-1820. (b) Taft, R. W.; Anvia, F.; Gal, J.-F.; Walsh, S.; Capon, M.; Holmes, M. C.;

- Hosn, K.; Oloumi, G.; Vasanwala, R.; Yazdani, S. *Pure & Appl. Chem.* **1990**, *62*, 17-23. (c) Deakyne, C. A.; Meot-Ner (Mautner), M. *J. Am. Chem. Soc.* **1985**, *107*, 474-479. (d) Meot-Ner (Mautner), M.; Deakyne, C. A. *J. Am. Chem. Soc.* **1985**, *107*, 469-474.
19. (a) Canceill, J.; Lacombe, L.; Collet, A. *J. Chem. Soc., Chem. Commun.* **1987**, 219-221. (b) Garel, L.; Lozach, B.; Dutasta, J. P.; Collet, A. *J. Am. Chem. Soc.* **1993**, *115*, 11652-11653. (c) Garel, L.; Dutasta, J. P.; Collet, A. *Angew. Chem. Int. Ed. Engl.* **1993**, *32*, 1169-1171. (d) Collet, A. *Tetrahedron* **1987**, *43*, 5723-5759. (e) Collet, A.; Dutasta, J. P.; Lozach, B.; Canceill, J. *Topics in Current Chemistry* **1993**, *165*, 104-129.
20. (a) Burley, S. K.; Petsko, G. A. *FEBS Lett.* **1986**, *203*, 139-143. (b) Burley, S. K.; Petsko, G. A. *Weakly Polar Interactions in Proteins*; Academic Press, Inc.: 1988; Vol. 39, pp 125-189.
21. (a) Stauffer, D. A.; Barrans, R. E., Jr.; Dougherty, D. A. *Angew. Chem. Int. Ed. Engl.* **1990**, *29*, 915-918. (b) McCurdy, A.; Jimenez, L.; Stauffer, D. A.; Dougherty, D. A. *J. Am. Chem. Soc.* **1992**, *114*, 10314-10321.
22. Stauffer, D. A.; Dougherty, D. A. *Tetrahedron Lett.* **1988**, *29*, 6039-6042.
23. Acetylcholine (ACh) binds to esterases with  $K_d$  of  $\sim 1$  mM.<sup>24</sup> At the McPC603 binding site,  $K_d$  is  $\sim 10$   $\mu$ M for phosphocholine, and 1 mM for choline.<sup>25</sup> Binding to the ACh receptors is complex, involving two positively cooperative, nonequivalent sites, and at least four functional states in the nicotinic receptor. The value of  $K_d$  obtained depends on the type of measurement being made; for further discussion see Ochoa, E. L. M.; Chattopadhyay, A.; McNamee, M. G. *Cell. Mol. Neurobiol.* **1989**, *9*, 141-178.

- Karlin, A. In *The Cell Surface and Neuronal Function*; Cotman, C. W.; Poste, G.; Nicolson, G. L., Eds.; Elsevier/North Holland Biomedical: Amsterdam, 1980; pp 191-260.
24. (a) Hasan, F. B.; Cohen, S. G.; Cohen, J. B. *J. Biol. Chem.* 1980, 255, 3898-3904.  
(b) Hasan, F. B.; Elkind, J. L.; Cohen, S. G.; Cohen, J. B. *J. Biol. Chem.* 1981, 256, 7781-7785. (c) Cohen, S. G.; Lieberman, D. L.; Hasan, F. B.; Cohen, J. B. *J. Biol. Chem.* 1982, 257, 14087-14092.
25. (a) Satow, Y.; Cohen, G. H.; Padlan, E. A.; Davies, D. R. *J. Mol. Biol.* 1986, 190, 593-604. (b) Gettins, P.; Potter, M.; Leatherbarrow, R. J.; Dwek, R. A. *Biochemistry* 1982, 21, 4927-4931. (c) Getzoff, E. D.; Tainer, J. A.; Lerner, R. A.; Geysen, H. M. *Adv. Immunol.* 1988, 43, 1-98. (d) Schultz, P. G. *Science* 1988, 240, 426-433.
26. (a) Abramson, S. M.; Li, Y.; Culver, P.; Taylor, P. *J. Biol. Chem.* 1989, 264, 12666-12672. (b) Cohen, J. B.; Sharp, S. D.; Liu, W. S. *J. Biol. Chem.* 1991, 266, 23354-23364. (c) Dennis, M.; Giraudat, J.; Kotzyba-Hibert, F.; Goeldner, M.; Hirth, C.; Chang, J. Y.; Lazure, C.; Chrétien, M.; Changeux, J. P. *Biochemistry* 1988, 27, 2346-2357. (d) Galzi, J. L.; Revah, F.; Black, D.; Goeldner, M.; Hirth, C.; Changeux, J. P. *J. Biol. Chem.* 1990, 65, 10430-10437. (e) Kao, P. N.; Dwork, A. J.; Kaldany, R-R. J.; Silver, M. L.; Wideman, J.; Stein, S.; Karlin, A. *J. Biol. Chem.* 1984, 259, 11662-11665. (f) Pedersen, S. E.; Cohen, J. B. *Proc. Natl. Acad. Sci.* 1990, 87, 2785-2789.
27. (a) Chaturvedi, V.; Donnelly-Roberts, D. L.; Lentz, T. L. *Biochemistry* 1992, 31, 1370-1375. (b) Chaturvedi, V.; Donnelly-Roberts, D. L.; Lentz, T. L. *Biochemistry* 1993, 32, 9570-9576.



28. Fraenkel, Y.; Gershoni, J. M.; Navon, G. *FEBS Lett.* 1991, 291, 225-228.
29. Novotny, J.; Bruccoleri, R. E.; Saul, F. A. *Biochemistry* 1989, 28, 4735-4749.
30. Dougherty, D. A.; Stauffer, D. A. *Science* 1990, 250, 1558-1560.
31. Sussman, J. L.; Harel, M.; Frolow, F.; Oefner, C.; Goldman, A.; Toker, L.; Silman, I. *Science* 1991, 253, 872-879.
32. Trump-Kallmeyer, S.; Hoflack, J.; Bruinvels, A.; Hibert, M. *J. Med. Chem.* 1992, 35, 3448-3462.
33. (a) Heginbotham, L.; MacKinnon, R. *Neutron* 1992, 8, 483-491. (b) MacKinnon, R.; Yellen, G. *Science* 1990, 250, 276-279.
34. Kumpf, R. A.; Dougherty, D. A. *Science* 1993, 261, 1708-1710.
35. (a) Paudler, W. W.; Jovanovic, M. V. *Org. Magn. Reson.* 1982, 19, 192-195. (b) Speranza, M. In *Advances in Heterocyclic Chemistry*; Academic Press, Inc.: 1986, Vol. 40, pp 25-104.
36. (a) Tarrago, G.; Marzin, C.; Najimi, O.; Pellegrin, V. *J. Org. Chem.* 1990, 55, 420-425. (b) Griffing, J. M.; Salisbury, L. F. *J. Am. Chem. Soc.* 1948, 70, 3416-3419.
37. Diederich, F. *Angew. Chem. Int. Ed. Engl.* 1988, 27, 362-386.
38. Barrans, R. E., Jr.; Dougherty, D. A. *Supramolecular Chemistry*, in press.
39. The binding energies calculated are strictly  $\Delta E$  values, but may be reasonably compared to  $\Delta H$  values. Assuming  $\Delta S^\circ$  contributions to binding are

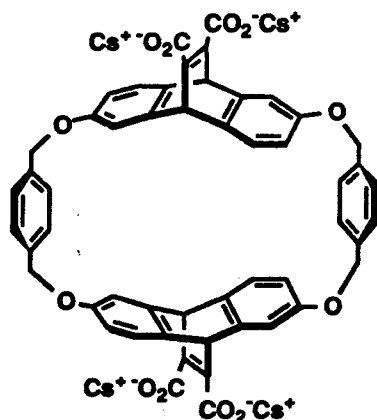
relatively constant for closely related host/guest pairs, trends in  $-\Delta G^\circ$  values can be directly related to the calculations.

**Chapter 2: The Aqueous Binding of Guanidinium Guests to a Cyclophane  
Receptor.**

## Introduction

In 1981, Kebarle observed the gas-phase binding of  $K^+$  to benzene, and determined a surprisingly large enthalpy of binding, 19 kcal/mol.<sup>1</sup> In the complex, the ion is positioned directly above the center of the ring. Since then, many studies have demonstrated that the face of a benzene ring possesses a substantial partial negative charge, and that it can bind quite strongly to cationic structures, both in the gas phase and in solution. We refer to this effect as the "cation- $\pi$  interaction." In our own work, we have been especially interested in understanding the nature of this effect, and in quantifying its magnitude in solution. Our studies of molecular recognition by cyclophane hosts have provided some of the most compelling evidence for the importance of the cation- $\pi$  interaction in aqueous binding (see Chapter 1).

In our early work on cation- $\pi$  binding, we focused primarily on the complexation of tetraalkylammonium and alkylated iminium (alkylated quinolines, isoquinolines, pyridines, and related structures) guests with the host P, 1.<sup>2</sup> The important neurotransmitter acetylcholine (ACh) is a quaternary ammonium compound, and we have shown that it binds tightly to host P ( $-\Delta G^\circ = 6.2$  in aqueous borate buffer).<sup>3</sup> This observation led to our unconventional proposal that the aromatic rings of Tyr, Trp, and Phe contribute significantly to ACh binding at biological receptors through cation- $\pi$  interactions.<sup>3</sup> Subsequent studies on natural binding sites for ACh provided support for our prediction,<sup>4</sup> and it is now generally accepted that the binding sites of both the enzyme acetylcholine esterase (AChE) and the nicotinic acetylcholine receptor (nAChR) are rich in aromatic residues and that cation- $\pi$  interactions are involved in ACh binding.

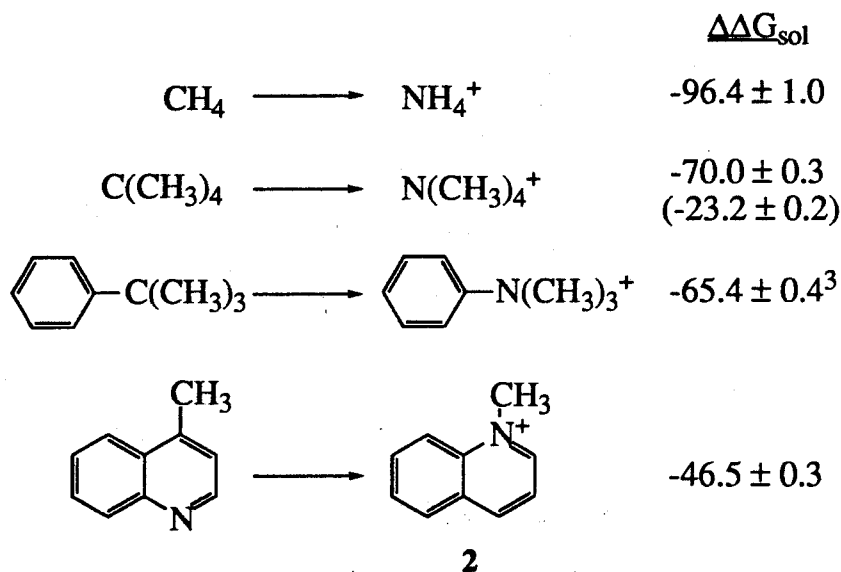


Studies of biological receptors have also provided evidence that the quaternary ammonium ion of ACh can be replaced by other cationic structures. For example, the X-ray structure of fasciculin 1, a potent AChE inhibitor from green mamba snake venom, revealed several well-ordered lysine and arginine residues that are located at relatively exposed positions on the protein.<sup>5</sup> It has been postulated that binding of the inhibitor involves interactions between the cationic side chains of these amino acids and the aromatic residues of the enzyme. In addition, a variety of curaremimetic neurotoxins, such as bungarotoxin and erabutoxin, all contain a highly conserved arginine.<sup>6</sup> These toxins recognize and block the nAChR with high affinity and selectivity. It is believed that the arginine side chain represents the counterpart of the head group of ACh.

Given that the protonated amine group of lysine and the guanidinium group of arginine are both capable of participating in cation- $\pi$  interactions in natural receptors, it seemed logical to investigate whether these types of compounds bind to the host P. Earlier work in the group had shown that protonated amine ( $\text{RNH}_3^+$ ) guests were not measurably bound by host P in aqueous solution.<sup>2c</sup>

We assumed that this was because the much greater water solubility of these ions reduced the hydrophobic component of binding. This hypothesis was consistent with the computational studies described below.

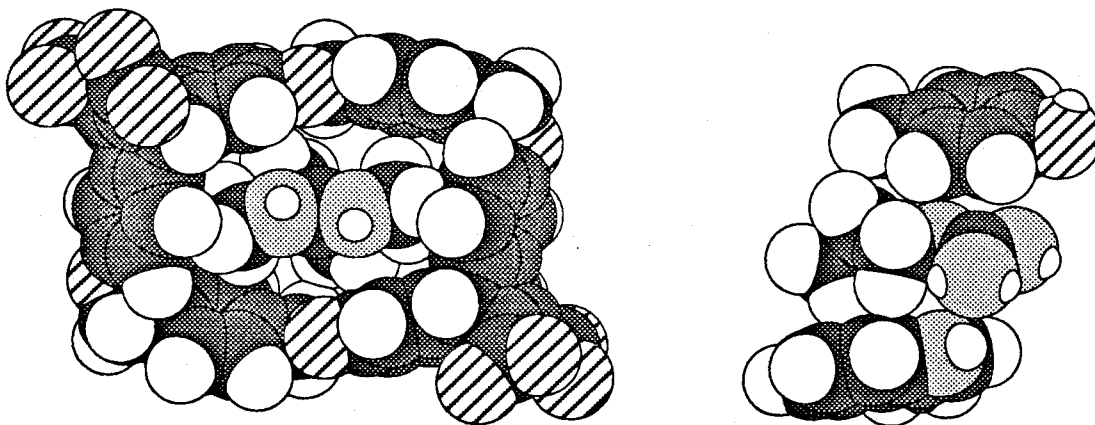
Using statistical perturbation theory (SPT) and Monte Carlo (MC) simulations, we found that relative to a reference hydrocarbon, a protonated amine is indeed much better solvated than a tetraalkylammonium (see Figure 2.1).<sup>3,7</sup> An alternative way of expressing this is to note that the aqueous solvation energy of  $\text{NH}_4^+$  is approximately 30 kcal/mol larger than that of  $\text{N}(\text{CH}_3)_4^+$ . These results implied that with the host P, the cation- $\pi$  interaction cannot overcome the desolvation penalty for protonated amines.



**Figure 2.1.** Calculated relative aqueous (chloroform) solvation energies (kcal/mol) for cations and analogous neutral compounds.

We then turned our attention toward the binding of guanidinium ions. Alkylated guanidines are very strong bases,  $\text{pK}_a = 13\text{-}14$ , so they are protonated in the pH  $\sim 9$  borate buffer we use in our binding studies. CPK models

suggested that the flat, delocalized guanidinium cation would be especially well-suited to the rhomboid form of host P (see Figure 2.2). In the rhomboid conformation, the aromatic rings of the host can stack on either side of a guanidinium guest. A similar type of arrangement has been observed in the crystal<sup>8</sup> and solution<sup>9</sup> structure of the  $\alpha$ -amylase inhibitor Tendamistat, where an arginine residue is sandwiched between the aromatic rings of a tryptophan and a tyrosine (see Figure 2.2). Furthermore, recent studies of the interaction between the side chains of aromatic amino acids and the side chain of arginine in protein structures have established that the guanidinium group prefers to stack directly over the center of the ring.<sup>10</sup> This stacked geometry is distinct from the other reasonable alternative, a T-shaped interaction in which the guanidinium NH points towards the face of the phenyl ring in a manner suggestive of a hydrogen bond.



**Figure 2.2.** A guanidinium ion stacked between aromatic rings. **Left:** Host P in the rhomboid conformation found in the crystal structure of the tetraester<sup>11</sup> with guanidinium guest 3 docked into a viable binding position. **Right:** The side chains of the residues Trp18-Arg19-Tyr20 in the protein Tendamistat, taken from reference 9.

## Results and Discussion

**Binding Studies.** A number of guanidinium guests were synthesized, and their binding affinities to host P in deuterated borate buffer (referred to as borate-d) were determined. The binding studies were conducted using the NMR methods that were described previously in Chapter 1. The data are shown in Figure 2.3. We estimate that the error bars for the  $\Delta G^\circ$  values reported are  $\pm 0.2$  kcal/mol.

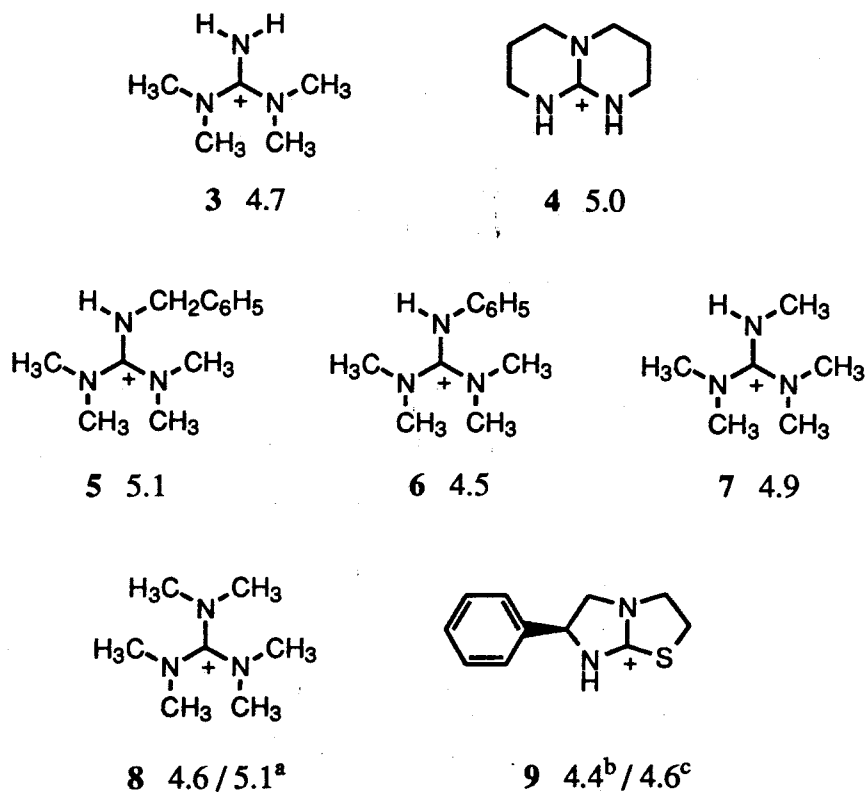


Figure 2.3.  $-\Delta G^\circ$  (kcal/mol) in borate-d for guanidinium guests binding to host P.

<sup>a</sup> The two values are for the two enantiomers of the guest.

<sup>b</sup> *R,R,R,R*-host.

<sup>c</sup> *S,S,S,S*-host.

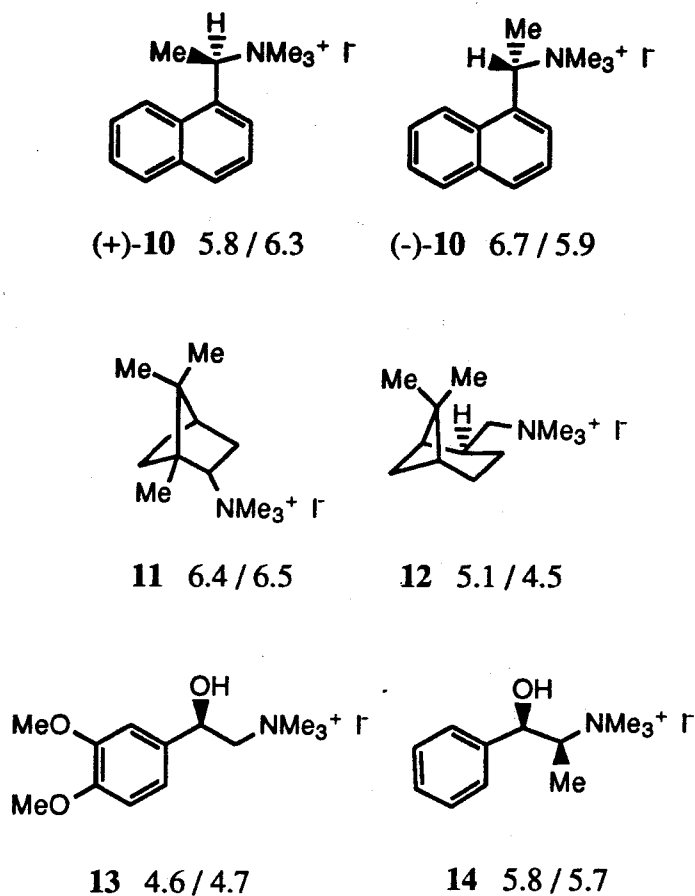


The binding affinities of the guanidinium guests (4-5 kcal/mol) are somewhat lower than those of other cationic guests such as the iminium and tetraalkylammonium compounds, whose binding energies in borate-d are in the 6-8 kcal/mol range. (See Chapter 1 for a more detailed discussion of positively-charged guests binding to host P.) This probably reflects the high water solubility of the guanidinium guests. We measured the solubility of **4** in borate buffer and found it to be approximately 4.8 M. For comparison, the solubility of a typical iminium guest N-methylquinolinium, **2**, is 0.52 M in borate-d.<sup>2c</sup> As was seen with the protonated amines, some alkylation was necessary to achieve measurable binding. Thus tetramethylguanidinium, **3**, and related structures were well bound, whereas arginine (not pictured) was not measurably bound. We believe that it is both the small size and the high water solubility of molecules such as arginine which limit their binding to the macrocycle.

Levamisole hydrochloride, **9**, has been included in this list, although strictly it is an imidazo[2,1-b]thiazolium rather than a guanidinium compound. Molecule **9** is an effective anthelmintic drug, and has been the subject of recent attention because of its immunomodulatory and anticancer activities.<sup>12</sup> We became interested in **9** because it resembles the guanidinium structures and because it contains a chiral center.

The enantioselective binding of host P has been examined previously,<sup>2c</sup> and the binding constants for a number of chiral guests are shown in Figure 2.4. These results demonstrate that host P displays moderate discrimination between the enantiomers of some guests. We wished to see whether **9** was also bound preferentially by one of the enantiomers of the host. Therefore, the binding constants for this guest were measured with both the *R,R,R,R* and *S,S,S,S* absolute configurations of the host. The  $\Delta G^\circ$  values for **9** suggest that the guest is better bound by the *S,S,S,S*-host, but the difference in binding constants falls

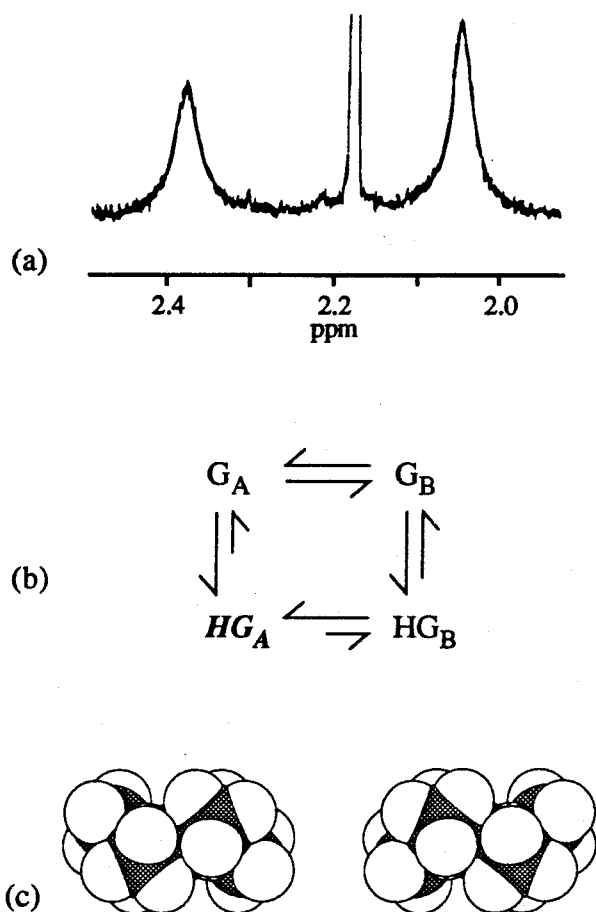
within the error bars. Significant enantioselectivity was observed, however, with the conformational enantiomers of the guanidinium guest **8**. This is described in detail in the next section.



**Figure 2.4.**  $-\Delta G^\circ$  (kcal/mol) for enantiomerically pure guests binding to host P in borate-d. The numbers are reported for (*R,R,R,R*-host/*S,S,S,S*-host). Values are accurate to  $\pm 0.2$  kcal/mol.

**Hexamethylguanidinium.** Hexamethylguanidinium, **8**, proved to be a particularly interesting guest. At room temperature, the  $^1\text{H}$  NMR spectrum of **8** in borate consists of a single resonance. In the presence of host P, the singlet

splits into two peaks; this is illustrated in Figure 2.5a. Raising the temperature of the solution by approximately 15° causes the peaks to coalesce, and a singlet is once again observed.



**Figure 2.5.** (a) NMR resonances of hexamethylguanidinium, **8**, when binding to host P.  $[Guest]_0 = 0.16$  mM;  $[Host]_0 = 0.24$  mM in borate buffer. The peak at 2.19 ppm (3,3-dimethylglutarate, internal standard) has been truncated for clarity. (b) Equilibrium relationships between the enantiomers of **8** ( $G_A$  and  $G_B$ ) and their complexes with P ( $HG_A$  and  $HG_B$ ). (c) CPK models of the two enantiomers of **8** based on calculated structures.

Molecular models and computational modelling<sup>13</sup> indicate that steric crowding between the methyl groups of **8** forces the molecule to adopt a nonplanar conformation. X-ray crystallography<sup>14</sup> has shown that **8** possesses a propeller-like structure which is  $D_3$ -symmetric, and therefore chiral. The energy barriers to rotation about the carbon-nitrogen bonds have been measured for a number of substituted guanidinium salts including **6** and related molecules.<sup>15</sup> Based on these studies, one would expect a barrier of rotation, and thus racemization, to be in the range of 14-16 kcal/mol for **8**. At room temperature, the rate of racemization is fast ( $10$ - $100$  sec<sup>-1</sup>), so isolation of the individual enantiomers is not possible. On the NMR time-scale, however, the rate of interconversion is slow, and when placed in an appropriately chiral environment, separate resonances for the two enantiomers are observed. In our case, host **P** provides the chiral environment which produces the two NMR signals.

Host **P**, however, acts as more than simply a chiral shift reagent. The truly remarkable feature of the NMR spectrum shown in Figure 2.5a is that the two singlets are *unequal* in intensity. This is explained by preferential binding of the host to one of the enantiomers of **8**. As shown in Figure 2.5b, this shifts the equilibrium away from a 50:50 mixture of enantiomers and causes one of the signals to be significantly larger than the other.

To determine the magnitude of the enantioselectivity ( $\Delta\Delta G^\circ$ ), we conducted a binding study of **8**, titrating a solution of the host with a solution of the guest. As was mentioned previously in Chapter 1, our host-guest systems show only time-averaged signals of complexed and uncomplexed guest. Therefore, each enantiomer displayed only one NMR signal. At several different concentrations of host and guest, we carefully integrated the two peaks of **8**. This was only carried out for spectra in which the peaks were fully resolved and were large

enough to be easily integrated. At each concentration, the weighted average of the chemical shifts of the two enantiomers was calculated, and these data were fit to a single  $K_a$  using the least-squares fitting program MULTIFIT.<sup>16</sup> Knowing this average  $K_a$  allowed us to obtain the percentage of free guest at a particular concentration. We assumed that neither enantiomer was preferred in the uncomplexed form, so the free guest consisted of a 50:50 mixture of enantiomers. From this information (the percentage of each free enantiomer) and the measured peak areas [the percentage of each enantiomer (free + bound)], we were able to calculate the percentage of each bound enantiomer. Their ratio then yielded  $\Delta\Delta G^\circ$ . The  $\Delta G^\circ$  values for the two enantiomers could then be obtained because both the average  $K_a$  and  $\Delta\Delta G^\circ$  were known.

The data analysis indicated that host P binds one of the enantiomers approximately 500 cal/mol more tightly than the other. The magnitude of the selectivity is comparable to that observed with other chiral guests (see Figure 2.4). At the present time, we are unable to determine which is the preferred enantiomer.

Both the X-ray crystallographic data<sup>13</sup> and calculations<sup>12</sup> indicate that the extent of twisting in **8** is near 30°. Figure 2.5c shows space-filling models of the enantiomers which illustrate the similarity of the structures. We consider it quite impressive that host P is able to differentiate between the two conformations. The macrocycle possesses  $C_2$  symmetry in the rhomboid conformation and is also twisted in a sense. Perhaps it is this feature which allows host P to sense the subtle differences between the enantiomers of **8**.

## Conclusions

We have synthesized a number of guanidinium compounds, and examined their binding to the host P in aqueous solution. These molecules represent a new class of cationic guests for our receptor. Although the amino acid arginine did not show measureable binding, several alkylated guanidinium compounds exhibited fairly large binding affinities, especially considering the high water solubility of these guests. In addition, the host was able to discriminate between the two enantiomers of hexamethylguanidinium, a nonplanar molecule with  $D_3$  symmetry.

In protein structures, arginine has been shown to interact frequently with aromatic residues. The preferred geometry has the guanidinium ion of the arginine stacked in a parallel fashion directly over the face of the aromatic ring. This cation- $\pi$  interaction is analogous to that seen in the binding of guanidinium guests by the host P. Thus, we believe that our studies have implications for designing artificial binding sites for arginine. This is explored more fully in the following chapter.

## Experimental Section

Guests 3 and 9 were purchased from commercial sources. Guests 4-8 were prepared according to literature procedures.<sup>17</sup> Enantiomerically pure host P, 1, was synthesized as described previously in Chapter 1.

All binding studies were performed on a Bruker AM-500 NMR spectrometer. Spectra from the binding studies were referenced to an internal standard of 3,3-dimethylglutarate (DMG  $\delta$  1.09). All host solutions were prepared in borate-d buffer as detailed previously in Chapter 1. The host solutions were quantified by NMR integrations against a primary standard solution of DMG in borate-d. Guest solution concentrations were determined either by weight of solute or through NMR integrations against DMG. All binding studies were performed by adding aliquots of the guest solutions to an NMR tube containing a solution of host that was initially approximately 250  $\mu$ M. The binding data were fit to an appropriate association constant using the nonlinear least-squares fitting program, MULTIFIT. For the integration of the two enantiomer resonances of guest 8, a pulse delay of 10 sec ( $5 \cdot T_1$ ) was included in the NMR acquisition parameters to ensure accurate peak areas.

**References**

1. Sunner, J.; Nishizawa, K.; Kebarle, P. *J. Phys. Chem.* **1981**, *85*, 1814-1820.
2. (a) Shepodd, T. J.; Petti, M. A.; Dougherty, D. A. *J. Am. Chem. Soc.* **1986**, *108*, 6085-6087. (b) Shepodd, T. J.; Petti, M. A.; Dougherty, D. A. *J. Am. Chem. Soc.* **1988**, *110*, 1983-1985. (c) Petti, M. A.; Shepodd, T. J.; Barrans, R. E., Jr.; Dougherty, D. A. *J. Am. Chem. Soc.* **1988**, *110*, 6825-6840.
3. Dougherty, D. A.; Stauffer, D. A. *Science* **1990**, *250*, 1558-1560.
4. (a) Sussman, J. L.; Harel, M.; Frolow, F.; Oefner, C.; Goldman, A.; Toker, L.; Silman, I. *Science* **1991**, *253*, 872-879. (b) Harel, M.; Schalk, I.; Ehret-Sabatier, L.; Bouet, F.; Goeldner, M.; Hirth, C.; Axelsen, P. H.; Silman, I.; Sussman, J. L. *Proc. Natl. Acad. Sci.* **1993**, *90*, 9031-9035. (c) Changeux, J.-P.; Devillers-Thiéry, A.; Galzi, J.-L.; Bertrand, D. *TiPS* **1992**, *13*, 299-301.
5. le Du, M. H.; Marchot, P.; Bougis, P. E.; Fontecilla-Camps, J. C. *J. Biol. Chem.* **1992**, *267*, 22122-22130.
6. (a) Lentz, T. L. *Biochemistry* **1991**, *30*, 10949-10957. (b) Pillet, L.; Trémeau, O.; Ducancel, F.; Drevet, P.; Zinn-Justin, S.; Pinkasfeld, S.; Boulain, J.-C.; Ménez, A. *J. Biol. Chem.* **1993**, *268*, 909-916.
7. Kearney, P. C.; Mizoue, L. S.; Kumpf, R. A.; Forman, J. E.; McCurdy, A.; Dougherty, D. A. *J. Am. Chem. Soc.* **1993**, *115*, 9907-9919.
8. Pflugrath, J. W.; Wiegand, G.; Huber, R. *J. Mol. Biol.* **1986**, *189*, 383-386.
9. Kline, A. D.; Braun, W.; Wüthrich, K. *J. Mol. Biol.* **1986**, *189*, 377-382.



10. (a) Flocco, M. M.; Mowbray, S. L. *J. Mol. Biol.* **1994**, *235*, 709-717. (b) Mitchell, J. B. O.; Nandi, C. L.; McDonald, I. K.; Thornton, J. M. *J. Mol. Biol.* **1994**, *239*, 315-331. (c) Nandi, C. L.; Singh, J.; Thornton, J. M. *Protein Eng.* **1993**, *6*, 247-259.
11. Forman, J. E.; Marsh, R. E.; Schaefer, W. P.; Dougherty, D. A. *Acta Cryst.* **1993**, *B49*, 892-896.
12. Kovach, J. S.; Svingen, P. A.; Schaid, D. J. *J. Nat'l Cancer Inst.* **1992**, *84*, 515-519.
13. (a) We have calculated the AM1 structure of **40**, and found that it agrees very well with the x-ray structure.<sup>12</sup> (b) Gobbi, A.; Frenking, G. *J. Am. Chem. Soc.* **1993**, *115*, 2362-2372.
14. Boese, R.; Bläser, D.; Petz, W. *Z. Naturforsch.* **1988**, *43b*, 945-948.
15. (a) Kessler, H.; Leibfritz, D. *Tetrahedron Lett.* **1969**, *6*, 427-430. (b) Kessler, H.; Leibfritz, D. *Chem. Ber.* **1971**, *104*, 2158-2169. (c) Sapse, A. M.; Snyder, G.; Santoro, A. V. *J. Phys. Chem.* **1981**, *85*, 662-665. (d) Rabiller, C.; Ricolleau, G.; Martin, M. L.; Martin, G. J. *Nouv. J. Chim.* **1980**, *4*, 35-42. (d) Santoro, A. V.; Mickevicius, G. *J. Org. Chem.* **1979**, *44*, 117-120.
16. MULTIFIT differs from most fitting procedures in that chemical shift changes from *all* protons are considered together in a single least-squares fit. This maximizes the ratio of observations to fit parameters, thereby producing an optimal fit. Full details are given in the following: Barrans, R. E., Jr. Ph.D. Thesis, California Institute of Technology, 1992. Barrans, R. E., Jr.; Dougherty, D. A. *Supramolecular Chemistry*, in press.

17. Guest 4: Schmidtchen, F. P. *Chem. Ber.* 1980, 113, 2175-2182. 5, 6:  
Bredereck, H.; Bredereck, K. *Chem. Ber.* 1961, 94, 2278-2295. 7: Angyal, S.  
J.; Warburton, W. K. J. *Chem. Soc.* 1951, 2492-2494. 8: Lecher, H.; Graf, F.  
*Chem. Ber.* 1923, 56, 1326-1330.

**Chapter 3: Progress Toward the Synthesis of Macrocycles with Appended  
Amide or Carboxylate Groups**

## Introduction

The ability of aromatic rings to participate in electrostatic interactions has been the subject of considerable attention recently. The cation- $\pi$  effect, which involves stabilization of a positive charge by the electron-rich face of an aromatic ring, is a dramatic example of this kind of phenomenon. Many studies, including our own, have shown that this effect can provide a powerful force for molecular recognition (see Chapter 1 for further discussion).

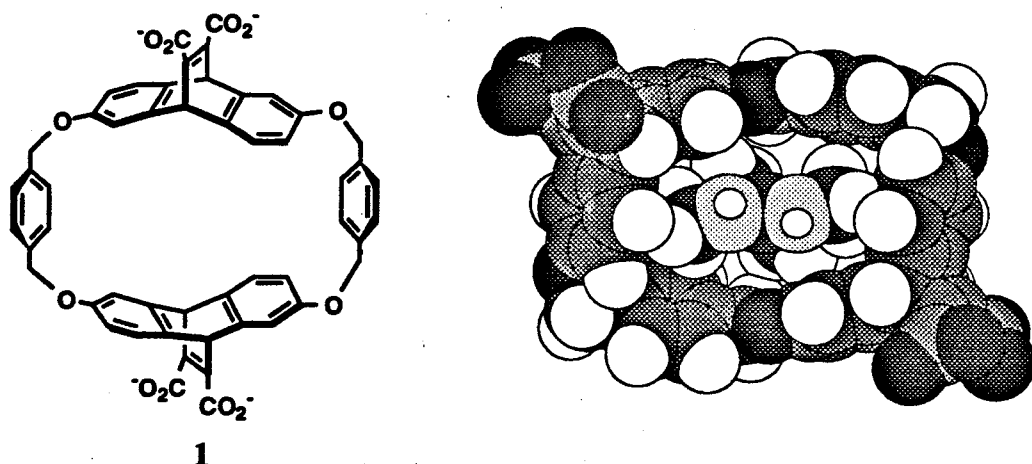
Given that an aromatic ring can bind quite strongly to cations, it should not be surprising that it also binds effectively to partial positive charges. Recent gas-phase studies have shown that water<sup>1</sup> and ammonia<sup>2</sup> bind to benzene with interaction energies of 1.8 and 1.4 kcal/mol respectively. In both complexes, the  $\pi$ -cloud of the benzene ring acts as a hydrogen-bond acceptor.

Perutz made an early observation of this type of hydrogen-bonding interaction in the crystal structure of a hemoglobin-drug complex.<sup>3</sup> He noted that the amide hydrogens of an asparagine residue of the hemoglobin pointed toward the face of an aromatic ring of the bound drug. This observation prompted Burley and Petsko to conduct a survey of then available protein crystal structures to search for similar interactions.<sup>4</sup> These authors concluded that there was a general tendency for the positively-charged or  $\delta(+)$  side chains of lysine, arginine, asparagine, glutamine, and histidine to interact with the center of an aromatic ring in a manner suggestive of a hydrogen bond. They referred to the effect as the "amino-aromatic interaction." The strength of this interaction has since been calculated to be approximately 3 kcal/mol, which is about half as strong as a conventional hydrogen bond.<sup>5</sup>

More recent studies of the geometries of amino-aromatic interactions in protein crystal structures have questioned the conclusions drawn by Burley and Petsko. A study by Thornton and coworkers focused specifically on  $sp^2$  hybridized nitrogen-bearing groups that lie above the aromatic rings of phenylalanine and tyrosine.<sup>6</sup> They found that while amino-aromatic hydrogen bonds do occur, they are extremely rare. In most instances, the preferred conformation is one in which the  $sp^2$  nitrogen atom is approximately coplanar with the aromatic ring.

A different study conducted by Flocco and Mowbray showed that such stacked arrangements are clearly favored for arginine-aromatic interactions in proteins.<sup>7</sup> This cation- $\pi$ -type of interaction has been noted in several recent crystal structures, including the periplasmic ribose-binding protein of *E. coli*,<sup>8</sup> P2 myelin,<sup>9</sup> and cellobiohydrolase II.<sup>10</sup> In each case, the guanidinium moiety of an arginine residue is parallel stacked directly over the center of an aromatic side chain. Similarly, computational studies of the guanidinium ion-benzene complex in water indicate that a stacked geometry is the lowest energy structure.<sup>11</sup>

In Chapter 2, we demonstrated that the host P, 1, bound various alkylated guanidinium guests with binding energies of 4-5 kcal/mol in aqueous borate buffer. Arginine was not bound by our host, presumably because of its small size and high water solubility. In our host-guest complexes, the flat guanidinium cation intercalates between the aromatic rings of the host to maximize hydrophobic and cation- $\pi$  interactions (see Figure 3.1). This type of binding geometry is analogous to the stacked structures seen between the arginine and aromatic residues in proteins.



**Figure 3.1.** Host P shown with a CPK representation of a host-guest complex. The complex shows the host P in the conformation found in the crystal structure of the tetraester<sup>12</sup> with the guanidinium guest 5 docked into a viable binding position.

One of the apparent functions of the aromatic ring in arginine-aromatic stacked pairs is to orient the guanidinium ion so that its NH groups can form conventional hydrogen bonds to other groups in the protein or to solvent.<sup>6,7</sup> Thus, we were interested in investigating whether a hydrogen-bond acceptor placed near the cavity of our macrocycle would enhance binding of guanidinium guests. Recent work by Pat Kearney in the group had already begun to explore this possibility.<sup>13</sup>

Pat synthesized the host CP, 2. The CP host possesses a single carboxylate group located adjacent to the binding cavity. The carboxylate is in a well-solvated aqueous environment, but is positioned such that it can form close contacts with bound guest molecules (see Figure 3.2). Pat determined the aqueous binding affinities of a wide variety of neutral and cationic guests to the host CP, and compared them to those of host P. He found that the additional carboxylate did not alter the hydrophobic nature of the binding site, and that it did not affect the binding orientations of any of the guests. The

binding energies of several guanidinium compounds to both hosts are shown in Figure 3.3. The estimated error in the  $-\Delta G^\circ$  values shown is  $\pm 0.2$  kcal/mol.

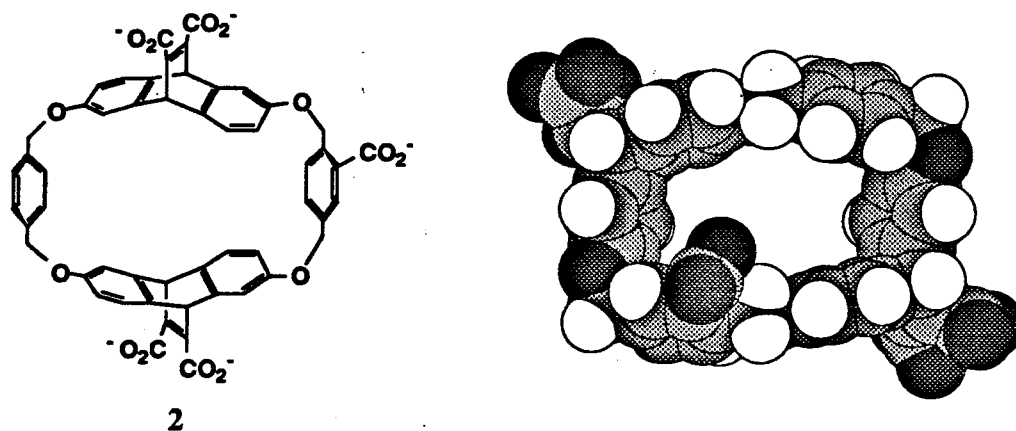


Figure 3.2. Host CP shown with a CPK representation of the host structure in one of several possible rhomboid conformations of the molecule. The additional carboxylate is shown in the lower left-hand side of the diagram.

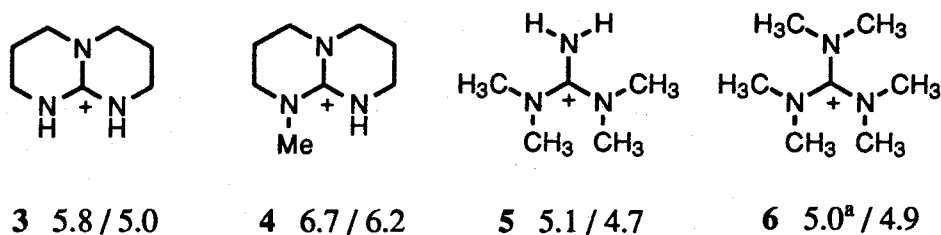
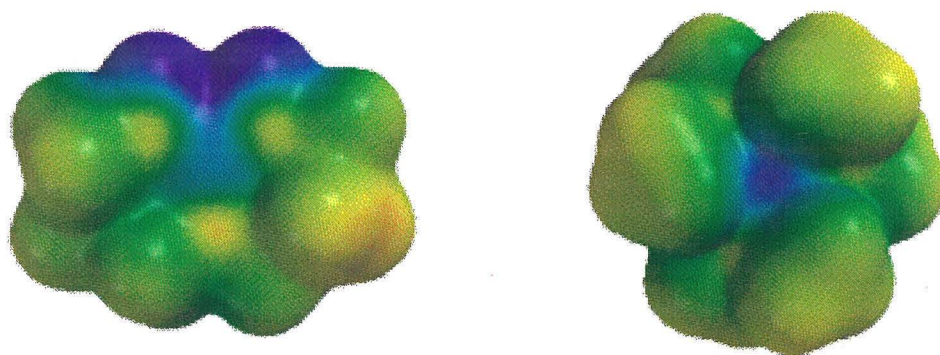


Figure 3.3.  $-\Delta G^\circ$  (kcal/mol) in aqueous borate buffer for binding to Host CP/P. <sup>a</sup>Values reported are weighted averages for the binding of the two enantiomers.

Most of the guanidinium guests, with the exception of hexamethylguanidinium, **6**, showed enhanced binding to the CP host. Interestingly, increased binding affinities were observed only for those guests that possess NH groups. While it is tempting to attribute these results to hydrogen-bond formation between the host carboxylate and the guanidinium

NH groups, an investigation of the electrostatic potentials of the guest molecules suggests a different explanation.

The AM1 electrostatic potentials of the guests **3** and **6** were calculated and mapped onto surfaces of total molecular electron density. They are shown in Figure 3.4. For the guest **3**, which displayed a substantial enhancement in its binding affinity for CP, strongly positive values of electrostatic potential are observed on exposed regions, centered on the NH atoms. These regions of high electrostatic potential are also ideally located such that they can point out of the binding cavity and up toward the negatively-charged carboxylate group of CP. In contrast, guest **6**, which showed no binding enhancement, does not display comparable regions of high positive electrostatic potential on exposed surface regions. These observations suggest that the formation of contact ion-pairs between the guest and the added carboxylate of the CP host may account for the increases in binding affinities.



**Figure 3.4.** Calculated AM1 electrostatic potential surfaces for the guanidinium guests **3** (left) and **6** (right). The electrostatic potential surface values range from 73.66 (red) to 122.4 (blue) kcal/mol.

To gain additional insight into the nature of the binding enhancements seen with host CP, we decided to synthesize the hosts **7a**, **7b**, and **7c** shown in



Figure 3.5. In the host **7a**, the negatively-charged carboxylate of host CP has been replaced by a neutral hydrogen-bond acceptor to investigate whether true hydrogen bonding can occur between the carbonyl of the amide and a guanidinium guest. In the hosts **7b** and **7c**, a methylene unit has been inserted between the host cavity and the carboxylate/amide group to investigate whether increased flexibility of the tethered group produces tighter binding of the guanidinium guest to the host cavity. The carboxylate/amide of **7b** and **7c** can position itself to optimize its interactions with a bound guest, but at an entropic cost. We anticipated that these studies would eventually lead to the design of hosts that recognize and bind arginine in water through a combination of cation- $\pi$  effects and hydrogen bonding.

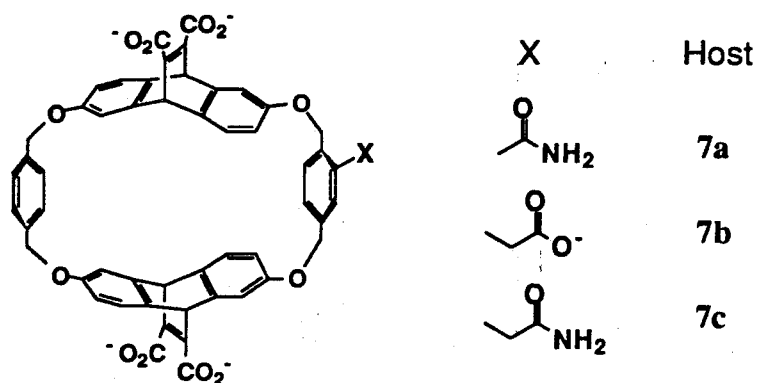


Figure 3.5. Definition of Host Structures.

## Results and Discussion

The proposed syntheses of the hosts are shown in Figure 3.6. The strategy is identical to the one used to synthesize host CP. The macrocycles are constructed in a stepwise manner, first reacting an excess of enantiomerically pure ethenoanthracene **8**, with cesium carbonate and  $\alpha,\alpha'$ -dibromo-*p*-xylene

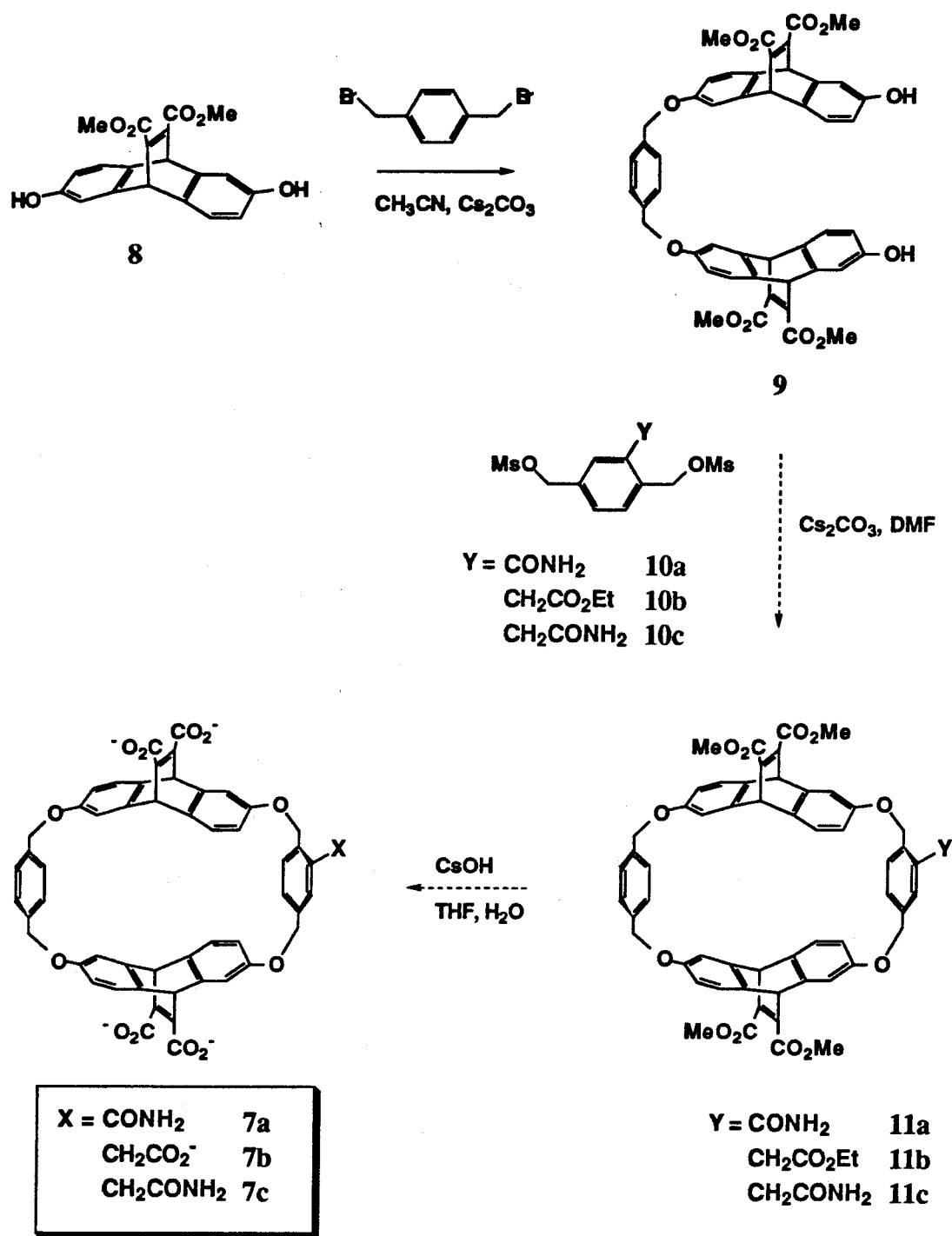
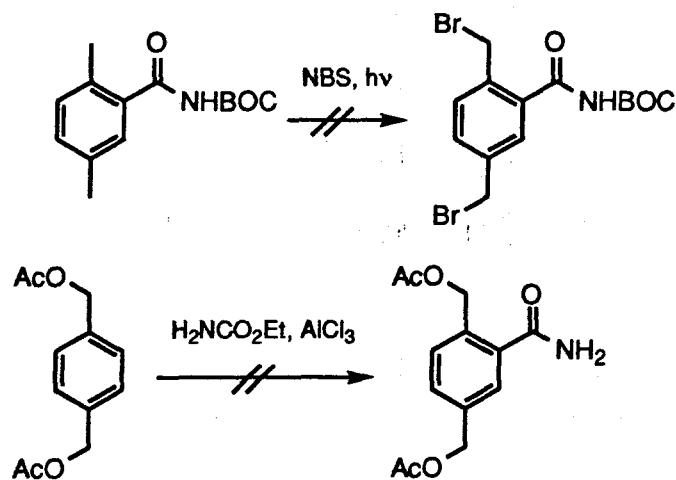


Figure 3.6. Proposed synthesis of hosts 7a, 7b, and 7c.

to produce compound **9**. Coupling of **9** with the appropriate linker molecule (**10a**, **10b**, or **10c**) then yields the desired macrocycle (**11a**, **11b**, or **11c**). Cleavage of the ester groups with cesium hydroxide in THF/H<sub>2</sub>O produces a water-soluble tetra(or penta)acid (**7a**, **7b**, or **7c**) that is suitable for binding studies. These hydrolysis conditions have been used previously in the group to selectively cleave methyl esters in the presence of amides.<sup>14</sup>

In order to synthesize the desired hosts, the appropriate linker molecules, **10a-c** must first be made. Unfortunately, due to time constraints on the author's graduate career, the syntheses of these compounds were not completed. However, several precursor molecules were made whose syntheses are documented in the following pages as they may be useful for future work in this area.

**Progress Towards the Synthesis of the Amide Linker, 10a.** The attempted synthesis of the amide linker, **10a**, is shown in Figure 3.7. The scheme is admittedly rather complicated for such a simple molecule. However, it was undertaken only after initial attempts to generate the desired linker via NBS bromination and via Friedel-Crafts-type acylation (shown below) were unsuccessful.



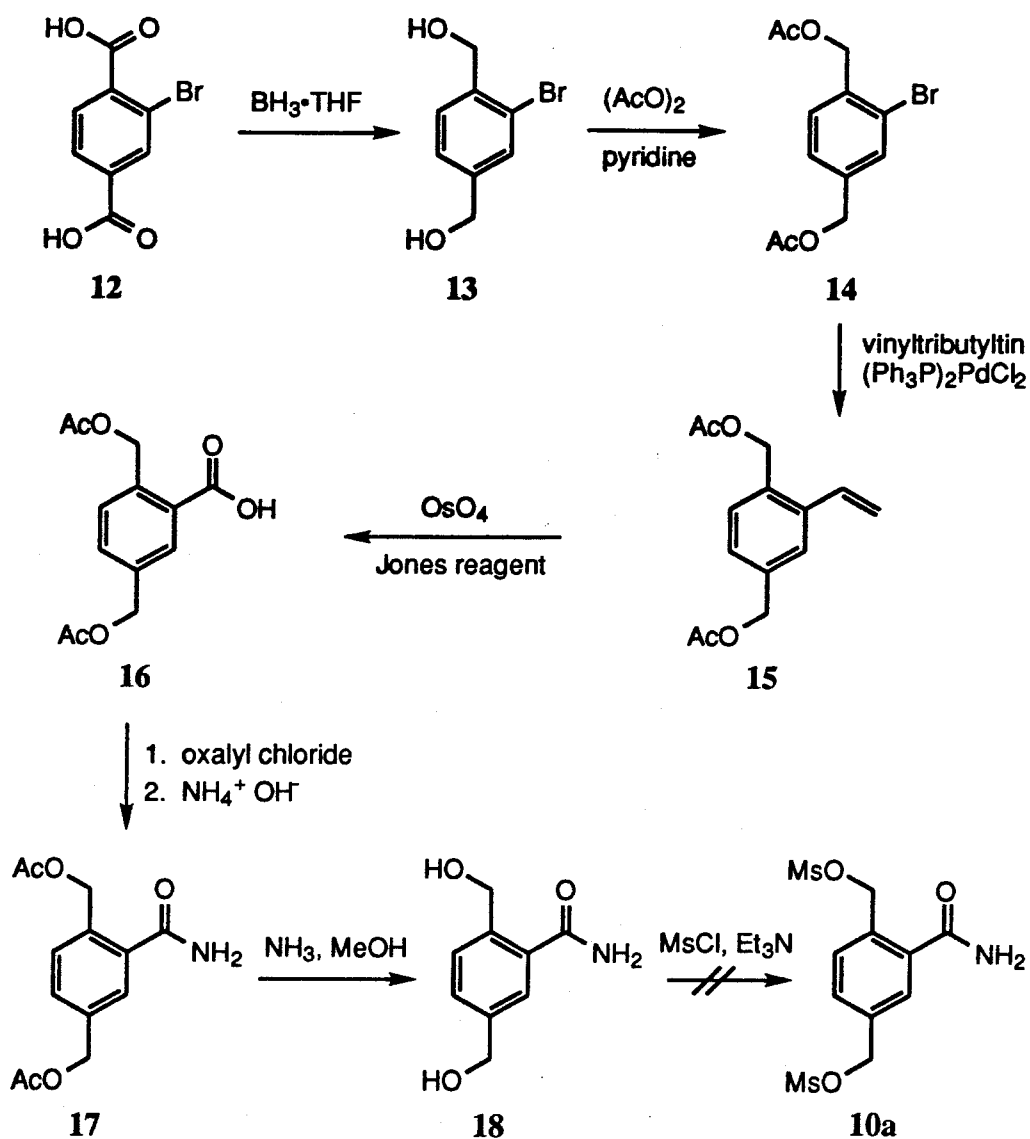


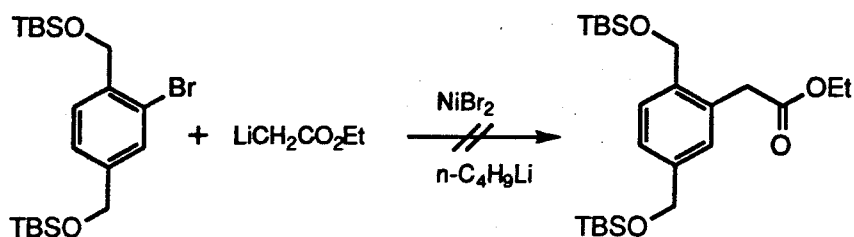
Figure 3.7. Attempted synthesis of the Linker 10a.

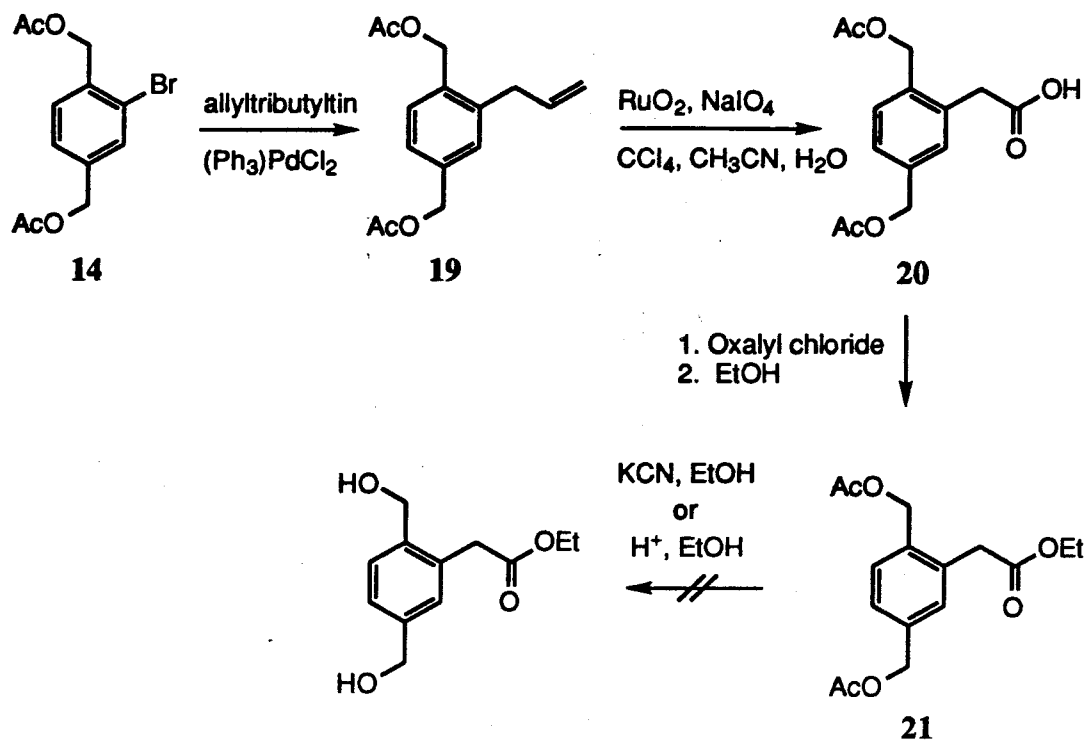
Commercially available 2-bromoterephthalic acid, **12**, was quantitatively reduced to the diol **13** using  $\text{BH}_3 \cdot \text{THF}$ . The reaction proceeds cleanly, so the product was used directly in the next step without further purification. Acetate protection of **13** was accomplished using acetic anhydride in pyridine. Compound **14** was also used without further purification. Stille coupling of

**14** with vinyltributyltin in refluxing dioxane produced the styrene **15** in good yield. However, the next step, oxidative cleavage of **15** to the benzoic acid **16**, was problematic. This reaction was tried a number of times using various oxidizing agents, but the yields never exceeded 50%. The best yields and the cleanest products were obtained using  $\text{OsO}_4$ /Jones reagent, so this method is reported here. Conversion of **16** to the acid chloride using oxalyl chloride followed by quenching of the reaction with saturated aqueous ammonium hydroxide produced the amide **17**. The acetate esters of **17** were then cleaved in a solution of methanol saturated with ammonia to obtain the diol **18**.

The final step, formation of the dimesylate **10a**, was expected to be facile, but this reaction repeatedly generated multiple products. We then tried to introduce alternative leaving groups, such as tosylates or bromides, but similar problems were encountered. It is now believed that the desired compounds decompose quickly, which preclude their isolation. A possible solution to this problem might be to convert the alcohols of **18** to less reactive leaving groups such as chlorides.

**Progress Towards the Synthesis of the Ester Linker, 10b.** Initially, we tried to synthesize the linker **10b** via a nickel-catalyzed substitution reaction (see below). Unfortunately, only starting material was recovered from this reaction. Therefore, we decided to synthesize **10b** using a route similar to the one proposed for **10a**. Part of the synthetic scheme is shown in Figure 3.8.



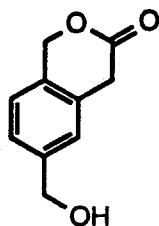


**Figure 3.8.** Attempted Synthesis of the Ester Linker 10b.

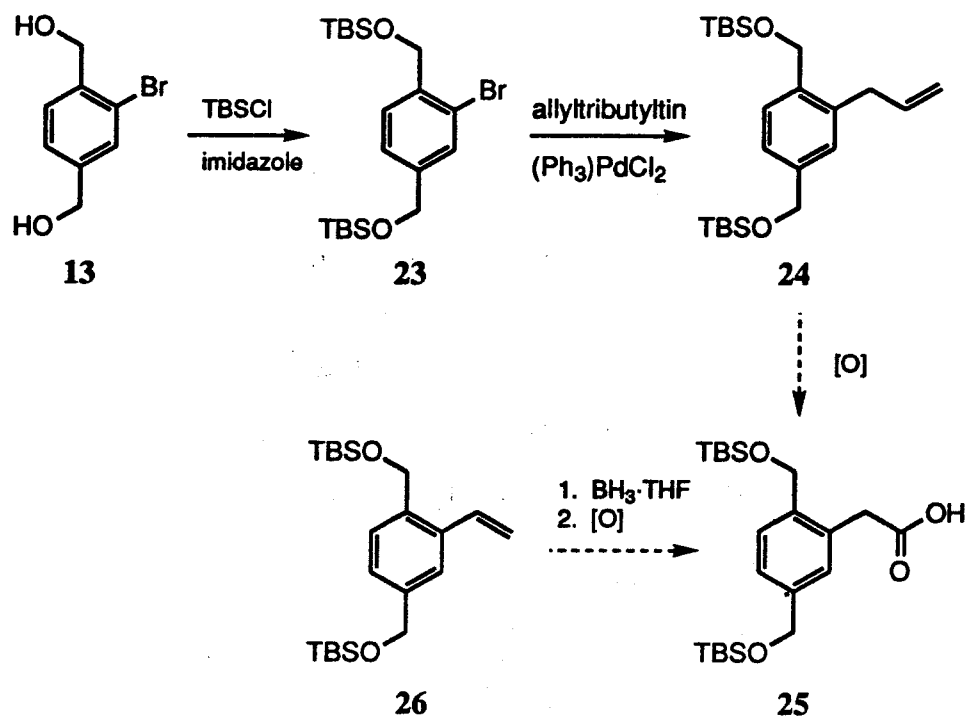
Synthesis of the compound **14** was described in the last section. Stille coupling of **14** with allyltributyltin produced the allylbenzene **19** in good yield. Problems were again encountered with the next step, the oxidative cleavage of **19** to form the carboxylic acid **20**. Various oxidizing agents were tried, but the yields from the reactions were quite low, ranging from 30-40%. Hydroboration of the styrene **15** followed by oxidation to the carboxylic acid **20** was also attempted, but the overall yield from these reactions was equally low. The cleanest product was obtained from the oxidative cleavage using  $\text{RuO}_2$  and  $\text{NaIO}_4$  in  $\text{CCl}_4$ ,  $\text{CH}_3\text{CN}$ , and  $\text{H}_2\text{O}$ , so this method is reported here.

Esterification of **20** was accomplished by formation of the acid chloride using oxalyl chloride, followed by quenching with ethanol. The next step, cleavage of the acetyl esters of **21** by transesterification, was unsuccessful.

Reaction of **21** in refluxing ethanol containing catalytic acid led to multiple products. The major component of the mixture is believed to be the cyclized compound **22**. Similar results were obtained when the transesterification was carried out under milder conditions (catalytic KCN in ethanol at room temperature).

**22**

We then decided to try the same synthetic route, but using a different protecting group for the alcohols of **13** (see Figure 3.9). *t*-Butyldimethylsilyl (TBS) ethers were chosen since they can be cleaved easily with acid. This synthesis was only partially completed. Bromide **13** was reacted with *t*-butyldimethylsilyl chloride to produce the compound **23** in good yield. Stille coupling of **23** with allyltributyltin to obtain **24** was also readily accomplished. Oxidative cleavage of **24** using RuO<sub>4</sub>, however, was unsuccessful. A test reaction was conducted substituting KMnO<sub>4</sub> as the oxidizing agent. The desired carboxylic acid, **25**, was isolated, but in very low yield. Optimization of this reaction will be necessary in future work. Alternatively, **25** could be synthesized by hydroboration of the styrene **26** followed by oxidation. Esterification of **25**, cleavage of the TBS ethers, and finally mesylation of the diol should produce the desired linker, **10b**.



**Figure 3.9.** A revised synthetic route towards the linker 10b.

**Progress Towards the Synthesis of the Amide Linker, 10c.** The synthesis of the linker 10c uses the same strategy that was proposed for the synthesis of 10a (see Figure 3.10). Synthesis of the carboxylic acid 20 was described in the previous section. Formation of the acid chloride followed by quenching with ammonium hydroxide produced the amide 27. Alcohol deprotection of 27 was accomplished using  $K_2CO_3$  in methanol/ $H_2O$ ; this reaction proceeded in poor yield. It was later discovered in the synthesis of 10a that acetate esters could be cleaved in excellent yield using methanol saturated with ammonia; this procedure should be used in the future. The final step, formation of the dimesylate 10c, was not attempted because of the minute quantities of 28 that were isolated from the previous reaction. In light of the problems



encountered in trying to form the dimesylate 10a, it may be advisable to convert the alcohols of 28 to less reactive leaving groups.

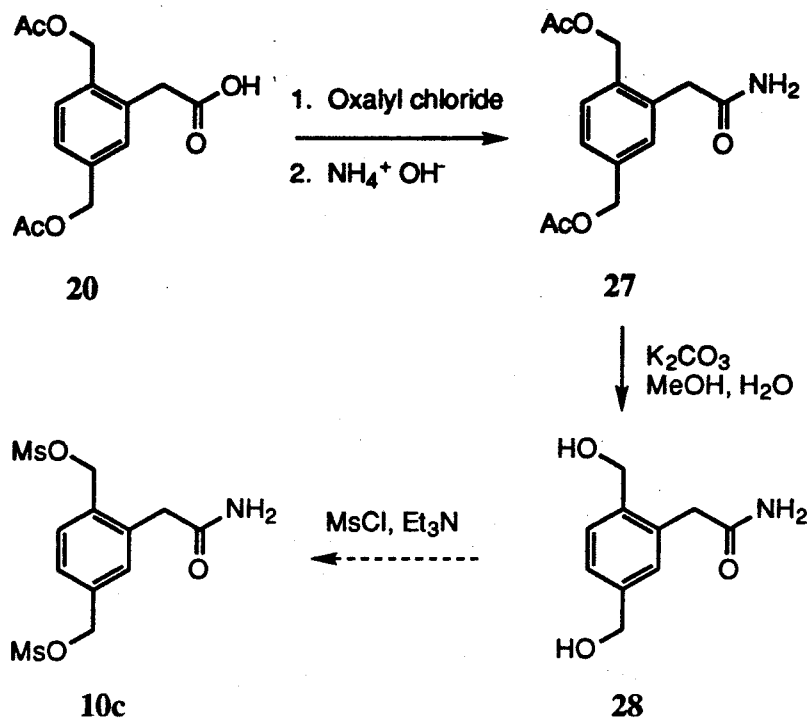


Figure 3.10. Synthesis of the Linker 10c.

### Concluding Remarks.

This chapter has documented significant progress towards the synthesis of three new host structures. The macrocycles are modified versions of the host P, each containing either an amide or a carboxylate group appended to the rim of the binding cavity. Due to time constraints on the author's graduate career, this project was not completed. However, studies of these macrocycles still represents a worthwhile goal, as they will help to clarify the role that a hydrogen-bond acceptor can play in the binding of a guest that contains complementary hydrogen-bond donors. It is anticipated that this information

will aid in the development of novel hosts that use a combination of cation- $\pi$  interactions and hydrogen bonding to bind arginine and other highly water-soluble guests in aqueous media.

## Experimental Section

**General Methods.** The NMR spectra were recorded on either a General Electric QE-300, JEOL JNM GX-400, or Bruker AM-500 spectrometer. Routine spectra were referenced to the residual proton signals of the solvents, and are reported in ppm downfield of 0.0 as  $\delta$  values. All coupling constants,  $J$ , are reported in Hz. Melting points were determined on a Thomas Hoover melting point apparatus, and are corrected. Routine mass spectral analyses were performed either on a Hewlett Packard 5890/5970 GC/MS or at the University of California, Riverside. All high resolution mass spectral analyses were performed at the University of California, Riverside. All reactions were stirred magnetically under argon unless otherwise noted. THF was distilled from sodium benzophenone ketyl.  $\text{CH}_2\text{Cl}_2$  was distilled from  $\text{CaH}_2$ . Anhydrous dioxane, DMF, and pyridine were obtained from commercial sources. Jones reagent was prepared as described in the literature.<sup>15</sup>

**2-Bromo-1,4-benzenedimethanol (13).** 2-Bromoterephthalic acid (5 g, 0.020 mol, 1 equiv) was placed in a dry, 250 mL, 3-neck round-bottom flask equipped with a reflux condenser. The diacid was dissolved in dry THF (50 mL), and then  $\text{BH}_3 \cdot \text{THF}$  (1.0 M solution in THF, 50 mL, 0.05 mol, 2.5 equiv) was slowly injected into the solution, which caused the solution to gently foam. Shortly after the addition was complete, a large amount of white precipitate formed, and the solution became very warm. The mixture was then refluxed for 3 hours, during which time most of the solid dissolved. The reaction was then cooled to room temperature, and water was added. *Caution: Foaming at first!* The mixture was extracted twice with ether, and

the combined organic layers were washed first with NaHCO<sub>3</sub> (saturated aqueous), and then with water. The solution was dried over MgSO<sub>4</sub>, filtered, and the solvents removed under reduced pressure, leaving 4.37 g of a white solid: 99% yield. The compound was used without further purification. m.p. 111-113 °C; <sup>1</sup>H NMR (acetone-d<sub>6</sub>) δ 7.54 (m, 2H), 7.33 (dd, 1H, *J* = 1, 8), 4.64, 4.61 (2d, 4H, *J* = 6, collapsed to two singlets upon addition of D<sub>2</sub>O), 4.47 (t, 1H, *J* = 6, D<sub>2</sub>O exchangeable), 4.37 (t, 1H, *J* = 6, D<sub>2</sub>O exchangeable); <sup>13</sup>C NMR (acetone-d<sub>6</sub>) δ 144.27, 140.32, 130.92, 128.81, 126.41, 122.00, 64.12, 63.64; EI-MS *m/e* 218 (M<sup>++</sup> 2), 216 (M<sup>+</sup>), 187, 185, 159, 157, 137.

**1-Bromo-2,5-bis(acetyloxymethyl)benzene (14).** Diol 13 (1.24 g, 5.7 mmol, 1 equiv) was dissolved in a minimal amount of anhydrous pyridine (~ 5 mL). Acetic anhydride (1.6 mL, 1.73 g, 17 mmol, 3 equiv) was added, and the solution was stirred at room temperature for 12 hours. Water was added, and the solution was extracted twice with ether. The combined ether layers were washed twice with HCl (5% aqueous), and then once with water. The solution was dried over MgSO<sub>4</sub>, filtered, and concentrated to obtain 1.72 g of an off-white solid: 89% yield. The compound was used without further purification. m.p. 66-68 °C; <sup>1</sup>H NMR (acetone-d<sub>6</sub>) δ 7.65 (d, 1H, *J* = 2), 7.49 (d, 1H, *J* = 8), 7.41 (dd, 1H, *J* = 2, 8), 5.15 (s, 2H), 5.09 (s, 2H), 2.08 (s, 3H), 2.06 (s, 3H). <sup>13</sup>C NMR (CDCl<sub>3</sub>) δ 170.74, 170.69, 137.95, 135.24, 132.42, 129.97, 127.25, 123.52, 65.61, 64.99, 21.01, 20.96; CI-MS *m/e* 320 (MNH<sub>4</sub><sup>++</sup> 2), 318 (MNH<sub>4</sub><sup>+</sup>), 240 (M<sup>+-</sup>OAc); HRMS 318.0338, calc. for C<sub>12</sub>H<sub>13</sub>BrO<sub>4</sub>NH<sub>4</sub>: 318.0341.

**2,5-Bis(acetyloxymethyl)styrene (15).** Bromide 14 (2.5 g, 8.3 mmol, 1 equiv), vinyltributyltin (4 mL, 4.34 g, 13.7 mmol, 1.6 equiv), and anhydrous dioxane (10 mL) were placed in a 100 mL, 3-neck round-bottom flask equipped with a reflux condenser. The flask was evacuated and purged with argon several

times, and then bis(triphenylphosphine)palladium(II)chloride (175 mg, 0.249 mmol, 3 mol %) was quickly added. The solution was refluxed for 4 hours, during which time the solution turned from yellow, to green, and finally to black. The mixture was cooled, diluted with ether, and then washed with water. The ether layer was dried over  $\text{MgSO}_4$ , filtered, concentrated, and purified by chromatography over silica gel ( $R_f$  0.39 in  $\text{CH}_2\text{Cl}_2$ ) giving 1.95 g of a slightly yellow oil (95% yield). Note: The product slowly polymerized over the course of several days.  $^1\text{H}$  NMR (acetone- $d_6$ )  $\delta$  7.49 (d, 1H,  $J = 1$ ), 7.26 (d, 1H,  $J = 8$ ), 7.18 (dd, 1H,  $J = 2, 8$ ), 6.90 (dd, 1H,  $J = 11, 17$ ), 5.67 (dd, 1H,  $J = 1, 17$ ), 5.61 (dd, 1H,  $J = 1, 11$ ), 5.04 (s, 2H), 4.98 (s, 2H), 1.93, 1.90 (2s, 6H);  $^{13}\text{C}$  NMR ( $\text{CDCl}_3$ )  $\delta$  170.88, 170.84, 137.72, 136.60, 133.33, 132.80, 130.19, 127.65, 125.95, 117.40, 65.96, 64.00, 21.08, 21.01; MS  $m/e$  248 ( $\text{M}^+$ ), 206 ( $\text{M}^+ - \text{Ac}$ ), 194, 164, 146, 117.

**2,5-Bis(acetyloxymethyl)benzoic acid (16).** Styrene 15 (867 mg, 3.49 mmol, 1 equiv) was dissolved in acetone (15 mL) and  $\text{OsO}_4$  (0.43 mL of a 4 wt % solution in  $\text{H}_2\text{O}$ , 2 mol %) and Jones Reagent (4.9 mL, 16.9 mmol of  $\text{Cr}^{\text{VI}}$ , 3.5 equiv) were added. The mixture was stirred for 20 hours at room temperature, during which time the solution separated into two phases. Isopropanol (~ 1 mL) was added followed by  $\text{NaHSO}_3$  (0.27 g). The mixture was diluted with  $\text{H}_2\text{O}$  (~ 10 mL), and stirred until a dark green homogenous solution was obtained. The solution was diluted with  $\text{H}_2\text{O}$  and extracted several times with ethyl acetate. The organic extracts were combined, dried over  $\text{MgSO}_4$ , filtered, and concentrated. Thin layer chromatography on silica plates showed that the product streaks near the baseline in 25% THF in  $\text{CH}_2\text{Cl}_2$ , and is weakly UV active. Purification by chromatography over silica gel (5-25% THF in  $\text{CH}_2\text{Cl}_2$ ) produced 445 mg of a cloudy oil which solidified

upon standing (45% yield).  $^1\text{H}$  NMR (acetone- $d_6$ )  $\delta$  7.92 (s, 1H), 7.47 (m, 2H), 5.04 5.03 (2s, 4H), 1.97, 1.93 (2s, 6H);  $^{13}\text{C}$  NMR (acetone- $d_6$ )  $\delta$  170.90, 170.81, 168.04, 138.99, 137.17, 132.67, 131.28, 129.97, 128.87, 65.64, 64.65, 20.72; CI-MS  $m/e$  284 ( $\text{MNH}_4^+$ ), 240 ( $\text{MNH}_4^+ - \text{Ac}$ ), 224 ( $\text{MNH}_4^+ - \text{OAc}$ ).

**2,5-Bis(acetyloxymethyl)benzamide (17).** Benzoic acid 16 (367 mg, 1.38 mmol, 1 equiv) was dissolved in dry  $\text{CH}_2\text{Cl}_2$  (~ 5 mL). The solution was cooled to 0 °C, and oxalyl chloride (132  $\mu\text{L}$ , 192 mg, 1.66 mmol, 1.2 equiv) was added. One drop of DMF was added to the mixture, which caused it to vigorously foam. The solution was warmed to room temperature, stirred for 30 min, and then evaporated under reduced pressure. The resulting yellow oil was dissolved in a minimal amount of dry THF, and poured onto a chilled solution of ammonium hydroxide (saturated aqueous, ~ 5 mL). A white precipitate formed immediately. After stirring for 15 min, water was added, and the solution was extracted several times with ethyl acetate. The combined organic layers were dried over  $\text{MgSO}_4$ , filtered, and concentrated to yield 267 mg of an off-white solid: 79% yield. The compound was used in the next step without further purification.  $^1\text{H}$  NMR ( $\text{CDCl}_3$ )  $\delta$  7.49 (s, 1H), 7.36 (m, 2H), 6.4 (br s, 1H), 5.9 (br s, 1H), 5.24 (s, 2H), 5.01 (s, 2H), 2.01, 2.00 (2s, 6H);  $^{13}\text{C}$  NMR ( $\text{CDCl}_3$ )  $\delta$  170.92, 170.86, 170.62, 136.48, 135.18, 134.24, 130.45, 129.95, 127.70, 65.37, 63.90, 21.03; EI-MS  $m/e$  283 ( $\text{MNH}_4^+$ ), 266 ( $\text{MH}^+$ ), 225 ( $\text{M}^+ - \text{Ac}$ ), 208 ( $\text{M}^+ - \text{OAc}$ ), 147 ( $\text{M}^+ - 2\text{OAc}$ )

**2,5-Bis(hydroxymethyl)benzamide (18).** Benzamide 17 (300 mg, 1.13 mmol, 1 equiv) was placed in a dry, 50 mL, 3-neck round bottom flask equipped with a dry ice condenser. The amide was dissolved in methanol (~ 20 mL, spectral grade), and the flask was cooled in a dry ice/acetone bath. Ammonia was then condensed into the flask until a saturated solution was achieved. The

flask was warmed to room temperature, stoppered, and stirred for 12 hours. The solvent was then removed under reduced pressure, and the resulting residue was purified by crystallization from methanol/CH<sub>2</sub>Cl<sub>2</sub>: 197 mg white crystals, 93% yield. <sup>1</sup>H NMR (DMSO-d<sub>6</sub>) δ 7.85 (br s), 7.40 (m, 3H), 5.24 (m, 2H, D<sub>2</sub>O exchangeable), 5.25 (d, 2H, *J* = 6, collapsed to a singlet upon addition of D<sub>2</sub>O), 5.21 (d, 2H, *J* = 6, collapsed to a singlet upon addition of D<sub>2</sub>O).

**2,5-Bis(acetyloxymethyl)allylbenzene (19).** Bromide **14** (1.5 g, 4.98 mmol, 1 equiv), allyltributyltin (3 mL, 3.2 g, 9.68 mmol, 2.0 equiv), and DMF (15 mL) were placed in a 100 mL, 3-neck round-bottom flask equipped with a reflux condenser. The flask was evacuated and purged with argon several times, and then bis(triphenylphosphine)palladium(II)chloride (105 mg, 0.150 mmol, 3 mol %) was quickly added. The yellow solution was heated at 95 °C for 4 hours, during which time the solution gradually turned black. The mixture was cooled, diluted with ether and then washed with H<sub>2</sub>O. The ether layer was dried over MgSO<sub>4</sub>, filtered, concentrated, and purified by chromatography over silica gel (*R<sub>f</sub>* 0.53, CH<sub>2</sub>Cl<sub>2</sub>) to give 965 mg of a clear, colorless oil, 74% yield. <sup>1</sup>H NMR (acetone-d<sub>6</sub>) δ 7.37 (d, 1H, *J* = 8), 7.25 (m, 2H), 5.97 (m, 1H), 5.12 (s, 2H), 5.07 (s, 2H), 5.03 (m, 2H), 3.47 (d, 2H, *J* = 6), 2.04, 2.03 (2s, 6H); <sup>13</sup>C NMR (CDCl<sub>3</sub>) δ 170.91, 170.86, 139.06, 136.49, 133.90, 130.02, 129.79, 126.45, 116.40, 65.99, 63.97, 36.88, 21.09, 21.06; EI-MS *m/e* 262 (M<sup>+</sup>), 220 (M<sup>+</sup> - Ac), 202 (M<sup>+</sup> - OAc), 142 (M<sup>+</sup> - 2OAc).

**2,5-Bis(acetyloxymethyl)phenylacetic acid (20).** A flask was charge with CH<sub>3</sub>CN (4 mL), CCl<sub>4</sub> (4 mL), H<sub>2</sub>O (6 mL), allylbenzene **19** (528 mg, 2.0 mmol, 1 equiv) and NaIO<sub>4</sub> (1.77 g, 8.3 mmol, 4.1 equiv). RuO<sub>2</sub> (8 mg, 3 mol %) was added to this biphasic solution, which caused the mixture turned yellow-brown. The solution was stirred vigorously for 2 hours at room temperature,

and then filtered through celite. The filtrate was diluted with  $\text{CH}_2\text{Cl}_2$ , and the phases were separated. The aqueous phase was extracted several times with ethyl acetate. The combined organic extracts were dried over  $\text{MgSO}_4$ , filtered, and concentrated. Purification by chromatography over silica gel (5-15% THF in  $\text{CH}_2\text{Cl}_2$ ;  $R_f$  0.40 in 25% THF in  $\text{CH}_2\text{Cl}_2$ ) produced 182 mg of a grayish oil (32% yield) that solidified upon standing.  $^1\text{H}$  NMR (acetone- $d_6$ )  $\delta$  7.39 (d, 1H,  $J = 8$ ), 7.30 (m, 2H), 5.15 (s, 2H), 5.08 (s, 2H), 3.76 (s, 2H), 2.05, 2.03 (2s, 6H);  $^{13}\text{C}$  NMR ( $\text{CDCl}_3$ )  $\delta$  177.00, 171.01, 170.86, 136.76, 134.62, 133.01, 130.90, 130.59, 127.71, 65.72, 64.18, 38.23, 21.07, 20.90; EI-MS  $m/e$  298 ( $\text{MNH}_4^+$ ).

**2,5-Bis(acetyloxymethyl)ethyl phenylacetate (21).** Benzoic acid **20** (638 mg, 2.28 mmol, 1 equiv) was dissolved in dry  $\text{CH}_2\text{Cl}_2$  (~ 5 mL), cooled to 0 °C, and oxalyl chloride (251 mL, 365 mg, 2.87 mmol, 1.2 equiv) was added. One drop of DMF was added to the mixture, which caused it to vigorously foam. The solution was warmed to room temperature, stirred for 30 min, and then quenched with several drops of anhydrous ethanol. The mixture was stirred for another 15 min, and then evaporated. Purification by chromatography over silica gel ( $R_f$  0.40, 5% ethyl acetate in  $\text{CH}_2\text{Cl}_2$ ) produced a clear, colorless oil in 60-70% yield.  $^1\text{H}$  NMR ( $\text{CDCl}_3$ )  $\delta$  7.30 (d, 1H,  $J = 8$ ), 7.18 (m, 2H), 5.04 (s, 2H), 4.99 (s, 2H), 4.05 (q, 2H), 3.62 (s, 2H), 2.00, 1.97 (2s, 6H), 1.16 (t, 3H,  $J = 7$ );  $^{13}\text{C}$  NMR ( $\text{CDCl}_3$ )  $\delta$  171.02, 170.73, 170.62, 136.57, 134.60, 133.71, 130.70, 130.29, 127.33, 65.67, 64.04, 61.05, 38.43, 21.01, 20.96, 20.89, 14.19.

**1-Bromo-2,5-bis(*tert*-butyldimethylsilyloxymethyl)benzene (23).** Bromide **13** (1.5 g, 6.9 mmol, 1 equiv), *tert*-butyldimethylsilylchloride (2.6 g, 0.17 mol, 2.5 equiv), and imidazole (1.88 g, 0.28 mol, 4 equiv) were dissolved in anhydrous DMF (~ 25 mL), and the reaction mixture was stirred overnight at 40 °C. The DMF was removed under reduced pressure, and the residue was dissolved in



CH<sub>2</sub>Cl<sub>2</sub>. After washing with water, the organic phase was dried over MgSO<sub>4</sub>, filtered, and concentrated. The residue was loaded onto a pad of silica gel, and eluted with CH<sub>2</sub>Cl<sub>2</sub> which produced 529 mg (93% yield) of a cloudy, white oil. <sup>1</sup>H NMR (acetone-d<sub>6</sub>) δ 7.54 (m, 2H), 7.37 (d, 1H), 4.77, 4.75 (2s, 4H), 0.96, 0.94 (2s, 18H), 0.14, 0.11 (2s, 12H).

**2,5-Bis(*tert*-butyldimethylsiloxymethyl)allylbenzene (24).** This compound was prepared using the same procedure that was used to synthesize compound 19, but substituting compound 23 for compound 14. Purification by chromatography over silica gel (*R<sub>f</sub>* 0.62, 1:1 isooctane/CH<sub>2</sub>Cl<sub>2</sub>) produced a clear colorless oil in 75% yield. <sup>1</sup>H NMR (CDCl<sub>3</sub>) δ 7.38 (d, 1H), 7.15 (d, 1H), 7.10 (s, 1H), 5.92 (m, 1H), 5.92 (m, 1H), 4.61 (s, 1H), 3.37 (d, 2H), 0.95 (s, 18H), 0.14 (s, 12H).

**2,5-Bis(acetyloxymethyl)phenylacetamide (27).** This compound was prepared using the same procedure that was used to synthesize compound 17, but substituting compound 20 for the compound 16. <sup>1</sup>H NMR (CDCl<sub>3</sub>) δ 7.31 (d, 1H, *J* = 8), 7.19 (m, 2H), 5.65 (br s), 5.50 (br s), 5.04 (s, 2H), 4.99 (s, 2H), 3.57 (s, 2H), 2.01, 1.97 (2s, 6H); CI-MS *m/e* 297 (MNH<sub>4</sub><sup>+</sup>), 280 (MH<sup>+</sup>), 220 (M<sup>+</sup> - OAc); HRMS 297.1445, calc. for C<sub>14</sub>H<sub>17</sub>NO<sub>5</sub>: 297.1450.

**2,5-Bis(hydroxymethyl)phenylacetamide (28).** Compound 27 (83 mg, 0.30 mmol, 1 equiv) was dissolved in MeOH (~ 3 mL, spectral grade), and a solution of K<sub>2</sub>CO<sub>3</sub> (82 mg, 0.59 mmol, 2 equiv) in a minimal amount of H<sub>2</sub>O was added. The solution was stirred for 5 hours at room temperature, and then evaporated. The resulting residue was taken up in CH<sub>2</sub>Cl<sub>2</sub> and washed with water. The organic layer was dried over MgSO<sub>4</sub>, filtered, and concentrated to obtain 10 mg of a white solid (17% yield). Note: It was later

discovered, in the synthesis of compound 18, that acetyl esters could be cleaved in excellent yield using methanol saturated with ammonia.  $^1\text{H}$  NMR (DMSO- $d_6$ )  $\delta$  7.41 (br s, 1H), 7.16 (d, 2H,  $J = 8$ ), 7.00 (m, 2H), 6.86 (br s, 1H), 5.10 (t, 1H,  $J = 5$ ,  $\text{D}_2\text{O}$  exchangeable), 5.04 (t, 1H,  $J = 5$ ,  $\text{D}_2\text{O}$  exchangeable), 4.35 (d, 2H,  $J = 5$ , collapsed to a singlet upon addition of  $\text{D}_2\text{O}$ ), 4.31 (d, 2H,  $J = 5$ , collapsed to a singlet upon addition of  $\text{D}_2\text{O}$ ), 3.30 (s, 2H); CI-MS  $m/e$  196 ( $\text{MH}^+$ ); HRMS 196.0969, calc. for  $\text{C}_{10}\text{H}_{13}\text{NO}_3$ : 196.0974.

**References**

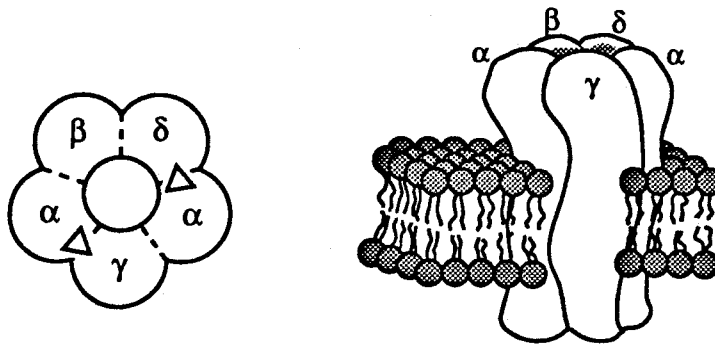
1. Suzuki, S.; Green, P. G.; Burngarner, R. E.; Dasgupta, S.; Goddard, W. A.; Blake, G. A. *Science* **1992**, *257*, 942-945.
2. Rodham, D. A.; Suzuki, S.; Suenram, R. D.; Lovas, F. J.; Dasgupta, S.; Goddard, W. A.; Blake, G. A. *Nature* **1993**, *362*, 735-737.
3. Perutz, M. F.; Fermi, G.; Abraham, D. J.; Poyart, C.; Bursaux, E. *J. Am. Chem. Soc.* **1986**, *108*, 1064-1078.
4. Burley, S. K.; Petsko, G. A. *FEBS Lett.* **1986**, *203*, 139-143.
5. Levitt, M.; Perutz, M. *J. Mol. Biol.* **1988**, *201*, 751-754.
6. Mitchell, J. B. O.; Nandi, C. L.; McDonald, I. K.; Thornton, J. M. *J. Mol. Biol.* **1994**, *239*, 315-331.
7. Flocco, M. M.; Mowbray, S. L. *J. Mol. Biol.* **1994**, *235*, 709-717.
8. Mowbray, S. L.; Cole, L. B. *J. Mol. Biol.* **1992**, *225*, 155-175.
9. Cowan, S. W.; Newcomer, M. E.; Jones, T. A. *J. Mol. Biol.* **1993**, *230*, 1225-1246.
10. Rouvinen, J.; Bergfors, T.; Teeri, T.; Knowles, J. K. C.; Jones, T. A. *Science* **1990**, *249*, 380-386.
11. Duffy, E. M.; Kowalczyk, P. J.; Jorgensen, W. L. *J. Am. Chem. Soc.* **1993**, *115*, 9271-9275.
12. Forman, J. E.; Marsh, R. E.; Schaefer, W. P.; Dougherty, D. A. *Acta Cryst.* **1993**, *B49*, 892-896.

13. Kearney, P. C. Ph.D. Thesis, California Institute of Technology, 1993.
14. J. E. Forman, unpublished results.
15. Hudlicky, M. *Oxidations in Organic Chemistry*; ACS Monograph 186; American Chemical Society: Washington, DC, 1990; p 273.

**Chapter 4: Design of a Disulfide-Containing Macrocyclic, a Model of the  
Nicotinic Acetylcholine Receptor Binding Site.**

## Introduction

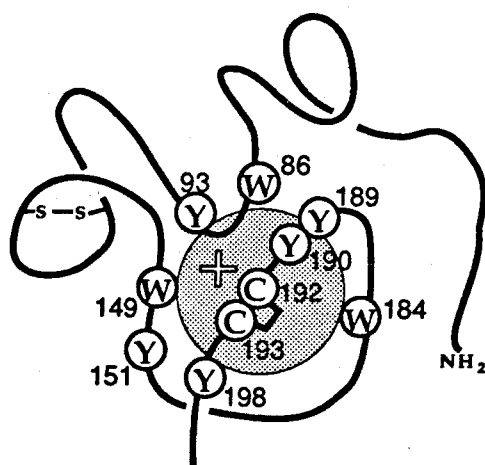
The nicotinic acetylcholine receptor (nAChR) is a ligand-gated ion channel that is involved in signal transduction at vertebrate neuromuscular junctions and at cholinergic synapses of the central nervous system.<sup>1</sup> The nAChR of skeletal muscle and of the *Torpedo* electric organ is a large (290 kD) transmembrane glycoprotein. The receptor is a pentamer composed of four distinct but homologous subunits with the stoichiometry  $\alpha_2\beta\gamma\delta$ . As is true of most membrane proteins, the X-ray crystallographic structure of the receptor has not been determined. Electron micrographs of *Torpedo* nAChR indicate that the subunits are arranged pseudo-symmetrically around a central axis that lies perpendicular to the plane of the membrane.<sup>2</sup> The subunits surround the ion channel situated in the center of the cluster. Figure 4.1 shows the presumed ordering of the subunits.



**Figure 4.1.** Schematic representation of a model of the nAChR. **Left:** Top view of the receptor showing a possible arrangement of the subunits surrounding the central ion channel. The ACh binding sites are represented as triangles. **Right:** Side view of the receptor showing transmembrane organization.

Agonists, such as acetylcholine (ACh), bind to two inequivalent sites on the receptor and cause opening of the ion channel which is selective for

sodium, potassium, and other small cations. Affinity labeling studies have shown that the ACh binding sites are formed primarily by the  $\alpha$  subunits, and are located at the interfaces between the  $\alpha$  and  $\gamma$  and between the  $\alpha$  and  $\delta$  subunits.<sup>3</sup> Many of the same studies, as well as some additional work involving site-directed mutagenesis<sup>4</sup> and NMR experiments<sup>5</sup> have identified a number of amino acids near the binding site. The residues are situated in three distinct regions of the large, amino-terminal, extracellular portion of the  $\alpha$  subunit and include Trp 86, Tyr 93, Trp 149, Tyr 151, Trp 184, Tyr 189, Tyr 190, Cys 192, Cys 193, and Tyr 198 (see Figure 4.2). All of these amino acids are rigorously conserved in the  $\alpha$  subunits of muscle nAChR, with the exception of Trp 184 and Tyr 189 which are less well conserved.



**Figure 4.2.** A schematic model of the nAChR agonist binding site of *Torpedo marmorata*, adapted from reference 1c. The amino-terminal, extracellular segment of the  $\alpha$  subunit is shown. The large sphere represents the space occupied by ACh. Circled residues have been identified near the binding site. C, Cys; W, Trp; Y, Tyr.

It was widely believed that the negatively-charged carboxylate groups of aspartate and glutamate were responsible for binding the positively-charged

head group of ACh. Consequently, the presence of several aromatic amino acids at the binding site was quite surprising. The findings are completely consistent, however, with a model of the ACh binding site proposed by the Dougherty group, in which the electron-rich rings of aromatic amino acids bind the quaternary ammonium ion of ACh through cation- $\pi$  interactions.<sup>6</sup> (A more detailed discussion of the cation- $\pi$  effect is given in Chapter 1.).

The role of the two cysteines, 192 and 193, is enigmatic. Mutagenesis of either residue to serine decreased the affinity of the receptor for agonists and eliminated the receptor's response to ACh.<sup>7</sup> Cys 192 and Cys 193 are conserved in all  $\alpha$  subunits sequenced to date and are unique to the  $\alpha$  subunit. Furthermore, in the native receptor the two cysteines are disulfide linked to each other.<sup>8</sup> Adjacent cysteines are not uncommon in sequences of proteins, but a disulfide bridge between them is extremely rare. A vicinal disulfide has been observed in only one protein structure, methanol dehydrogenase.<sup>9</sup> The disulfide is located at the enzyme's active site, but its significance is not yet known.

The presence of an unusual disulfide near the binding site for ACh in the nAChR suggests that it may have an important function. Karlin and coworkers demonstrated that the disulfide bond is readily reduced by dithiothreitol.<sup>10</sup> They also showed that in the presence of saturating concentrations of an agonist, the rate of reduction of the disulfide decreases by one or two orders of magnitude.<sup>10</sup> More potent agonists give more effective protection against reduction. A similar effect was not seen with competitive antagonists. This implies that the disulfide is involved in local conformational changes in the vicinity of the ACh binding site that lead to activation of the ion channel.



A disulfide exists in one of two preferred conformations that are mirror images of each other with dihedral angles of approximately  $\pm 90^\circ$ . Therefore, Karlin and coworkers proposed that binding of ACh causes a change in the conformation of the disulfide that ultimately triggers opening of the ion channel.<sup>8</sup> The hypothesis is still purely speculative; the disulfide may instead play a structural role in the protein.

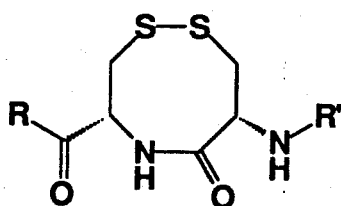
Karlin's proposal inspired us to design a host modeled after the nAChR binding site for ACh. Earlier work in the Dougherty group had demonstrated that relatively simple synthetic models can be used to gain considerable insight into complex interactions present in biological systems.<sup>6</sup> We anticipated that studies on such a host might begin to elucidate the role of the disulfide in the nAChR. Aside from its possible biological relevance, we hoped that the work would eventually lead to novel hosts that exploit the redox and conformational switching capabilities of the disulfide.

One of the specific questions regarding the nAChR that we had hoped to address was whether the disulfide is directly involved in binding ACh. Previous work in our group had established that the electron-rich faces of aromatic rings can produce strong binding to cations.<sup>11</sup> A disulfide possesses a large surface of lone pair electrons which could function much like a benzene ring, and act as a recognition element for the tetramethylammonium ion of ACh. In addition, a gas-phase *ab initio* calculation measured a stabilizing interaction of 22 kcal/mol between  $\text{Na}^+$  and dimethyldisulfide,<sup>12</sup> comparable to the value of 24 kcal/mol between  $\text{Na}^+$  and benzene.<sup>13</sup>

As was mentioned earlier, an 80-fold decrease in the rate of disulfide reduction occurred in the presence of a saturating concentration of ACh. However, a positive charge in the vicinity of the disulfide would be expected

to enhance the rate of reduction by thiolate. This raises another question: Does the presence of a positive charge next to the disulfide alters its redox potential and makes it less susceptible to reduction?

The third and perhaps most interesting question was whether binding of a guest causes a change in the conformation of the disulfide. The cyclic dipeptide N-BOC[cyclo-(R)-cysteinyl-(R)-cysteine]*tert*-butyl ester **1** was found to exist in chloroform as a mixture of two conformers that interconvert slowly on the NMR time-scale.<sup>14</sup> Both conformers possess a *cis* amide bond but differ in the chirality of the disulfide. In DMSO, the NMR data indicated that three conformers were present, but they were not further characterized. These results appear to be consistent with computational studies on compound **2**. *Ab initio* and molecular mechanics calculations predicted two low energy *cis* amide conformers of **2** which can be interconverted by rotation about the disulfide bond. A *trans* amide conformer lies 1 or 2 kcal/mol higher in energy.<sup>15</sup>

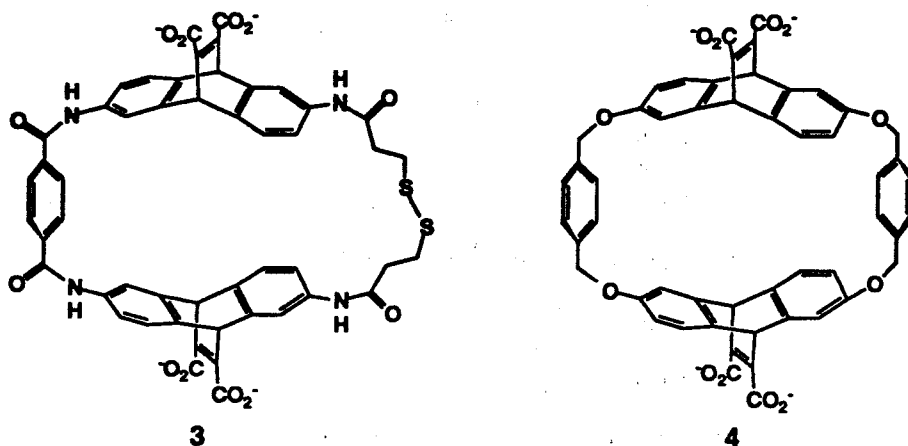


**1** R=O<sup>t</sup>Bu, R'=BOC

**2** R=NHMe, R'=Ac

As an initial attempt at creating a simple model of the nAChR binding site, we intended to synthesize the macrocycle **3**. Host **3** can be viewed as a modified version of our prototypical and best-studied receptor, host **4**. (For a detailed description of the binding properties of **4**, see Chapter X.) We had already demonstrated that host **4** binds ACh with a  $K_d = 25 \mu\text{M}$  at 298 °K in aqueous buffer,<sup>16</sup> a value comparable to that of the nAChR.<sup>17</sup> The tight

binding exhibited by **4** is primarily a result of cation- $\pi$  interactions between the quaternary ammonium group of ACh and the electron-rich aromatic rings of the host.



The host **3** retains the basic structure of host **4**, but introduces a disulfide moiety. The new binding cavity is surrounded by several aromatic rings and a disulfide, an arrangement that is not too unlike the model of the nAChR binding site (see Figure 4.2). Amide bonds were chosen to construct the molecule because they provided a great deal of synthetic flexibility; we anticipated that modification of the macrocycle for subsequent studies would be extremely facile.

## Results and Discussion

Unfortunately, the project did not proceed quite as we had envisioned. Although we were able to synthesize the host **3**, it was insoluble in most organic solvents and in water, which precluded its purification and its study in solution. N-Methylation of the amides of **3** improved its solubility properties somewhat, but the molecule was still not soluble enough for

binding studies to be conducted in aqueous media. Nonetheless, the work represents significant exploratory work towards producing a host model of the nAChR. Several new molecules were synthesized, and they are documented in the following pages together with suggestions for future efforts in this area.

**Disulfide Host Synthesis.** Building the amide-linked host **3** required production of a whole new series of compounds whose synthesis is shown in Figure 4.3. Commercially available 2,6-diaminoanthraquinone **5** was reduced with sodium borohydride to produce 2,6-diaminoanthracene **6**. The purity of the product seemed to depend largely upon the purity of the starting material. Cleaner products and better yields were obtained when **5** was newly-purchased. The anthracene **6** was soluble only in polar, organic solvents such as DMF and DMSO, and it decomposed fairly quickly in solution. Therefore, this compound was not purified further, but was used directly in the next step. The amino groups of **6** were protected using di-*tert*-butyl dicarbonate to produce **7**. Due to its poor solubility properties, compound **7** was only partially purified before reacting it with dimethyl acetylenedicarboxylate in refluxing dioxane to obtain the racemic Diels-Alder adduct **8**. Removal of the BOC protecting groups with TFA gave the basic building block of the host, ethenoanthracene **9**.

The macrocycle was constructed in a stepwise manner. First, an excess of ethenoanthracene **9** was reacted with terephthaloyl chloride to produce molecule **10**. Since compound **9** was racemic, both *meso* and *dl* isomers of **10** were obtained. Reverse-phase high pressure liquid chromatography (HPLC)

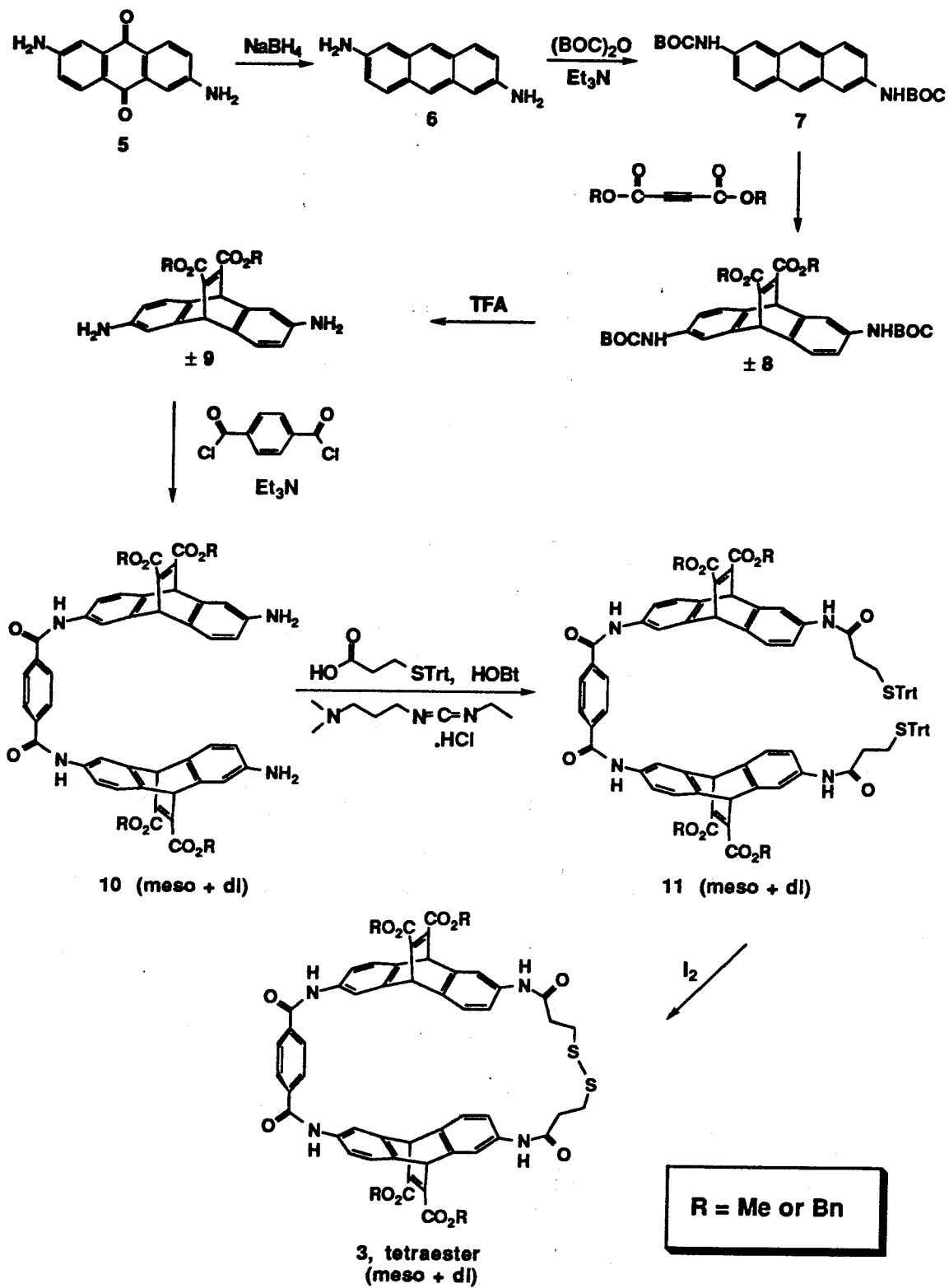


Figure 4.3. Synthesis of a Disulfide-Containing Macrocyclic.

was unsuccessful at separating the isomers so a mixture of **10** was coupled to 3-(triphenylmethylthio)propionic acid to give **11**. Finally, iodine oxidation cleaved the thiol-protecting trityl groups and closed the macrocycle, producing *meso* and *dl* forms of the desired host **3**, tetraester.

The tetramethyl ester of **3** did not crystallize, and it was soluble only in polar, organic solvents such as DMF and DMSO. Consequently, it was not possible to fully purify the host, or to separate the *meso* and *dl* isomers. In an effort to increase the macrocycle's solubility in organic solvents and thereby enable purification, the methyl esters of **3** were replaced with more hydrophobic benzyl esters. This was accomplished by substituting dibenzyl acetylenedicarboxylate in the Diels-Alder reaction (see Figure 4.3).

The benzyl groups did very little to alter the solubility properties of the host. A few NMR binding studies of tetrabenzyl ester **3** were attempted in DMSO- $d_6$ , but guests were not measurably bound in this solvent; this was hardly surprising given the absence of a hydrophobic effect. To obtain a water-soluble host that could be purified by HPLC and that could be used in aqueous binding studies, we hydrolyzed the benzyl esters with trifluoromethanesulfonic acid. Contrary to our expectations, the resulting compound, the putative tetraacid, did not dissolve in basic, aqueous media. This result forced us to redesign the receptor.

**Modification of the Disulfide Host.** In pH ~ 9 buffer, the hydrolyzed host **3** should have existed as a tetracarboxylate, so we were not entirely sure why the molecule was insoluble in both aqueous and mixed aqueous (5-25% v/v acetonitrile added) media. Presumably, the poor solubility of **3** stemmed from the presence of the four amides in the molecule. The amide linkages undoubtedly rigidified the host structure and probably created favorable

packing interactions. Internal hydrogen-bonding may have also discouraged its solvation. We reasoned that these problems might be overcome by N-methylating the amides, which would block hydrogen-bonding sites and which would also lower the barrier of rotation about the amide bond.

To accomplish this task, we first tried to N-methylate all four amides of the macrocycle precursor **11**. A variety of methods were used, but they produced mixtures of tri- and tetra-methylated products which could not be separated. Better results were obtained when the amino groups of ethenoanthracene **9** were methylated. Synthesis of the desired macrocycle is shown in Figure 4.4.

Monomethylation of **9** was achieved by reaction with formaldehyde and benzotriazole to form a diaminomethylbenzotriazole derivative which was then reduced with sodium cyanoborohydride to give **12**. The etheno bridge of **9** was susceptible to reduction under these conditions, and consequently it was difficult to avoid production of a small amount of an overreduced side-product during this reaction. Compound **12** was reacted with terephthaloyl chloride to form **13** as a *meso* + *dl* mixture. Standard coupling reactions between **13** and 3-(triphenylmethylthio)propionic acid were unsuccessful, presumably due to steric hindrance by the added methyl groups on the amines. Compound **14** was instead obtained by reaction of **13** with 3-(triphenylmethylthio)propanoyl chloride which was generated *in situ* from the carboxylic acid using dichlorotriphenylphosphorane. Iodine oxidation of **14** then produced the desired macrocycle **15**.

Thin layer chromatography of the crude product mixture of **15** revealed two-closely running spots which were separated by preparative centrifugal chromatography. The  $^1\text{H}$  NMR spectra of both compounds showed extremely broad resonances which yielded little information and which did not sharpen

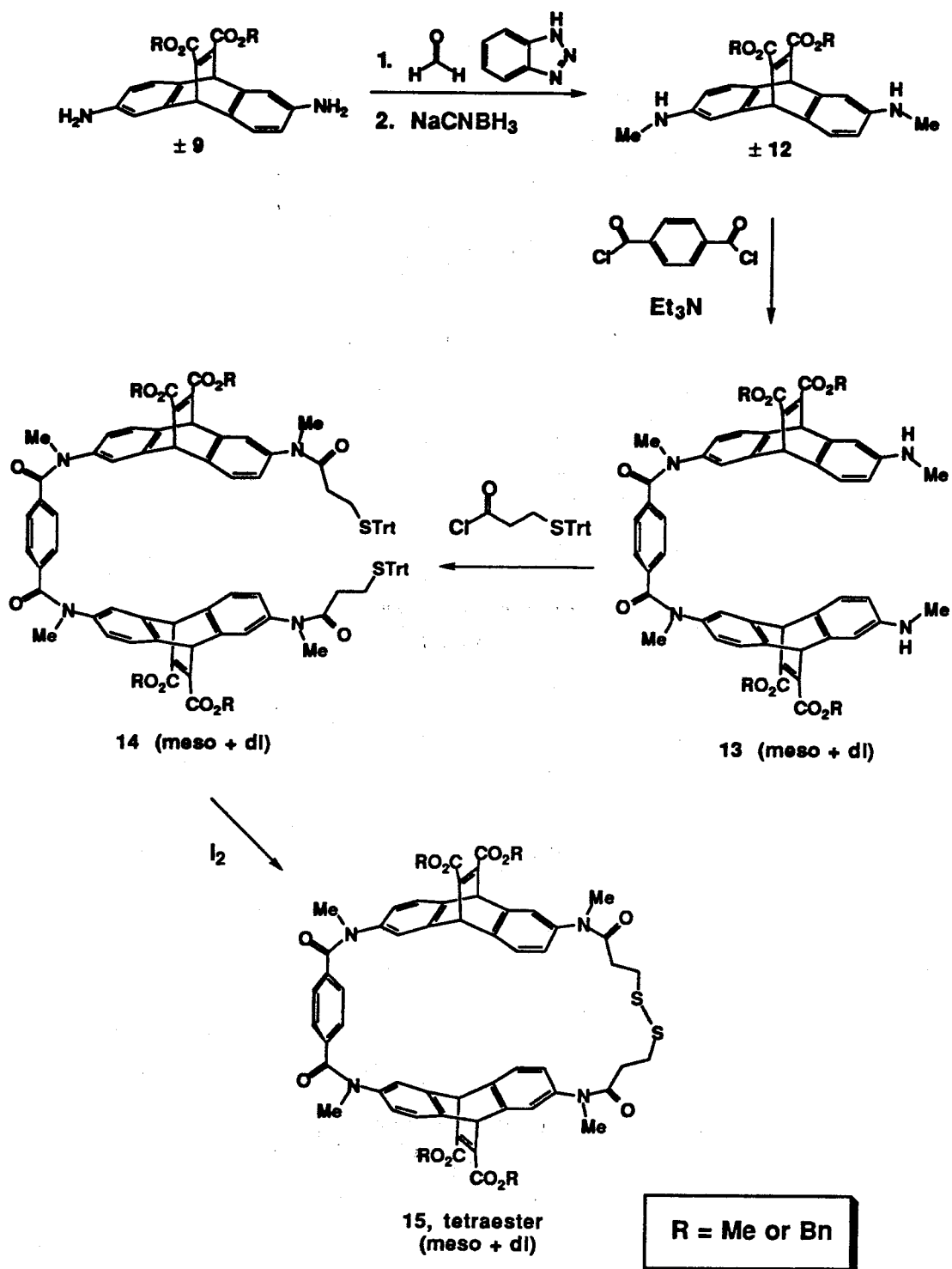
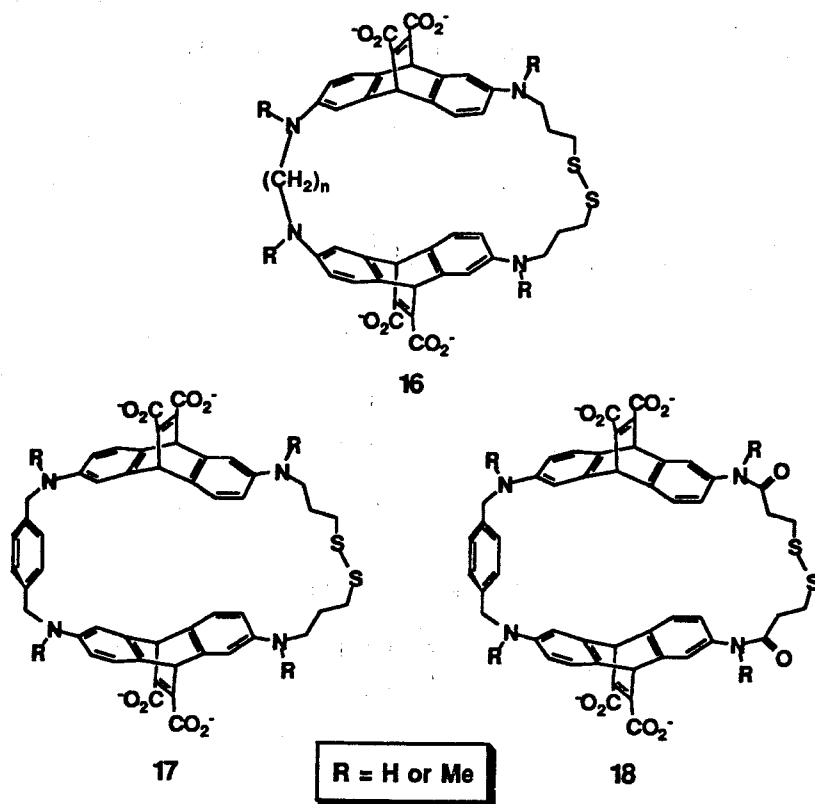


Figure 4.4. N-Methylated Disulfide Host Synthesis.



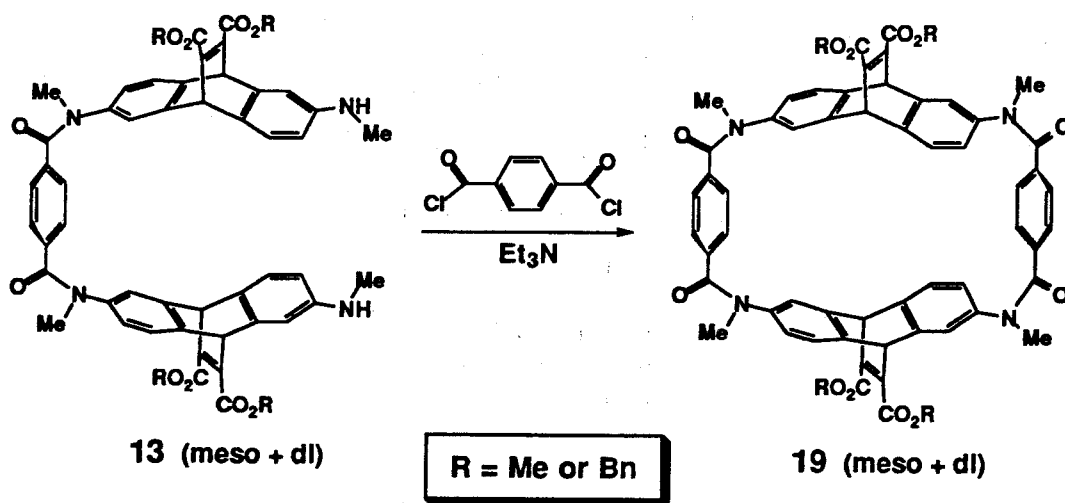
upon heating. The reason for the broadening is not known, but it may have been due to slow rotation about the amide or disulfide bonds. The mass spectral data identified both molecules as the desired disulfide macrocycle, so we concluded that we had isolated *meso* and *dl* hosts, but we were unable to identify which compound was which isomer. Hydrolysis of either molecule failed to generate a water-soluble product, so these macrocycles were not studied further.

At this point, our efforts to produce a disulfide host that was suitable for solution studies essentially ended. A few other ideas were considered, such as host 16, in which the phenyl linker is replaced by a more flexible alkyl chain. A macrocycle containing amine linkages 17 or a combination of amine and amide linkages 18 were two other possibilities. The syntheses of these molecules were initiated, but were not completed.



**An N-Methyl Amide Macrocyclic.** A final molecule that is worth mentioning is the host **19**. The macrocycle is essentially a modified version of the host **4** in which N-methyl amides rather than ethers hold the macrocycle together. It was originally intended to be used for comparison with the disulfide host **15** and is notable for its unusual behavior in solution.

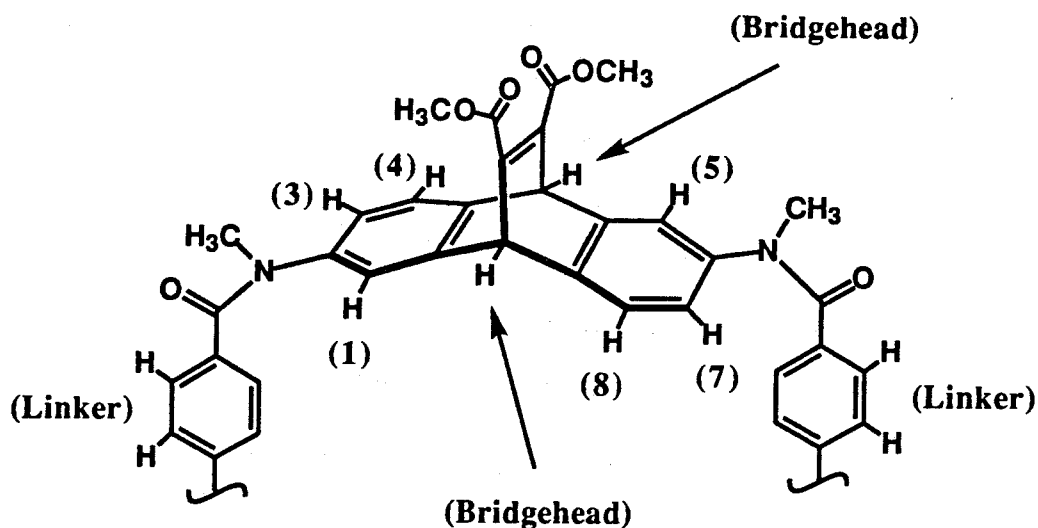
Host **19** was easily prepared by reacting diamine **13** with terephthaloyl chloride in dilute solution. The crude product mixture of the reaction contained equal amounts of two compounds which were isolated by chromatography. Their mass spectral data displayed identical molecular ion peaks, so it was assumed that the *meso* and *dl* isomers had been separated. The  $^1\text{H}$  NMR spectrum of one of the isomers displayed broad resonances and was not studied further. The other isomer, however, displayed sharp NMR resonances and was examined in greater detail. The following sections refer specifically to this isomer of **19**.



The tetramethyl ester of **19** was soluble in a wide range of solvents such as chloroform, acetone, acetonitrile, methanol, and DMSO. It was also soluble in mixed aqueous solutions containing either DMSO or acetonitrile. The

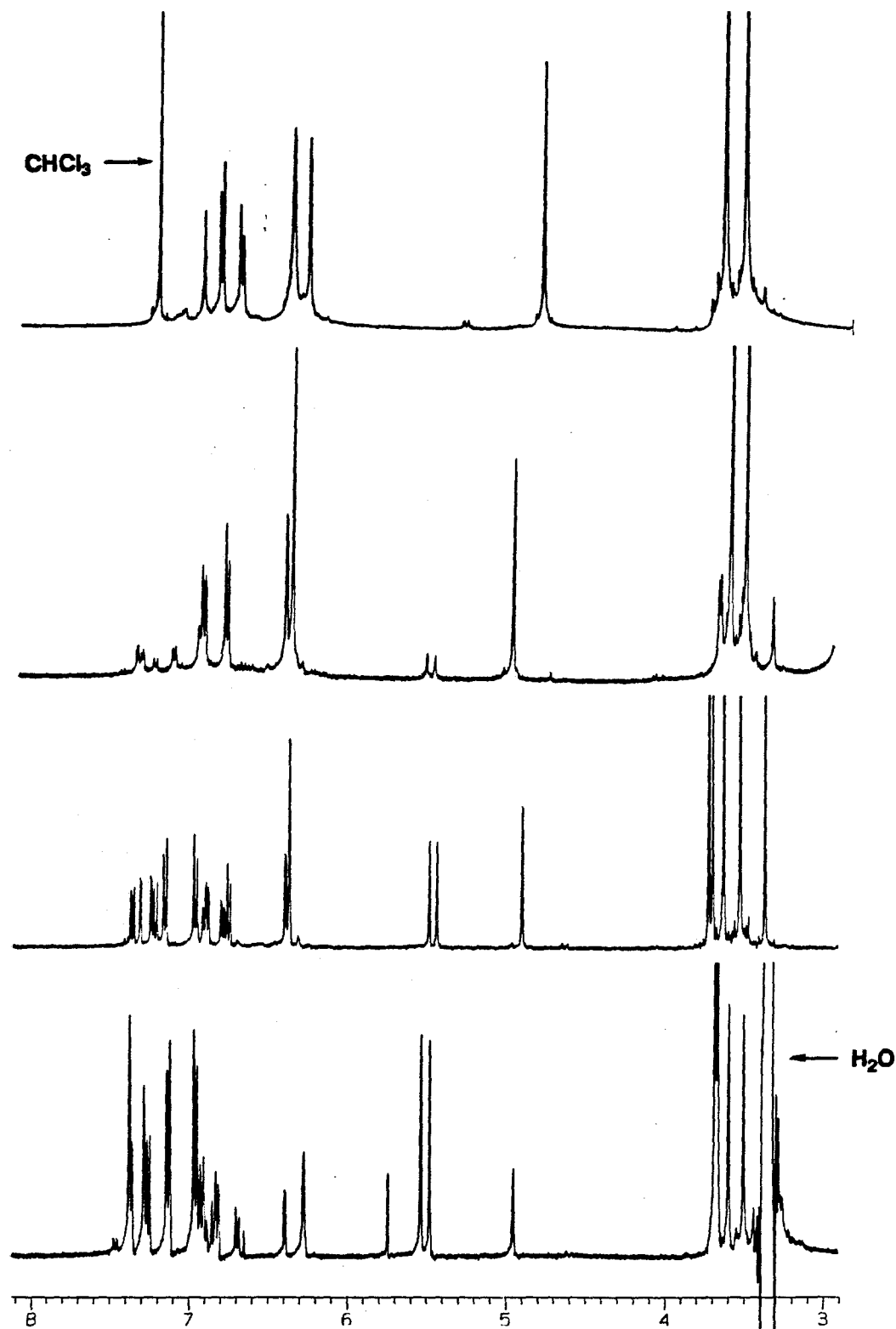
NMR data revealed a mixture of two conformers whose interconversion was slow on the NMR time-scale. Interestingly, the ratio of conformers present in solution depended upon the polarity of the medium.

The  $^1\text{H}$  NMR spectra of tetramethyl ester **19** in a variety of solvents are illustrated in Figure 4.5, next page. In  $\text{CDCl}_3$  (top spectrum), the molecule exists almost exclusively in one conformation. Switching to progressively more polar solvents causes the peaks belonging to another conformer to appear. This is most easily seen by following the bridgehead protons of the host across the series of solvents. (The labelling scheme of the host protons is shown in Figure 4.6.)



**Figure 4.6.** Labelling Scheme for the Protons of Tetramethyl ester **19**. The name of the proton is shown in parentheses next to the atom.

In  $\text{CDCl}_3$ , the bridgehead protons resonate as a sharp singlet at 4.9 ppm. Upon moving to acetone- $d_6$ ,  $\text{CD}_3\text{CN}$  and finally  $\text{DMSO}-d_6$ , the peak shrinks in size. At the same time, two singlets of equal intensity centered at 5.5 ppm



**Figure 4.5.**  $^1\text{H}$  NMR spectra of macrocycle 19 in organic solvents. From top to bottom, the solvents are:  $\text{CDCl}_3$ , acetone- $\text{d}_6$ ,  $\text{CD}_3\text{CN}$ , and  $\text{DMSO-d}_6$ . The peaks between 3-4 ppm have been truncated for clarity.

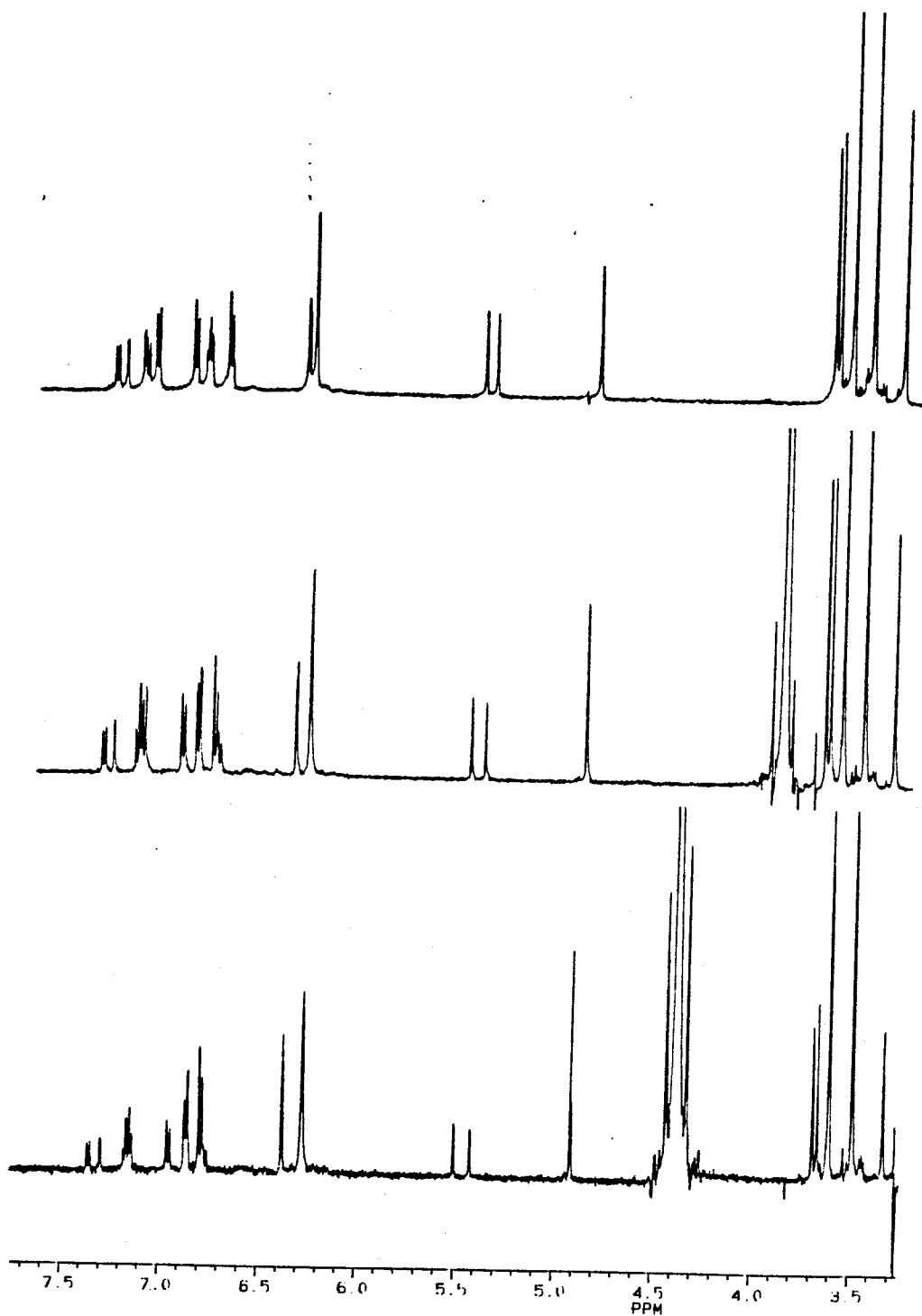
gradually grow in. The bridgehead protons are inequivalent in the new conformer which suggests that it is of lower symmetry.

Changes occur in other parts of the spectrum as well. In the aromatic region, the  $\text{CDCl}_3$  spectrum shows four peaks that can be easily assigned [ $\delta$  (proton type): 6.85 (4, 8); 6.73 (3, 7); 6.40 (linker); 6.30 (1, 5)]. (The singlet at 6.7 ppm is due to an impurity.) As these peaks become smaller, several peaks with more complicated splitting patterns appear further downfield. The complexity of the peaks in the aliphatic region also increases in the more polar solvents.

For unknown reasons, the trend seen in organic solvents reverses itself when water is added. Figure 4.7 shows  $^1\text{H}$  NMR spectra of the tetramethyl ester of 19 in mixed solutions of  $\text{CD}_3\text{CN}$  and  $\text{D}_2\text{O}$ . Both conformations of the host are present in the spectra. As the concentration of water increases, creating a more polar medium, the amount of the lower-symmetry conformer decreases. This is again most easily discerned by noting the relative peak heights of the two sets of bridgehead protons ( $\delta$  5.5 and 4.9) in the various solvents. Similar results were obtained in  $\text{DMSO-d}_6/\text{D}_2\text{O}$  solutions.

To ensure that we were observing a conformational effect and not an irreversible process, we lyophilized the NMR sample containing  $\text{DMSO-d}_6$  and redissolved it in  $\text{CDCl}_3$  which again produced the top spectrum in Figure 4.5. Steady-state magnetization transfer experiments conducted in  $\text{CD}_3\text{CN}$  determined the rate of interconversion between the conformers to be  $2 \text{ sec}^{-1}$  at  $300 \text{ }^\circ\text{K}$ . We speculated that the conformers were interconverting by rotation around one or more of the amide bonds, but were unable to confirm this hypothesis.

A few NMR binding studies of the tetramethyl ester of 19 were conducted in organic ( $\text{CDCl}_3$ ,  $\text{DMSO-d}_6$ ) and mixed aqueous (40%  $\text{CD}_3\text{CN}$  in  $\text{D}_2\text{O}$ ) media,



**Figure 4.7.**  $^1\text{H}$  NMR spectra of macrocycle 19 in mixed aqueous solvents. From top to bottom, the solutions contain 4%, 29% and 62% v/v  $\text{D}_2\text{O}$  in  $\text{CD}_3\text{CN}$ . The peak at 3.9 ppm (middle) and at 4.4 ppm (bottom) are due to water and have been truncated for clarity. The peaks at 3.6 and 3.5 ppm have also been truncated for clarity.

but guests were not measurably bound by the host. This was hardly surprising since hydrophobic effects do not dominate complexation in these solvents. The tetrabenzyl ester of **19** was hydrolyzed with triflic acid in TFA to give a molecule, the putative tetraacid, which was fully soluble in unbuffered D<sub>2</sub>O. The <sup>1</sup>H NMR spectrum of this molecule in D<sub>2</sub>O resembled that of the tetramethyl ester in CDCl<sub>3</sub>; only the high symmetry conformer appeared to be present. Several NMR binding studies on the hydrolyzed host were carried out in pure D<sub>2</sub>O and in pH ~ 9 buffer, but again measurable binding of guests was not observed. The results were quite unexpected since purely hydrophobic binding should have occurred in these systems.

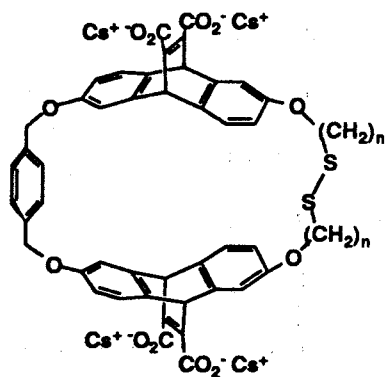
A possible explanation for the lack of guest binding is that the macrocycle adopts a collapsed conformation, and that it is too rigid to reorganize into a conformation suitable for guest binding. X-ray structure analysis and examination of NMR spectra showed that N-methylbenzanilide exists solely as a *cis* amide in the crystal and in solution, whereas benzanilide is a *trans* amide.<sup>18</sup> Corey-Pauling-Koltun (CPK) models of **19** in which all of the amides are constrained in the *cis* configuration produces a structure that no longer contains a binding pocket. In the <sup>1</sup>H NMR spectra of **19** in CDCl<sub>3</sub> and in D<sub>2</sub>O, the phenyl linker groups are shifted considerably further upfield (6.4 ppm) than one would expect. This suggests that the protons are being shielded by the other aromatic rings of the host, and may be indicative of a collapsed conformation.

In the low-symmetry conformer of the tetramethyl ester of **19**, the phenyl group resonances appear further downfield which could mean that the conformation is more open, and therefore better suited for complexation. Unfortunately, we could not adequately test this hypothesis since significant amounts of the low-symmetry conformer are only present in solvents where

the hydrophobic effect is either absent or severely diminished. More studies are needed to better understand this system.

### Concluding Remarks.

Although we were quite disappointed that our efforts to produce a soluble disulfide-containing host were unsuccessful, we still believe that it is a worthwhile goal. Synthesis of hosts 17 or 18 may be feasible, but it is uncertain whether their construction will be particularly facile. A different option might be to synthesize the ether-linked macrocycle 20. This strategy has the decided advantage of starting with molecules that can be produced enantiomerically pure, and in good yield.



20

Ironically, host 20 was the molecule that we had envisioned making when the project was first conceived. At that time, the synthetic routes towards 20 were both limited and problematic, so the idea was quickly abandoned. A very recent publication, however, used benzyltriethylammonium tetrathiomolybdate to synthesize a variety of dithia-crown ethers and other



macrocyclic disulfides.<sup>19</sup> This sulfur transfer reagent may be suitable for our purposes. A possible synthetic scheme is illustrated in Figure 4.8.

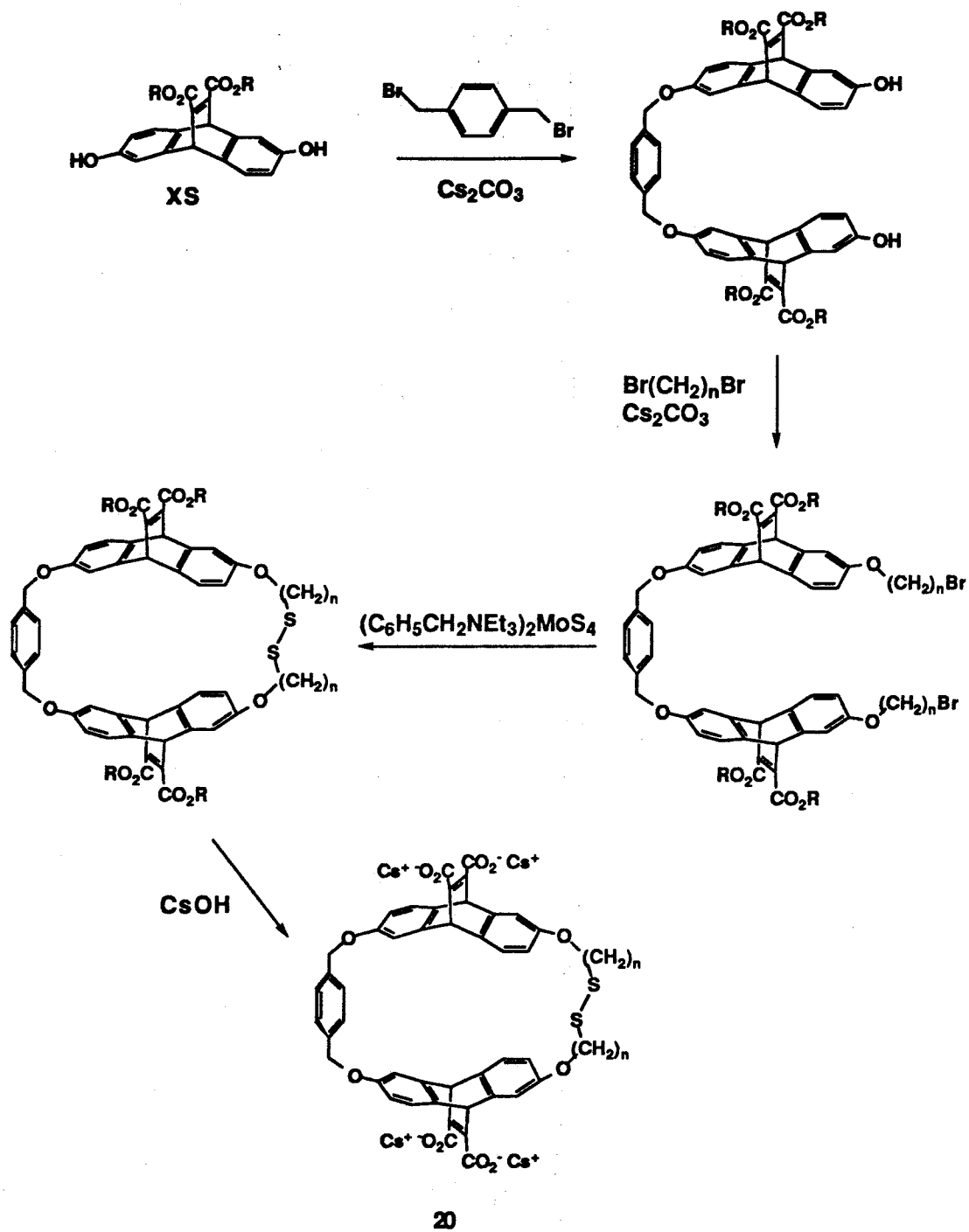


Figure 4.8. Proposed Synthesis of a Disulfide Host.

On a final note, it might also be interesting to go back and structurally characterize the two conformers of host **19**. To do so would first require identification of the isomer as either *meso* or *dl*. Wilcox recently devised a method for synthesizing enantiomerically pure ethenoanthracene **9**, dimethyl ester.<sup>20</sup> From this compound, a single enantiomer of **19** could be prepared for comparison with the unknown isomer. Alternatively, it may be possible to grow crystals of **19**.

## Experimental Section

**General Methods.** The NMR spectra were recorded on either a General Electric QE-300, JEOL JNM GX-400, or Bruker AM-500 spectrometer. Routine spectra were referenced to the residual proton signals of the solvents and are reported in ppm downfield of 0.0 as  $\delta$  values. All coupling constants,  $J$ , are reported in Hz. Preparative centrifugal chromatography was performed on a Harrison Research Chromatotron model 792T using silica plates. Melting points were determined on a Thomas Hoover melting point apparatus, and are corrected. All mass spectral analyses were performed at the University of California, Riverside. All reactions were stirred magnetically under argon unless otherwise noted. Dibenzyl acetylenedicarboxylate was prepared as described in the literature.<sup>21</sup>

**2,6-Diaminoanthracene (6).** 2,6-Diaminoanthraquinone (10 g, 0.042 mol, 1 equiv), NaBH<sub>4</sub> (16 g, 0.43 mol, 10 equiv) and isopropanol (500 mL) were placed in a dry 1000 mL flask. The solution was evacuated and purged several times with argon, and then refluxed for 24 hrs in the dark. Note: Longer reaction times led to significant amounts of an overreduced compound which could not be easily separated from the desired product. After cooling to room temperature, the brown solution was poured onto ~ 500 mL NaCl (saturated aqueous), and the resulting mixture was vigorously stirred while argon was bubbled through the solution. After 18 hrs, the solution was filtered through celite. The yellow (green fluorescent) filtrate was extracted twice with ethyl acetate, dried over MgSO<sub>4</sub> and concentrated to yield 2.93 g of a yellow-brown solid. The brown solid that remained on the celite was soxhlet extracted with ethyl acetate for 4 days. Note: It is extremely important to rigorously exclude oxygen during the soxhlet

extractions, otherwise the product turns dark brown, and the yield is greatly diminished. Yield from soxhlet extractions: 2.96 g, combined yield 67%. The product was stored in the dark at -100 °C and was used without further purification.  $^1\text{H}$  NMR (DMSO- $d_6$ )  $\delta$  7.80 (s, 2H), 7.61 (d, 2H,  $J = 9$ ), 6.90 (dd, 2H,  $J = 3, 9$ ), 6.78 (d, 2H,  $J = 2$ ), 5.2 (br s);  $^{13}\text{C}$  NMR (DMSO- $d_6$ )  $\delta$  144.74, 131.30, 128.62, 127.88, 122.00, 121.13, 104.36.

**2,6-Bis[N-(*tert*-butoxycarbonyl)amino]anthracene (7).** 2,6-Diaminoanthracene **6** (1.24 g, 5.96 mmol, 1 equiv), di-*tert*-butyl dicarbonate (3.25 g, 14.9 mmol, 2.5 equiv) and triethylamine (1.51 g, 2.1 mL, 14.9 mmol, 2.5 equiv) were dissolved in ~ 30 mL DMF. After heating at 50° C for 12 hrs, the DMF was removed under reduced pressure. The resulting orange-brown solid was suspended in ether and suction filtered. The solid was then rinsed with acetone which removed most of the brown color and left a yellowish powder that was used directly in the next step: yield 1.29 g (53%).  $^1\text{H}$  NMR (DMSO- $d_6$ )  $\delta$  9.57 (br s), 8.25 (s, 2H), 8.17 (br s, 2H), 7.90 (d, 2H,  $J = 9$ ), 7.46 (dd, 2H,  $J = 3, 9$ ), 1.51 (s, 18H);  $^{13}\text{C}$  NMR (DMSO- $d_6$ )  $\delta$  153.55, 136.49, 131.33, 129.33, 128.93, 125.01, 121.32, 112.80, 79.91, 28.83.

**2,6-Bis[N-(*tert*-butoxycarbonyl)amino]-9,10-dihydro-11,12-dicarbomethoxyethenoanthracene ( $\pm$  **8**, R = Me).** BOC-protected anthracene **7** (1.29 g, 3.16 mmol, 1 equiv) and dimethyl acetylenedicarboxylate (2.25 g, 1.95 mL, 15.8 mmol, 5 equiv) were suspended in 100 mL dioxane, and refluxed. The solid dissolved, and refluxing was continued for 3 days. The dioxane was removed under reduced pressure, and the resulting brown viscous oil was purified by chromatography over silica gel eluting with 5% ethyl acetate in  $\text{CH}_2\text{Cl}_2$  to obtain 1.54 g of a yellow solid (89% yield).  $^1\text{H}$  NMR ( $\text{CDCl}_3$ )  $\delta$  7.62 (br s), 7.12 (d, 2H,  $J = 8$ ), 6.72 (dd, 2H,  $J = 4, 8$ ), 6.68 (br s, 2H), 5.31 (s, 2H), 3.72 (s, 6H),

1.45 (s, 18H). **2,6-Bis[N-(*tert*-butoxycarbonyl)amino]-9,10-dihydro-11,12-dicarbobenzyloxyethenoanthracene ( $\pm 8$ , R = Bzl)** was prepared using the same procedure, but substituting dibenzyl acetylenedicarboxylate. Purified by chromatography over silica gel ( $R_f$  0.38 in  $\text{CH}_2\text{Cl}_2$ ): yield 73%.  $^1\text{H NMR}$  ( $\text{CDCl}_3$ )  $\delta$  7.59 (br s), 7.28, 7.23 (2 m, 10H), 7.19 (d, 2H,  $J = 8$ ), 6.77 (dd, 2H,  $J = 2$ , 12), 6.56 (br s, 2H), 5.36 (s, 2H), 5.00 (s, 4H).

**2,6-Diamino-9,10-dihydro-11,12-dicarbomethoxyethenoanthracene ( $\pm 9$ , R = Me)**. Diels-Alder adduct  $\pm 8$ , R = Me (1.05 g, 1.91 mmol, 1 equiv) was placed in a flask and TFA (~ 5 mL) was added. The solution was stirred for 15 min, and then made basic (pH ~ 8) with  $\text{NaHCO}_3$  (saturated aqueous). *Caution: foaming!* The solution was then extracted twice with  $\text{CH}_2\text{Cl}_2$ . The organic extracts were combined, dried over  $\text{MgSO}_4$ , filtered, concentrated, and purified by chromatography over silica gel ( $R_f$  0.38 in 5% ethyl acetate in  $\text{CH}_2\text{Cl}_2$ ), yielding 587 mg (88%) of an off-white foam.  $^1\text{H NMR}$  ( $\text{CDCl}_3$ )  $\delta$  7.05 (d, 2H,  $J = 8$ ), 6.70 (d, 2H,  $J = 2$ ), 6.21 (dd, 2H,  $J = 2$ , 8), 5.25 (s, 2H), 3.73 (s, 6H); EI-MS  $m/e$  350 ( $\text{M}^+$ ), 291 ( $\text{M}^+ - \text{CO}_2\text{Me}$ ), 208 ( $\text{M}^+ - \text{dimethyl acetylenedicarboxylate}$ ). **2,6-Diamino-9,10-dihydro-11,12-dicarbobenzyloxyethenoanthracene ( $\pm 9$ , R = Bn)** was prepared from  $\pm 8$ , R = Bn using the same procedure. Purified by chromatography over silica gel ( $R_f$  0.50 in 20% ethyl acetate in  $\text{CH}_2\text{Cl}_2$ ): yield 74%.  $^1\text{H NMR}$  ( $\text{CDCl}_3$ )  $\delta$  7.28, 7.23 (2 m, 10H), 7.05 (d, 2H,  $J = 8$ ), 6.69 (d, 2H,  $J = 2$ ), 6.21 (dd, 2H,  $J = 2$ , 8), 5.20 (s, 2H), 4.99 (s, 4H), 3.45 (br s).

**Compound 10, R = Me**. Diamine  $\pm 9$ , R = Me (500 mg, 1.43 mmol, 5 equiv) and triethylamine (72 mg, 100  $\mu\text{L}$ , 0.71 mmol, 2.5 equiv) were placed in a 100 mL flask and dissolved in 10 mL dry THF. Terephthaloyl chloride (58 mg, 0.29 mmol, 1 equiv) was placed in a dry flask and dissolved in 10 mL dry THF. This solution, along with two 5 mL rinsings of the flask were drawn into a 25 mL gas-

tight syringe and injected into the solution containing the amines at a rate of ~ 5 mL/hr. Five hours after the addition finished, the THF was removed under reduced pressure. The resulting residue was dissolved in ethyl acetate, washed twice with H<sub>2</sub>O, dried over MgSO<sub>4</sub>, filtered, and concentrated. Column chromatography over silica gel (1:1 ethyl acetate/CH<sub>2</sub>Cl<sub>2</sub>) was used to isolate unreacted **± 9** (*R<sub>f</sub>* 0.59) and 185 mg product (*R<sub>f</sub>* 0.38, an off-white foam, 78% yield). The product was a 1:1 mixture of *meso* + *dl* isomers. <sup>1</sup>H NMR (CDCl<sub>3</sub>) δ 8.63 (s, 2H), 7.79 (s, 2H), 7.61 (s, 4H), 7.15 (m, 4H), 7.01 (d, 2H *J* = 8), 6.70 (d, 2H, *J* = 3), 6.20 (dd, 2H, *J* = 3, 8), 5.27 (s, 2H), 5.24 (s, 2H), 3.74 (s, 6H), 3.70 (s, 6H); FAB-MS *m/e* 831 (MH<sup>+</sup>), 799 (M<sup>+</sup>-OCH<sub>3</sub>), 771 (M<sup>+</sup>-CO<sub>2</sub>CH<sub>3</sub>), 688 (M<sup>+</sup>-dimethyl acetylenedicarboxylate). **Compound 10**, R = Bn was prepared using the same procedure from **± 9**, R = Bn. Purified by chromatography over silica gel (*R<sub>f</sub>* 0.30 in 1:2 ethyl acetate/CH<sub>2</sub>Cl<sub>2</sub>): yield 78%. <sup>1</sup>H NMR (CDCl<sub>3</sub>) δ 8.37 (s, 2H), 7.74 (s, 2H), 7.65 (s, 4H), 7.20 (m, 20H), 6.98 (d, 4H, *J* = 8), 6.67 (s, 4H), 6.17 (d, 4H, *J* = 8), 5.26 (s, 8H), 4.95 (m, 4H).

**3-(Triphenylmethylthio)propionic acid.** 3-Mercaptopropionic acid (1.22 g, 1.0 mL, 0.011 mol, 1 equiv) and triphenylmethyl chloride (4.7 g, 0.017 mol, 1.5 equiv) were placed in a flask along with DMF (6 mL), and the mixture was stirred at room temperature. The triphenylmethyl chloride gradually dissolved, and then a few hours later a large amount of white precipitate appeared in the flask. After 2 days, 10% sodium acetate solution (50 mL) was added, and the white solid was filtered off and washed with water. Recrystallization of the solid from acetone produced 2.6 g product (70% yield). m.p. 209-211 °C, literature value<sup>22</sup> 206-207 °C; <sup>1</sup>H NMR (acetone-d<sub>6</sub>) δ 7.42 (d, 6H, *J* = 7), 7.32 (t, 6H, *J* = 6), 7.26 (t, 3H, *J* = 7), 2.41 (t, 4H, *J* = 6), 2.25 (t, 4H, *J* = 7).

**Compound 11, R = Me.** Compound 10, R = Me (*meso* + *dl* mixture, 180 mg, 0.22 mmol, 1 equiv), 1-hydroxybenzotriazole (73 mg, 0.54 mmol, 2.5 equiv) and 3-(triphenylmethylthio)propionic acid (182 mg, 0.54 mmol, 2.5 equiv) were placed in a flask and dissolved in 5 mL DMF. 1-(3-Dimethylaminopropyl)-3-ethylcarbodiimide hydrochloride (104 mg, 0.54 mmol, 2.5 equiv) was added to the reaction mixture. The solution was stirred at room temperature for 12 hours. The DMF was removed under reduced pressure, and the residue was dissolved in ethyl acetate and washed three times with water. The organic layer was dried over MgSO<sub>4</sub>, filtered, concentrated, and purified by chromatography over silica gel (30% ethyl acetate in CH<sub>2</sub>Cl<sub>2</sub>) to yield 259 mg white solid (80%). <sup>1</sup>H NMR (DMSO-d<sub>6</sub>) δ 10.32 (s, 2H), 9.90 (s, 2H), 8.05 (s, 4H), 7.92 (s, 2H), 7.79 (s, 2H), 7.5-7.2 (m, 38H), 5.60 (d, 2H, J = 4), 3.70 (s, 12H), 2.32 (m, 4H); FAB-MS *m/e* 1492 (MH<sup>+</sup>). **Compound 11, R = Bn** was prepared from compound 10, R = Bn using the same procedure. <sup>1</sup>H NMR (DMSO-d<sub>6</sub>) δ 10.32 (s, 2H), 9.90 (s, 2H), 8.05 (s, 4H), 7.92 (s, 2H), 7.79 (s, 2H), 7.3-7.1 (m, 58H), 5.62 (s, 4H), 5.04 (s, 8H), 2.32 (m, 4H).

**Disulfide macrocycle 3, R = Me.** Compound 11, R = Me (100 mg, 0.067 mmol, 1 equiv) was dissolved in 50 mL DMF. I<sub>2</sub> (35 mg, 0.14 mmol, 2 equiv) was added, and the orange solution was stirred in the dark for 2 days at room temperature. Sodium thiosulfate (saturated aqueous) was added, and the solution was extracted with CH<sub>2</sub>Cl<sub>2</sub>. The organic extract was washed with water, dried over MgSO<sub>4</sub>, filtered, and the solvent removed under reduced pressure to yield a beige solid (a mixture of *meso* + *dl* isomers) which was not purified further. <sup>1</sup>H NMR (DMSO-d<sub>6</sub>) δ 10.32 (s, 2H), 9.96 (s, 2H), 8.00 (s, 4H), 7.90 (s, 2H), 7.77 (s, 2H), 7.40 (m, 2H), 7.34 (m, 4H), 7.09 (m, 2H), 5.55 (s, 4H), 3.68 (s, 12H), 2.96 (m, 4H), 2.63 (m, 4H); FAB-MS *m/e* 1027 (MNa<sup>+</sup>). **Disulfide**

macrocycle (**3**, R = Bn) was prepared from compound **11**, R = Bn using the same procedure.  $^1\text{H}$  NMR (DMSO- $d_6$ )  $\delta$  10.34 (s), 10.00 (s), 9.90 (s), 8.02 (s), 7.95 (m), 7.80 (d), 7.50-7.10 (m), 6.88 (s), 6.65 (s), 5.62 (d), 5.05 (s), 2.98 (br t), 2.70 (br t), 2.33 (m). (Integrated peak values were unavailable for this compound); FAB-MS  $m/e$  1331 (MNa $^+$ ).

**2,6-Bis(N-methylamino)-9,10-dihydro-11,12-dicarbomethoxyethenoanthracene ( $\pm$  **12**, R = Me).** Diamine  $\pm$  **9**, R = Me (587 mg, 1.67 mmol, 1 equiv), benzotriazole (440 mg, 3.69 mmol, 2.2 equiv) and formaldehyde (37% aqueous solution, 277  $\mu\text{L}$ , 3.69 mmol, 2.2 equiv) were dissolved in  $\sim$  7 mL EtOH and refluxed for 15 min until a white precipitate formed. The solution was allowed to cool to room temperature and was stirred for an additional 12 hours. The solution was then cooled in an ice bath and stirred for another 2 hours. The solid was filtered off and dried to give 890 mg of the benzotriazole derivative. This solid and NaBH $_3$ CN (228 mg, 0.60 mmol, 2.5 equiv) were suspended in 40 mL dry THF and refluxed for 2 hours, during which time the solid gradually dissolved. Note: Longer reaction times led to increasing amounts of an overreduced side-product. The solution was cooled, water was added, and the solution was extracted twice with ethyl acetate. The organic extracts were combined, dried over MgSO $_4$ , filtered, concentrated, and then purified using preparative centrifugal chromatography (2mm thick plate, 5% ethyl acetate in CH $_2$ Cl $_2$ ) which yielded a viscous yellow oil, 279 mg (44% overall yield).  $^1\text{H}$  NMR (CDCl $_3$ )  $\delta$  7.15 (d, 2H,  $J$  = 8), 6.71 (d, 2H,  $J$  = 2), 6.19 (dd, 2H,  $J$  = 2, 8), 5.23 (s, 2H), 3.78 (s, 6H), 2.79 (s, 6H). **2,6-Bis(N-methylamino)-9,10-dihydro-11,12-dicarbobenzyloxyethenoanthracene ( $\pm$  **12**, R = Bn)** was prepared in an identical fashion from  $\pm$  **9**, R = Bn.  $^1\text{H}$  NMR (CDCl $_3$ )  $\delta$  7.30 (m, 10H), 7.14 (d, 2H,  $J$  = 8), 6.71 (d, 2H,  $J$  = 2), 6.20 (dd, 2H,  $J$  = 2, 8), 5.27 (s, 2H), 5.04 (s, 4H); EI-MS  $m/e$  531



(MH<sup>+</sup>), 441 (M<sup>+</sup>-Bzl), 237 (M<sup>+</sup>-dibenzyl acetylenedicarboxylate); HRMS 531.2285, calc. for C<sub>34</sub>H<sub>30</sub>N<sub>2</sub>O<sub>4</sub>: 531.2284.

**Compound 13, R = Me.** This molecule was prepared using the same procedure that was used to synthesize compound 10, but substituting ethenoanthracene 12, R = Me for molecule 9. Purification by chromatography over silica gel (15% THF in CH<sub>2</sub>Cl<sub>2</sub>) gave recovered starting material 12 (*R<sub>f</sub>* 0.69) and product (*R<sub>f</sub>* 0.25, mixture of *meso* and *dl* isomers): yield 68%. <sup>1</sup>H NMR (CDCl<sub>3</sub>) δ 7.10 (d, 2H, *J* = 8), 7.02 (m, 8H), 6.68 (s, 2H), 6.44 (br s, 2H), 6.18 (d, 2H, *J* = 8), 5.28 (s, 2H), 5.18 (s, 2H), 3.77 (s, 12H), 3.30 (s, 6H), 2.76 (s, 6H). **Compound 13, R = Bn** was prepared in an identical fashion but using ± 12, R = Bn. <sup>1</sup>H NMR (CDCl<sub>3</sub>) δ 7.25 (m, 20H), 7.08 (m, 2H), 6.99 (m, 8H), 6.67 (m, 2H), 6.38 (br s, 2H), 6.18 (m, 2H), 5.30 (d, 2H, *J* = 5), 5.18 (s, 2H), 5.00 (m, 8H), 3.29 (s, 6H), 2.75 (s, 6H); FAB-MS *m/e* 1213 (MNa<sup>+</sup>), 1192 (MH<sup>+</sup>); HRMS 1213.4387, calc. for C<sub>76</sub>H<sub>62</sub>N<sub>4</sub>O<sub>10</sub>Na: 1213.4364.

**Compound 14, R = Bn.** 3-(Triphenylmethylthio)propionic acid (303 mg, 0.87 mmol, 3.5 equiv) was dissolved in 8 mL THF. Dichlorotriphenylphosphorane (281 mg, 0.87 mmol, 3.5 equiv) was added, and the solution was stirred for 90 min. Compound 13, R = Bn (296 mg, 0.25 mmol, 1 equiv) and triethylamine (87 mL, 0.62 mmol, 2.5 equiv) were dissolved in 10 mL dry THF. This solution, along with two 5 mL rinsings of the flask were drawn into a 25 mL gas-tight syringe and injected into the solution containing the acid chloride, at a rate of 13.2 mL/hr. The solution turned cloudy. Twelve hours after the injection had finished, the THF was removed under reduced pressure. The resulting residue was dissolved in CH<sub>2</sub>Cl<sub>2</sub>, washed twice with H<sub>2</sub>O, dried over MgSO<sub>4</sub>, filtered, and concentrated. The product was isolated by chromatography over silica gel (*R<sub>f</sub>* 0.56, 1:2 ethyl acetate/CH<sub>2</sub>Cl<sub>2</sub>): 338 mg (73% yield) of an off-white solid. <sup>1</sup>H

NMR (CDCl<sub>3</sub>)  $\delta$  7.3-6.9 (m, 62H), 6.61 (br d, 2H), 6.48 (br s 2H), 5.32 (m, 4H), 4.95 (m, 8H), 3.25 (s, 6H), 3.01 (s, 6H), 2.35 (m, 4H), 1.75 (m, 4H); FAB-MS *m/e* 1875 (MNa<sup>+</sup>), 1388 (M<sup>+</sup>-2Trt).

**Disulfide macrocycle 15, R = Bn.** This molecule was prepared using the same procedure that was to synthesize the macrocycle 3 but substituting compound 14, R = Bn for molecule 11. Thin-layer chromatography on silica plates (12% THF in CH<sub>2</sub>Cl<sub>2</sub>) showed that the crude product contained unreacted 14 (*R<sub>f</sub>* 0.78) and two other spots (*R<sub>f</sub>* 0.38, 0.12). All three compounds were isolated by chromatography over silica (5-30% THF in CH<sub>2</sub>Cl<sub>2</sub>). *R<sub>f</sub>* 0.38 compound: FAB-MS *m/e* 1387 (MNa<sup>+</sup>); HRMS 1387.4160, calc. for C<sub>82</sub>H<sub>68</sub>N<sub>4</sub>O<sub>12</sub>S<sub>2</sub>Na: 1387.4173. *R<sub>f</sub>* 0.12 compound: FAB-MS *m/e* 1387 (MNa<sup>+</sup>); HRMS 1387.4095, calc. for C<sub>82</sub>H<sub>68</sub>N<sub>4</sub>O<sub>12</sub>S<sub>2</sub>Na: 1387.4173.

**Macrocycle 19, R = Me.** Compound 13, R = Me (24 mg, 0.027 mmol, 1 equiv) and triethylamine (9 mL, 0.065 mmol, 2.5 equiv) were dissolved in 10 mL dry THF. Terephthaloyl chloride (5 mg, 0.025 mmol, 1 equiv) was dissolved in 10 mL dry THF, taken up in a 25 mL gas-tight syringe, and injected into the solution containing the amines at a rate of 7.7 mL/hr. Twelve hours after the injection had finished, the THF was removed under reduced pressure. The resulting residue was dissolved in CH<sub>2</sub>Cl<sub>2</sub>, washed twice with H<sub>2</sub>O, dried over MgSO<sub>4</sub>, filtered, and concentrated. Preparative centrifugal chromatography (1 mm plate, 25% THF in CH<sub>2</sub>Cl<sub>2</sub>) was used to isolate two products that ran very close to one another on the plate. High-*R<sub>f</sub>* compound: <sup>1</sup>H NMR (CDCl<sub>3</sub>)  $\delta$  6.85 (d, 4H, *J* = 8), 6.73 (dd, 4H, *J* = 2, 8), 6.40 (br s, 8H), 6.30 (d, 4H, *J* = 2), 4.82 (s, 4H), 3.69 (s, 12H), 3.55 (s, 12H). **Macrocycle 19, R = Bn** was prepared from compound 13, R = Bn using the same procedure. High-*R<sub>f</sub>* compound: <sup>1</sup>H NMR (CDCl<sub>3</sub>)  $\delta$  7.25, 7.14 (2 m, 20H), 7.14 (d, 4H, *J* = 8), 6.69 (dd, 4H, *J* = 2, 8), 6.38 (br s, 8H), 6.25 (d, 4H, *J* =

2), 4.91 (s, 8H), 4.81 (s, 4H), 3.54 (s, 12H); FAB-MS *m/e* 1321 (MH<sup>+</sup>); HRMS 1321.4611 calc. for C<sub>84</sub>H<sub>64</sub>N<sub>4</sub>O<sub>12</sub>: 1321.4598. Low-*R<sub>f</sub>* compound: FAB-MS *m/e* 1321 (MH<sup>+</sup>).

**References**

1. For reviews on the nAChR see (a) Conti-Tronconi, B. M.; McLane, K. E.; Raftery, M. A.; Grando, S. A.; Protti, M. P. *Crit. Rev. Biochem.* 1994, 29, 69-123. (b) Devillers-Thiéry, A.; Galzi, J. L.; Eiselé, J. L.; Bertrand, S.; Bertrand, D.; Changeux, J. P. *J. Membrane Biol.* 1993, 136, 97-112. (c) Galzi, J. L.; Revah, F.; Bessis, A.; Changeux, J. P. *Ann. Rev. Pharmacol.* 1991, 31, 37-72. (d) Karlin, A. *Curr. Opin. Neurobiol.* 1993, 3, 299-309. (e) Karlin, A. *The Harvey Lectures* 1991, 85, 71-107.
2. Unwin, N. *J. Mol. Biol.* 1993, 229, 1101-1124.
3. (a) Abramson, S. M.; Li, Y.; Culver, P.; Taylor, P. *J. Biol. Chem.* 1989, 264, 12666-12672. (b) Cohen, J. B.; Sharp, S. D.; Liu, W. S. *J. Biol. Chem.* 1991, 266, 23354-23364. (c) Dennis, M.; Giraudat, J.; Kotzyba-Hibert, F.; Goeldner, M.; Hirth, C.; Chang, J. Y.; Lazure, C.; Chrétien, M.; Changeux, J. P. *Biochemistry* 1988, 27, 2346-2357. (d) Galzi, J. L.; Revah, F.; Black, D.; Goeldner, M.; Hirth, C.; Changeux, J. P. *J. Biol. Chem.* 1990, 65, 10430-10437. (e) Kao, P. N.; Dwork, A. J.; Kaldany, R-R. J.; Silver, M. L.; Wideman, J.; Stein, S.; Karlin, A. *J. Biol. Chem.* 1984, 259, 11662-11665. (f) Pedersen, S. E.; Cohen, J. B. *Proc. Natl. Acad. Sci.* 1990, 87, 2785-2789.
4. (a) Chaturvedi, V.; Donnelly-Roberts, D. L.; Lentz, T. L. *Biochemistry* 1992, 31, 1370-1375. (b) Chaturvedi, V.; Donnelly-Roberts, D. L.; Lentz, T. L. *Biochemistry* 1993, 32, 9570-9576.
5. Fraenkel, Y.; Gershoni, J. M.; Navon, G. *FEBS Lett.* 1991, 291, 225-228.
6. Dougherty, D. A.; Stauffer, D. A. *Science* 1990, 250, 1558-1560.

7. Mishina, M.; Tobimatsu, T.; Imoto, K.; Tanaka, K.; Fujita, Y.; Fukuda, K.; Kurasaki, M.; Takahashi, H.; Morimoto, Y.; Hirose, T.; Inayama, S.; Takahashi, T.; Kuno, M.; Numa, S. *Nature* 1985, 313, 364-369.
8. Kao, P. N.; Karlin, A. *J. Biol. Chem.* 1986, 261, 8085-8088.
9. (a) Blake, C. C. F.; Ghosh, M.; Harloos, K.; Avezoux, A.; Anthony, C. *Struct. Biol.* 1994, 1, 102-105. (b) White, S.; Boyd, G.; Mathews, F. S.; Xia, Z.; Dai, W.; Zhang, Y.; Davidson, V. L. *Biochemistry* 1993, 32, 12955-12958.
10. Damle, V. N.; Karlin, A. *Biochemistry* 1980, 19, 3924-3932.
11. Petti, M. A.; Shepodd, T. J.; Barrans, R. E., Jr.; Dougherty, D. A. *J. Am. Chem. Soc.* 1988, 110, 6825-6840.
12. A. P. West, unpublished results.
13. Kumpf, R. A.; Dougherty, D. A. *Science* 1993, 261, 1708-1710.
14. Horne, A.; North, M.; Parkinson, J. A.; Sadler, I. H. *Tetrahedron* 1993, 49, 5891-5904.
15. R. A. Kumpf, unpublished results.
16. Kearney, P. C.; Mizoue, L. S.; Kumpf, R. A.; Forman, J. E.; McCurdy, A.; Dougherty, D. A. *J. Am. Chem. Soc.* 1993, 115, 9907-9919.
17. Binding to the nAChR is complex involving two positively cooperative, nonequivalent sites, and at least four functional states. The value of  $K_d$  obtained depends on the type of measurement being made. Dose-response curves characterize a low-affinity conformation of the nAChR (50 to 100  $\mu$ M) associated with the resting state. Equilibrium binding studies identify a

- high-affinity conformation (~3 nM) associated with desensitized states. For further discussions see Ochoa, E. L. M.; Chattopadhyay, A.; McNamee, M. G. *Cell. Mol. Neurobiol.* **1989**, *9*, 141-178. Karlin, A. In *The Cell Surface and Neuronal Function*; Cotman, C. W.; Poste, G.; Nicolson, G. L., Eds.; Elsevier/North Holland Biomedical: Amsterdam, 1980; pp 191-260.
18. Itai, A.; Toriumi, Y.; Tomioka, N.; Kagechika, H.; Azumaya, I.; Shudo, K. *Tetrahedron Lett.* **1989**, *30*, 6177-6180.
19. Ramesha, A. R.; Chandrasekaran, S. *J. Org. Chem.* **1994**, *59*, 1354-1357.
20. C. S. Wilcox, private communication.
21. Lowe, G.; Ridley, D. D. *J. Chem. Soc., Perkin Trans. I* **1973**, 2024-2029.
22. Bray, A. M.; Kelly, D. P.; Mack, P. O. L.; Martin, R. F.; Wakelin, L. P. G. *Aust. J. Chem.* **1990**, *43*, 629-634.